Department of
Mineral and Petroleum Resources

EXPLANATORY NOTES

GEOCHEMICAL MAPPING OF THE NICHOLLS 1:100 000 SHEET

by A. J. Sanders

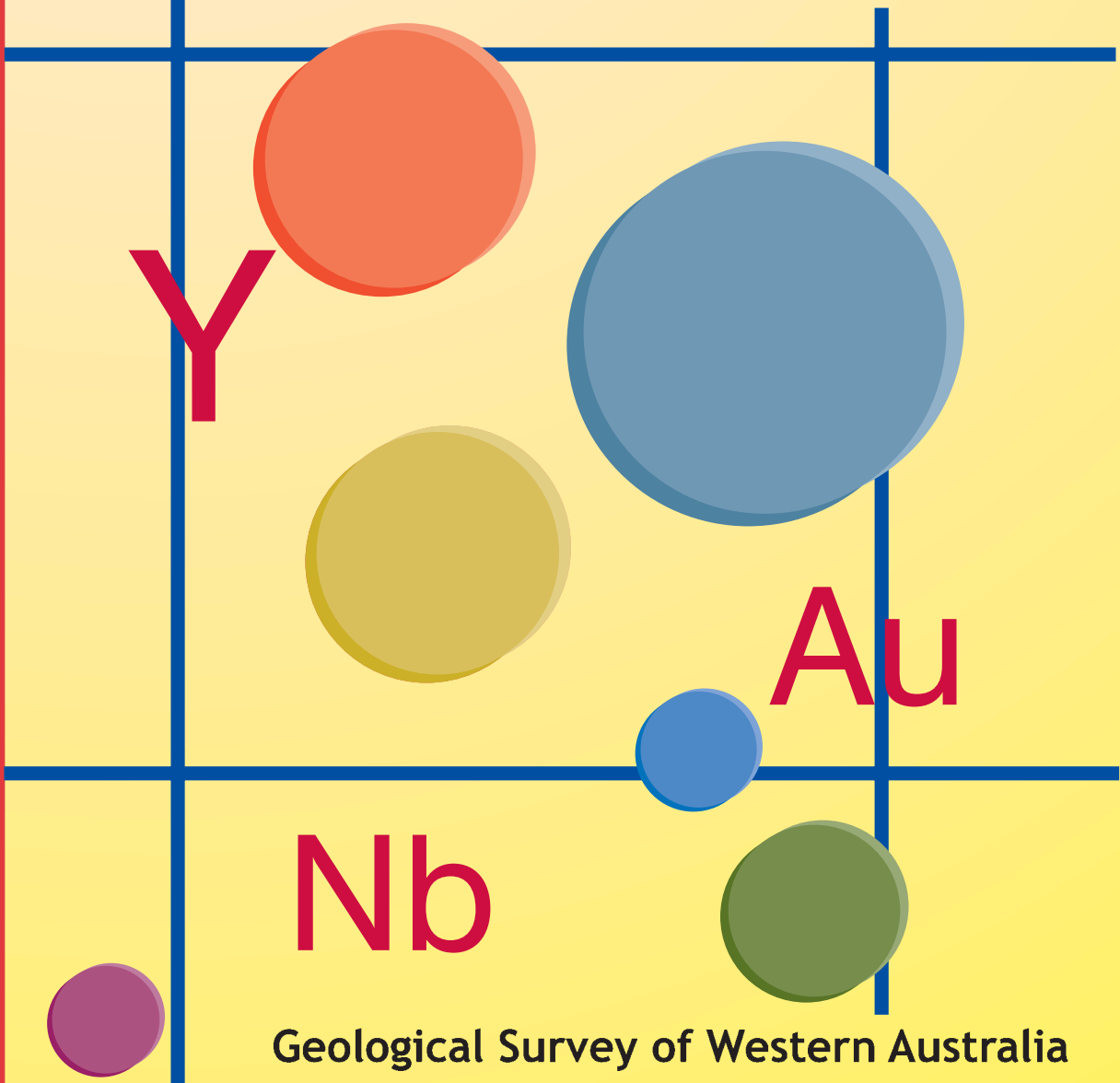

Geological Survey of Western Australia

GEOLOGICAL SURVEY OF WESTERN AUSTRALIA

GEOCHEMICAL MAPPING OF THE NICHOLLS 1:100 000 SHEET

by
A. J. Sanders

Perth 2002

MINISTER FOR STATE DEVELOPMENT
Hon. Clive Brown MLA

DIRECTOR GENERAL, DEPARTMENT OF MINERAL AND PETROLEUM RESOURCES
Jim Limerick

DIRECTOR, GEOLOGICAL SURVEY OF WESTERN AUSTRALIA
Tim Griffin

REFERENCE
The recommended reference for this publication is:
SANDERS, A. J., 2002, Geochemical mapping of the Nicholls 1:100 000 sheet: Western Australia Geological Survey, 1:100 000 Geological Series Explanatory Notes, 36p.

National Library of Australia Card Number and ISBN 0 7307 5727 7

ISSN 1321–229X

Grid references in this publication refer to the Geocentric Datum of Australia 1994 (GDA94). Locations mentioned in the text are referenced using Map Grid Australia (MGA) coordinates, Zone 51. All locations are quoted to at least the nearest 100 m.

Copy editor: J. A. Mikucki
Cartography: M. Vicentic, M. Prause
Desktop publishing: K. S. Noonan

Published 2002 by Geological Survey of Western Australia

Copies available from:
Information Centre
Department of Mineral and Petroleum Resources
100 Plain Street
EAST PERTH, WESTERN AUSTRALIA 6004
Telephone: (08) 9222 3459 Facsimile: (08) 9222 3444
This and other publications of the Geological Survey of Western Australia are available online through the Department's bookshop at www.mpr.wa.gov.au

Contents

Appendices

Plates (in pocket)

Figures (from p. 35)

Tables

Digital dataset (in pocket)

Geochemical mapping of the Nicholls 1:100 000 sheet

by

A. J. Sanders

Abstract

Regolith and geochemical mapping of the NICHOLLS 1:100 000 map sheet is based on regolith characteristics and sampling of regolith at 175 sites, comprising 28 sheetwash samples, 91 stream-sediment samples, 18 soil samples, 37 sandplain samples, and one lake-sediment sample. The nominal sampling density was one sample per 16 km^2. Each sample has been divided into two size fractions: <2 mm – >0.45 mm and <0.2 mm. The former fraction has been analysed for 57 elements after total digest and the latter fraction analysed for 53 elements after partial digest. Conductivity and pH values of the original sample are also presented. The distribution of selected elements is shown on spot-concentration maps.

A regolith-materials map has been produced using Landsat imagery, Aster imagery, aerial photography, and sample-site descriptions. Fifty-six percent of NICHOLLS is covered with sandplain, which has been divided into three sub-units on the basis of morphology and material. Exposed-regime regolith is the second most common regolith type, and is largely over the ridges of the Oldham and Cornelia ranges that strike northwest over the central part of the map sheet.

Comparison of total and partial digest data has shown that partial digest results are valuable for refining interpretations if the data is properly normalized to take account of variations in pH and organic content of the sample. Partial digest data are best displayed as normalized response ratios.

Regolith chemistry has identified potential areas of mineralization, including the Quadrio Lake – Phenoclast Hill area, which contains previously discovered barite–hematite stockworks with anomalous Au and Sb concentrations. Regolith chemistry suggests extensions to this mineralization towards the north, northeast, and southeast along the trend of the Cornelia Range. In addition, there appears to be a relationship between large regional structures, evident on gravity data, and anomalous regolith chemistry. Additive element-index maps highlight the Quadrio Lake – Phenoclast Hill area and its extensions, and suggest a possible metal zonation along the trend of the Cornelia Range. Other areas that show mineralization potential include the northeast, northwest, and southwest of the project area.

KEYWORDS: Nicholls, Trainor, barite, hematite, mineralization, Quadrio Lake, regolith, geochemistry, Oldham Sandstone, Cornelia Sandstone, Quadrio Formation.

Introduction

Regolith is unconsolidated or indurated weathered rock, including residual and transported material, which can obscure underlying bedrock. Large areas of Western Australia are covered by regolith. An understanding of the distribution of regolith and its chemistry offers significant insight into the nature of the bedrock, including the presence and extent of potentially economic mineralization.

Geochemical signatures of the underlying bedrock may be differentially enriched or diluted due to regolith-forming processes. Thus an understanding of regolith formation and the behaviour of elements in the regolith environment are useful mapping and exploration tools.

Regolith and geochemical mapping of the NICHOLLS* 1:100 000 map sheet is a trial project aimed at:

- providing baseline information on the chemistry of regolith to assist mineral exploration;
- identifying and defining specific areas with potential for undiscovered mineralization;

* Capitalized names refer to standard 1:100 000 map sheets, unless otherwise indicated.

- aiding in the identification of rock types and rock assemblages
- reviewing the most appropriate analytical size-fractions for regional geochemical surveys in sand-dominated terrain;
- identifying a range of analytical techniques (total and partial digest) for regional geochemical surveys in sand-dominated terrain; and
- trialling new geochemical processing and display techniques.

The regolith and geochemical mapping of NICHOLLS has many common characteristics with the regional regolith and geochemical mapping program of the Geological Survey of Western Australia (GSWA) that was initiated in 1994. To date, twenty 1:250 000-scale map sheets have been sampled and published in this program, covering parts of the northern Yilgarn Craton, Proterozoic rocks between the Yilgarn and Pilbara Cratons, the Northampton Complex, and areas of the Carnarvon Basin and Albany–Fraser Orogen (Fig. 1). The geochemical sampling of NICHOLLS follows a similar methodology to that of the 1:250 000 sampling with greater emphasis placed on media type and analytical technique in order to refine any future regional-scale sampling programs, particularly in sand-dominated environments.

Location and access

The NICHOLLS 1:100 000 (sheet 3448) is bounded by latitudes 24°30' and 25°00'S and longitudes 122°30' and 123°00"E (Fig. 2; Plate 1), and is the south-eastern 1:100 000 sheet of TRAINOR (1:250 000). The majority of the project area is dominated by sandplain and dune deposits of the Little Sandy Desert and strike ridges of the Cornelia and Oldham ranges. There are no settlements or pastoral leases on the map sheet. A gazetteer of topographic features is presented in Appendix 1.

Principal access to the project area is via a graded track from Sunday Well on Glenayle Station (on GLENAYLE) to the Trainor 1 stratigraphic well site of central-north NICHOLLS (Stevens and Adamides, 1998). The track is susceptible to washouts and inundations with loose sand making travel difficult in places. Access to Glenayle Station is via graded shire roads from the township of Wiluna.

Complex dune deposits, vegetation, and deep drainage incisions, both in the sand plain and along the slopes of the Cornelia and Oldham ranges, hinder access to the remainder of the project area. Easiest access is usually in the interdune areas, parallel with longitudinal dunes where near-surface iron-rich duricrust forms a pavement, or along the crest or base of the strike ridges.

Climate and vegetation

The climate on NICHOLLS is arid with a low and irregular rainfall. There are no meteorological stations, and climatic information is inferred from recordings made in nearby areas. Annual rainfall is between 100 and 300 mm, and in January the daily maximum temperature is 36–39°C with a minimum of 21–24°C. In July the daily maximum is 21–24°C with a mean daily minimum of 3–6°C*.

NICHOLLS largely lies in the Keartland Botanical District of the Eremean Botanical Province (Beard, 1974, 1990). The sand and dune-dominated areas are characterized by mixed shrubs of mainly *Acacia* and some *Hakea* species, with widespread spinifex cover (*Triodia* and *Plectrachne*). The upland slopes of the Oldham and Cornelia ranges are thickly covered with mulga scrub (*Acacia aneura*) in places, whereas the salt-lake dominated lowlands support saltbushes (*Atriplex*) and samphire (*Arthrocnemum*). Scattered desert oaks (*Allocasuarina decaisneana*) grow along calcreted palaeodrainage lines.

Physiography

Central NICHOLLS is dominated by the northwesterly trending Cornelia and Oldham ranges, which rise over 100 m above the surrounding plains. The southern margin of the sheet is characterized by boulder-strewn hills and breakaways, and in the north by scattered hills, some steeply incised. These elevated outcrop areas are interspersed with well-vegetated dune and sandplain deposits of the Little Sandy Desert. Dune types range from northwest-oriented longitudinal dunes, through to chain and net-like complexes. Longitudinal dunes are up to 15 km long and reach a maximum height of 10–12 m. In low-land areas and areas with rocky hills and ranges, chain and net-like dunes predominate, their formation probably caused by turbulent wind conditions. The northeast low-lands on NICHOLLS are characterized by a chain of lakes that form the terminus of the east- to northeast-sloping Ilgarari Palaeodrainage Basin (Williams, 1995). Upslope, the lake systems grade into broad, valley calcrete-filled palaeodrainages, now typically inundated with sand and dune deposits.

Topographic and remote-sensing datasets

Topographic information used on accompanying maps was obtained from the Department of Land Administration (DOLA) and Australian Land Information Group (AUSLIG). Sources include the WARBURTON (1:1 000 000) topographic map (1977), the TRAINOR (1:250 000) topographic map (1985), Landsat Thematic Mapper imagery (1994), Aster satellite imagery (2000), and 1:50 000-scale black and white aerial photographs (1995). Bouguer gravity data were acquired in 1995 for the central and western parts of the sheet as preliminary work before locating and drilling the GSWA Trainor 1 stratigraphic drillhole in the central north of NICHOLLS (Daishsat Proprietary Limited, 1995; Stevens and Adamides, 1998). The Water and Rivers Commission provided information on water bores on NICHOLLS and these are outlined in Stevens and Carlsen (1998, table 6.1).

* Climate data from Commonwealth Bureau of Meteorology website, 2002.

Geology

Geological setting

NICHOLLS lies in the eastern part of the northwestern Officer Basin in central Western Australia (Fig. 1). The northwestern Officer Basin is adjoined to the north by the Palaeoproterozoic Rudall Complex and Mesoproterozoic Yeneena Basin, to the west by the Mesoproterozoic Collier Basin, and to the south by the Palaeoproterozoic Earaheedy Basin. To the east, the Officer Basin is concealed beneath the Phanerozoic Gunbarrel Basin. The northwestern part of the Officer Basin is further subdivided into four Neoproterozoic subareas: the Gibson, Wells, and Blake Sub-basins, and the Trainor Platform (Hocking, 1994; Tyler and Hocking, 2001).

The northwestern part of the Officer Basin was originally regarded as the eastern part of the Mesoproterozoic Bangemall Basin (Daniels, 1975; Williams et al., 1976; Muhling and Brakel, 1985), although Grey (1978) inferred a younger age based on stromatolites. The Oldham and Cornelia ranges, which outcrop on NICHOLLS, were regarded as an inlier of older Proterozoic rocks. After discovery of an apparent unconformity within the rocks assigned to the Bangemall Group, and the recognition of glacigene sedimentary rocks that confirmed the Neoproterozoic age of the rocks above the unconformity, the area was elevated to separate basin status, termed the 900–600 Ma Savory Basin (Williams, 1987; Williams, 1992). Williams (1992) suggested that rocks of the Savory Group were deposited in a sag basin that developed marginal to the Capricorn Orogen, the site of the collision between the Archaean Pilbara and Yilgarn Cratons at c. 1830 Ma (Tyler et al., 1998; Occhipinti et al., 1999).

Although elevated to separate basin status, recognition of bio- and lithostratigraphic similarities between the Savory, Officer, and Amadeus Basins lead to the conclusion that all were essentially coeval, and probably linked under Phanerozoic cover (Grey, 1978, 1995; Williams 1992, p. 9). Hocking (1994), reassigned the Phanerozoic rocks in the Officer Basin, namely the Table Hill Volcanics and above, to the overlying Gunbarrel Basin.

Correlations between major Neoproterozoic basins of central Australia by Walter and Gorter (1994, fig. 1), Walter et al. (1995), and Grey (1995) suggest deposition commenced in a single large sag basin after 850 Ma, termed the Centralian Superbasin, which includes the Officer, Savory, Amadeus, Ngalia, and Georgina (part only) Basins. This superbasin was disrupted by uplift during the Paterson Orogeny (or Petermann Ranges Orogeny of central Australia; Walter et al., 1995) between 560 and 525 Ma, with separate depocentres forming in each of the basins. Walter and Gorter (1994) and Walter et al. (1995) recognized four major successions in the superbasin, referred to as Supersequences 1 to 4.

After mapping in the Paterson Orogen, Bagas et al. (1995) proposed that the Tarcunyah Group in the northeast of the area is a correlative of the lower Savory Group and that both are equivalent to Supersequence 1 of the Centralian Superbasin, and hence part of the Officer Basin. The argument was strengthened by detailed seismic interpretation (Perincek, 1996), as well as stromatolites and palynology, which led some workers to use the name Savory Sub-basin to indicate its position as a subcomponent of the Officer Basin (Grey and Cotter, 1996; Grey and Stevens, 1997; Stevens and Grey, 1997).

Bagas et al. (1999) suggested that the terms Savory Basin and Savory Sub-basin should be abandoned because the area is strictly not a separate basin or sub-basin, but simply the northwestern portion of the Officer Basin where there is no Phanerozoic cover, and hence should be referred to as the northwestern Officer Basin. They also abandoned the 'Savory Group' after recognizing a major hiatus of 150 to 200 m.y., replacing it with the Sunbeam Group (lower sequence) and the Disappointment Group (upper sequence). The Skates Hills Formation of the Sunbeam Group, which outcrops in the east and central north of NICHOLLS, includes the stromatolitic assemblage, *Acaciella australica*, and can be confidently assigned to Supersequence 1 (Grey, 1995). However, below the Skates Hills Formation, the assignment of the Brassey Range Formation to the lowermost successions of the Sunbeam Group is not unequivocal. Hocking and Grey (2000) recognized a problem with the westward palaeocurrent patterns for the Brassey Range Formation, where younger sequences are dominated by northerly trending palaeocurrent patterns. This, in conjunction with significant dolerite intrusions into the Brassey Range Formation, which are suggested to be correlatives of 1080 Ma dolerites of the western Edmund and Collier Basins (Wingate, 2002), led Hocking and Jones (2002) to include the Brassey Range Formation in a new group, the Salvation Group. The extent, age, and possible correlatives of the Salvation Group are uncertain, although it pre-dates the Centralian Superbasin and is either coeval with or slightly younger than the Collier Group (Hocking, R. M., 2002, written comm.).

The Ward and Oldham Inliers (Williams, 1992) form basement highs in the eastern parts of the northwestern Officer Basin and contain rocks formerly included in a single unit, the Cornelia Formation (Brakel and Leech, 1980; Williams, 1990, 1995). The unit is now subdivided into the steeply dipping, shale-dominated Quadrio Formation and Cornelia Sandstone, and the juxtaposed, moderately dipping Oldham Sandstone (Hocking et al., 2000a). Although these formations have not been dated, it appears that the Quadrio Formation and Cornelia Sandstone are older than the Oldham Sandstone because they dip more steeply, are relatively more tightly folded, and show a greater degree of silicification and quartz stockworking. The Quadrio Formation and Cornelia Sandstone possibly correlate with the early Mesoproterozoic Edmund Group of the Edmund Basin, and the Oldham Sandstone with the late Mesoproterozoic Collier Group of the Collier Basin (Martin et al., 1999; Hocking et al., 2000b). However, the Quadrio Formation and Cornelia Sandstone also resemble shale and sandstone units included in the Mesoproterozoic to Neoproterozoic Throssell Group of the Yeneena Basin (Hocking et al., 2000b), or could be equivalents of the Palaeoproterozoic Earaheedy Group (Hocking, R. M., 2002, written comm.). If the latter is the case, then the younger Oldham Sandstone

may actually be an Edmund Group equivalent and the overlying Brassey Range Formation a Collier Group equivalent (Hocking, R. M., 2002, written comm.). Further detailed mapping of the area is required to resolve these issues.

Simplified geology

The geology on NICHOLLS has been divided into seven lithological units, which form the basis for the assignment of geological codes in the accompanying datafiles NICHTOT.CSV and NICHPART.CSV. The simplified stratigraphy and descriptions for these units are presented in Table 1, Figure 2, and Plate 1.

The Quadrio Formation, which dominates northern Nicholls, is a steeply dipping, shale dominated-unit. Around Quadrio Lake it consists of ferruginized shale and siltstone that grades into banded and laminated chert in a prominent northwesterly trending ridge north of the lake. Above the chert are siltstone and sandstone units that are interpreted as coarsening-upward cycles laid down in offshore to foreshore shallowing-up episodes (Hocking et al., 2000b).

Differentiation of the Oldham and Cornelia Sandstones is based on changes in bedding characteristics and in magnetic character along the northern arm of the Oldham Range, which coincide with a fault. The more southerly Oldham Sandstone is a typically silicified, cross-bedded, and rippled quartz sandstone commonly dipping 15–20° to the southwest, with a highly magnetic signature. The Cornelia Sandstone to the north, is a steeper dipping, more intensely silicified and quartz stockworked sandstone, with a more subdued magnetic response. Both units are probably of broad fluvial origin (Hocking et al., 2000a,b, fig. 3). In the northeast of the project area, fault-bounded outcrops assigned to the Cornelia Sandstone include wacke and banded chert units that may be subfacies of the Cornelia Sandstone, or completely separate units whose relationships are yet to be established (Hocking, R. M., 2002, written comm.).

On NICHOLLS, the Oldham Inlier onlaps or is faulted against the Meso- to Neoproterozoic Salvation Group and the Neoproterozoic Sunbeam Group. The Brassey Range Formation (Salvation Group) outcrops in the south as low, rubbly hills and breakaways. The majority of the unit consists of fine- to coarse-grained, quartzose to feldspathic sandstone and siltstone. The Sunbeam Group consists of the shallowly dipping, moderately indurated quartz sandstone, basal conglomerate, and stromatolitic carbonate of the Skates Hills Formation. Stromatolitic carbonate units are common in the east and central north of NICHOLLS, where they outcrop as rugged, incised hills, capped by shallowly dipping quartz sandstone. Significant exposures of basal conglomerate are in the vicinity of Phenoclast Hill, and in the far northwest of the map sheet. Silicified sandstone clasts in the conglomerate were probably derived from the nearby Cornelia and Oldham Sandstones (Hocking et al., 2000a).

Rocks of the McFadden Formation (Disappointment Group) probably lie beneath shallow sand cover in the central north of the map sheet. The unit consists of fine- to coarse-grained sandstone, feldspathic sandstone, quartz wacke, and minor conglomerate and siltstone. The unit was intersected to a depth of 83.1 m in the Trainor 1 stratigraphic drillhole, where it unconformably overlies a mudstone-dominated unit, lithologically similar to the Quadrio Formation (Stevens and Adamides, 1998; Hocking et al., 2000c; Plate 1). However, Hocking (2002, written comm.) points out that due to its similarity with sandstone lenses of the Skates Hills Formation, its

Table 1. Simplified geological interpretation for NICHOLLS

PROTEROZOIC	*Ed*	Fine-grained dolerite dykes and sills, deeply weathered (kaolinized); various ages
Disappointment Group	*EDf*	**McFADDEN FORMATION** Laminated fine- to coarse-grained sandstone, feldspathic sandstone, quartz wacke; minor conglomerate, and siltstone
Sunbeam Group	*ESs*	**SKATES HILLS FORMATION** Stromatolitic dolomite and limestone, fine- to medium-grained sandstone, siltstone, shale; basal conglomerate
Salvation Group	*EVb*	**BRASSEY RANGE FORMATION** Fine- to coarse-grained sandstone and siltstone, quartzose and feldspathic; typically moderately indurated
Collier Group	*EMCo*	**OLDHAM SANDSTONE** Fine- to medium-grained silicified sandstone, siltstone; moderately dipping
Edmund Group	*EMEn*	**CORNELIA SANDSTONE** Fine- to medium-grained intensely silicified sandstone, siltstone, wacke; steeply dipping
	EMEq	**QUADRIO FORMATION** Shale, siltstone, minor sandstone, chert; steeply dipping to subvertical

designation on NICHOLLS as the McFadden Formation is not unequivocal.

Dolerite intrusions of unknown ages and various orientations are common on NICHOLLS, but most exposures are deeply weathered. A series of dominantly north-westerly trending sills are present in the Oldham Range, and narrow northerly to northeasterly trending dykes cut the Brassey Range Formation. Magnetic and gravity data suggest that dolerite sills and dykes are abundant, concealed within the sedimentary units, particularly south of a line that marks the boundary between the Oldham Sandstone and the Cornelia Sandstone ('magnetic terrace' of Hocking et al., 2000a, fig. 3). Narrow, northerly to northeasterly trending dolerites possibly extend along the eastern and northwestern margins of the project area, where they may be, in part, associated with iron-rich regolith units (Plate 2 — *Rf* and *Sf*).

Other recent GSWA work and known mineralization

The Trainor 1 stratigraphic well was drilled by GSWA in 1995 in the central north of NICHOLLS as part of the investigation of the hydrocarbon potential of the interior basins of Western Australia (Stevens and Adamides, 1998; Stevens and Carlsen, 1998; Plate 1). Trainor 1 was drilled to test the source-rock potential of the Neoproterozoic Skates Hills Formation and was fully cored from 5.8 m to its total depth of 709 m. The drillhole encountered flat-lying mudstone, sandstone, carbonate, and conglomerate from 9.1 to 83.1 m of the ?McFadden Formation (see **Simplified geology** above). Below 83.1 m is a moderately dipping, mudstone-dominated succession lithologically similar to the Quadrio Formation. No hydrocarbons were encountered in either unit, but minor amounts of hematite, pyrite, barite, and rare chalcopyrite were present in hydrothermally altered dark-grey mudstone in the lower unit (Stevens and Adamides, 1998). The drillcore is available for inspection, and is stored by GSWA in Perth.

Subsequent investigations of the geology in the vicinity of Quadrio Lake revealed the presence of barite–hematite stockworks containing anomalous quantities of gold, manganese, arsenic, and antimony (Hocking et al., 2000c). The mineralization is in the shale-dominated Quadrio Formation and was initially traced for about 2 km along the southern edge of Quadrio Lake. Further investigations carried out during this study reveal that the barite–hematite vein mineralization extends for at least 6 km between Quadrio Lake and Phenoclast Hill, and is typically orientated between 220 and 270°, with veins up to 50 cm across (Plate 1). The host rock near the veins is typically bleached, and silicified, and contains multiple silica-filled hairline fractures indicative of hydraulic fracturing (Hocking et al., 2000c).

Strontium isotope data (Hocking et al., 2000c) suggest that the deposition of barite occurred in an intracratonic environment. This is consistent with an intracratonic setting of the region, in which a Mesoproterozoic anoxic depositional setting is implied by the composition of the host rocks (shale and siltstone of the Quadrio Formation). This tectonic setting led Hocking et al. (2000c) to propose a sedex-style of mineralization based on the sedex-style sulfide deposits described by Goodfellow et al. (1993). Possible feeder channels include major faults and shear zones that are evident on gravity data such as those beneath the Cornelia Range. Hocking et al. (2000c) also propose other possible mineralization styles, including that of an intrusion-centred deposit, which is considered possible based on the gravity low immediately south of Phenoclast Hill.

Regolith sampling

Regolith sampling on NICHOLLS was carried out over two three-week periods (September–October 2000 and May–June 2001) by a two-person sampling team comprising a field assistant and geologist using a 4WD vehicle. At each sample site (Plate 1), characteristics of the regolith and surrounding geology were recorded on a standard form, presented in Appendix 2. Selection of sample sites made use of Landsat imagery and was based on a nominal 4 × 4 km grid, endeavouring to select the most representative material from the area. To this end, stream sediments with a catchment largely contained within the 4 × 4 km area were the priority sample media. In addition, certain regolith materials were more sought after as a sampling media than others. For instance, iron-rich duricrusts, with their established ability to concentrate trace elements (Butt et al., 2000), were targeted for sampling where appropriate, especially in sand-dune dominated terrains such as on NICHOLLS, where duricrust pavements are exposed in swales in places. The full approach to regolith sampling is discussed in Appendix 2.

Regolith-materials mapping

A regolith-materials map (Plate 2) has been produced for NICHOLLS using Landsat imagery, Aster imagery, 1:250 000 geological mapping of Williams (1995), aerial photography, and field observations recorded at each sample site (Appendix 2).

The regolith-materials map follows the current GSWA regolith-materials mapping scheme (Hocking et al., 2001). The assigned regolith codes for each sample on NICHOLLS are listed in the accompanying datafiles (NICHTOT.CSV, NICHPART.CSV) and these codes are described on Plate 2. Table 2 summarizes the occurrence of regolith units by area, sample type, and number of samples per regolith-materials division. A generalized version of the regolith-materials map is presented in Figure 3.

Major features of regolith on NICHOLLS are:

- low exposed-regime regolith and locally derived products associated with the Quadrio Formation, typically exposed in topographically low areas in the north;
- exposed-regime regolith, breakaways and locally derived products associated with the rugged and rubbly Skates Hills and Brassey Range Formations;

Table 2. Regolith units by area and number of samples

Regolith code	*Area (km²)*	*Percentage of total area*	*Number of samples*	*Percentage of total samples*
Residual				
Rf	70	2.5	16	9.1
Rk	0.26	0.01	0	0
Rl	7	0.2	1	0.6
Total	**77**	**2.7**	**17**	**9.7**
Exposed				
Xkc	24	0.9	2	1.1
Xls	31	1.1	5	2.9
Xls_m	22	0.8	7	4
Xls_s	18	0.6	2	1.1
Xmh	7	0.3	2	1.1
Xqs	37	1.3	3	1.7
Xqz1	302	10.8	8	4.6
Xqz2	147	5.3	4	2.3
Total	**588**	**21.0**	**33**	**18.8**
Colluvial				
Cf	10	0.3	1	0.6
Ck	8	0.3	2	1.1
Cl	114	4.1	11	6.3
Cq	129	4.6	10	5.7
Total	**261**	**9.3**	**24**	**13.7**
Low-gradient slope (sheetwash)				
Wd	118	4.2	11	6.3
Total	**118**	**4.2**	**11**	**6.3**
Alluvial				
A_c	36	1.3	37	21.1
A_d	30	1.1	1	0.6
A_dk	1	0.03	0	0
A_v	17	0.6	3	1.7
Total	**84**	**3.03**	**41**	**23.4**
Lacustrine				
L_l	44	1.6	3	1.7
L_m	62	2.2	3	1.7
Total	**106**	**3.8**	**6**	**3.4**
Sandplain				
Sd	1 002	35.8	18	10.3
Sf	254	9.1	11	6.3
Sk	311	11.1	14	8
Total	**1 567**	**56**	**43**	**24.6**
TOTAL	**2 801**	**175**	**99.9**	

- exposed-regime regolith and locally derived products associated with northwesterly trending strike ridges of the central Oldham and Cornelia ranges;
- deeply weathered, exposed-regime regolith associated with dolerites in the Oldham Range and Brassey Range Formation;
- narrow alluvial channels incising upland areas and fanning out into footslope sand plains;
- broad lake environments associated with palaeodrainages in the northeast;
- extensive valley calcrete along sand-filled palaeodrainages;
- iron-rich duricrust, forming low mounds and breakaways;
- local areas of sand with ironstone pebble veneer, typically associated with iron-rich duricrusts;
- extensive longitudinal and net-like dune fields (Little Sandy Desert).

Residual- and relict-regime regolith

Residual- and relict-regime regolith on NICHOLLS occupies nearly 3% by area and accounts for nearly 10% of regolith samples. Iron-rich residual-regime units (*Rf*) consist of ferruginous duricrust, with reworked material and overlying sand. They are commonly associated with areas of outcropping or shallowly buried dolerite and as capping to the ferruginized shale units of the Quadrio Formation, typified by arcuate duricrust around the shales bordering Quadrio Lake. The duricrust commonly consists of yellow, brown to black, pisolitic aggregations, and in the north of the sheet the pisolites may contain a shiny secondary siliceous coating. In the north and northwest of the sheet, it is probably extensive below sand cover and is often encountered through shallow digging in dune swales, forming iron-rich pavements within the sand environment. In the northeast part of the project area, a small relict carbonate-rich mound (*Rk*) has developed on the margin of the lake system. Relict carbonate-rich pavements are also thought to underlie some of the sandplain areas of central NICHOLLS, associated with valley calcrete in palaeodrainages and carbonate of the Skates Hills Formation. Mixed residual material (*Rl*) is exposed along the northern flank of the Cornelia Range and consists of cemented conglomeratic colluvium (likely derived from the Cornelia Range), and iron-rich material possibly associated with underlying ferruginized Quadrio Formation shales. A low, fan-shaped mound of mixed cobble and iron-rich material 1.5 km south of Quadrio Lake has also been coded as mixed residual material (*Rl*), and may be associated with the nearby conglomeratic units of the Skates Hills Formation at Phenoclast Hill and underlying Quadrio Formation shales.

Exposed-regime regolith

Areas of exposed bedrock or saprock (*X*) constitute 21% by area, and account for just under 19% of regolith samples collected on NICHOLLS. Exposed-regime regolith derived from youngest generation quartz-rich silicified sedimentary rock (*Xqz1*) is the dominant exposed-regime regolith type on NICHOLLS (occupying nearly 11% by area) and is associated with the sandstone strike ridges of the Oldham Range. The second most dominant exposed-regime unit is older generation silicified sedimentary rock (*Xqz2*) corresponding with the Cornelia Sandstone (5% by area). Both units owe their aerial extent to a strongly resistant nature, the quartz grains having undergone recrystallization forming an interlocking mosaic (Williams, 1995). In the northeast of the project area, exposed-regime regolith derived from sandstone-

dominated, heterogeneous sedimentary rock (Xls_s) has been tentatively assigned to the Cornelia Sandstone. Its mixed nature, including wacke and banded chert, sets it apart from the remainder of the Cornelia Sandstone (see **Simplified geology**).

Exposed-regime regolith derived from mudstone-dominated heterogeneous sedimentary rock (Xls_m) is largely on northern NICHOLLS, corresponding to the mixed units of the Quadrio Formation. Other than chert interbands, which appear as resistant ridges along the north side of Quadrio Lake, most of the unit is poorly exposed, which reflects the susceptibility to weathering of the dominantly mudstone lithology. Shale fragments are common in low-land, sheetwash and lacustrine environments of the north and suggest the Quadrio Formation, although not always exposed, is probably near surface throughout the lower topographic areas.

Carbonate-rich exposed-regime regolith (*Xkc*) derived from stromatolitic carbonate units of the Skates Hills Formation is common in the central north and along the eastern margin of the sheet. Due to the mixed nature of the Skates Hills Formation, the carbonate-rich unit (*Xkc*) is commonly associated with exposed-regime regolith derived from heterogeneous sedimentary rock (*Xls*), the parentage of which include, sandstone, siltstone, shale, conglomerate, and evaporite. The units are most prominent at Phenoclast Hill (*Xls* — largely basal conglomerate), and in the rugged hills 4 km to the northeast (*Xkc*, *Xls* — largely sandstone).

Quartz-rich exposed-regime regolith derived from sedimentary rocks (*Xqs*) is most common in the south of NICHOLLS, associated with low rubbly hills and breakaways of the Brassey Range Formation.

Exposed-regime regolith derived from dolerite sills (*Xmh*) is most common in the Oldham Range and in the Brassey Range Formation, where it is interlayered with regolith derived from silicified quartz-rich and quartz-rich sedimentary rocks (*Xqz1, Xqs*). The material is mostly kaolinized with little original fabric remaining.

Colluvial and low-gradient slope regolith

Colluvial (*C*) regolith occupies just over 9% of the project area and accounts for approximately 14% of regolith samples collected. Quartz-rich colluvium (*Cq*) is the dominant colluvial unit on NICHOLLS, found largely along the slopes of the Oldham and Cornelia ranges and in rubbly outcrops of the Brassey Range Formation. Heterogeneous colluvium (*Cl*) is distributed throughout the project area and results from input of mixed material. Along the footslopes of the Oldham Range, heterogeneous colluvium is a mixture of quartz- and ferromagnesian-rich detritus from sandstone and dolerite input respectively. In other areas, heterogeneous colluvium includes various proportions of quartz-, iron-, feldspathic- and carbonate-rich material depending on the upslope lithology. Carbonate-rich colluvium (*Ck*) is limited to the central north and east of the project area on the slopes and depressions bounding exposures of stromatolitic carbonate of the Skates Hills Formation. There are pockets of iron-rich colluvium (*Cf*), associated with iron-rich duricrust (*Rf*) around Quadrio Lake, and also in the southwest and northeast of the map sheet.

Undivided low-gradient slope material or sheetwash (*Wd*) accounts for just over 4% of regolith on NICHOLLS and approximately 6% of regolith samples collected. The unit is common along the low-gradient footslopes of the Oldham Range and in broad lowlands between Quadrio Lake and the Cornelia Range. In the east, this unit is associated with low outcrops of the Skates Hills Formation and manifests as vegetated depressions within the dominant sandplain environment. In places, the low-gradient sheetwash material progressively grades into undivided sandplain (*Sd*).

Alluvial regolith

Alluvial regolith (*A*) constitutes just over 3% by area of NICHOLLS and accounts for just over 23% of regolith samples. Along the flanks of the Oldham and Cornelia ranges and the rubbly hills of the Brassey Range Formation, there are periodically active channels (A_c). Although this unit constitutes only about 1% of regolith on the map sheet, it accounts for 21% of samples collected. The relatively high proportion of samples in this regime reflects the sampling priority for stream sediments (see **Appendix 2**). Where alluvial channels (A_c) leave the sloping uplands and enter flatter sand-dominated units, they commonly form alluvial fan or floodout deposits (A_v), the water eventually being fully absorbed by the sand. In a number of areas, active drainage (A_c) and sand-filled older generation drainage (*Sk* — see below) grade into broad, shallow alluvial depressions (A_d). The density of vegetation in the shallow alluvial depressions (A_d) suggests the soil remains damp throughout much of the year. Perhaps the shallow substrate (possibly shale) forms a barrier to water penetration causing greater saturation of the overlying regolith. In the northeast of the project area, a number of calcrete mounds follow recent alluvial depressions (A_dk).

Lacustrine regolith

Lacustrine regolith (*L*) is dominant in the northeast portion of the project area. It accounts for just under 4% by area of regolith on NICHOLLS and over 3% of the regolith samples collected. The majority of lacustrine regolith is within the main Ilgarari and Disappointment palaeo-drainages, and probably formed in small subdepressions in the palaeoslope, over a low permeability substrate. It is common to find ferruginized shale fragments at shallow depth in these lake environments. Playas and lakes (L_l) largely remain damp year round or contain shallow water, as is the case at Quadrio Lake, where several centimetres of fresh water commonly lie above brackish water. Dune and playa terrains (L_m) surround the lakes and contain partly consolidated clay, silt, sand, and evaporitic material.

Sandplain regolith

Sandplain (*S*) regolith is the most common unit on NICHOLLS, occupying 56% by area and accounting for

just under 25% of samples. Sandplain is characterized by a mixture of eolian, colluvial, and residual sand, and has been split into undivided sandplain (*Sd* — 36% by area), sandplain with an iron-rich pebble or granule veneer (*Sf* — 9%), and carbonate-rich (calcrete) dominated sandplain (*Sk* — 11%). At the footslopes of the Cornelia and Oldham ranges there tends to be a rapid change from the exposed and colluvial environments to flat-lying sand-dominated environments, suggesting the major trunk valleys are progressively filling with mobile sand.

Through central NICHOLLS, the dominant unit assigned as sandplain (*Sk*) actually represents an earlier generation of drainage and the unit is characterized by calcrete pavements, sandplain, and dunes in trunk depressions between major relief. The general flow direction is interpreted to have been towards the east, the area forming part of the Ilgarari palaeodrainage basin (Williams, 1995). Northeast of the Cornelia Range, the Ilgarari palaeodrainage connects with the northerly trending Disappointment palaeoriver (van de Graaff et al., 1977). The depression is now inundated with sand.

Sandplain with iron-rich pebble or granule veneer (*Sf*) is scattered throughout NICHOLLS, largely associated with iron-rich duricrust (*Rf*). The unit is well developed in the southwest associated with the Brassey Range Formation rocks and dolerites, and the pattern extends to the south onto STANLEY (1:250 000; Morris et al., 2000a). Field observations indicate that small iron-rich clasts (many of which are magnetic) are abundant above and within red quartz sand, and probably concentrate at the surface through wind deflation. The slope relationships between duricrust (*Rf*) and iron-rich sandplain (*Sf*), particularly on STANLEY (1:250 000; Morris et al., 2000a), suggest the iron-rich clasts may have both a residual and colluvial origin. In the dominantly sand-dune terrain of north and northwest NICHOLLS, iron-rich sandplain has developed where iron-rich duricrust juts through the sand cover, or iron-rich duricrust pavements are at shallow depth beneath the dunes, commonly exposed in the swales. In the southwest of the project area, a tongue of iron-rich sandplain (*Sf*) has encroached from the west. The iron-rich clasts are likely to have been derived from the residual capping on dolerites exposed to the west of the sheet. This pattern is well documented on STANLEY (1:250 000), where iron-rich sandplain has a shallow-angle colluvial relationship with iron-rich duricrust and dolerite (Morris et al., 2000a, fig. 53).

Undivided sandplain (*Sd*) is distributed throughout NICHOLLS. It is characterized by broad sandplains, and extensive longitudinal, chain, and net-like dune complexes. On STANLEY (1:250 000), areas dominated by dunes are coded as eolian (*E* — Morris et al., 2000a), and largely correspond with the southern extent of the Little Sandy Desert. On NICHOLLS, the complexity of differentiating colluvial, eolian, and residual sands made it more appropriate to combine the units (undivided) and the extent of eolian deposition is marked by the position of dune crests (Plate 2). The composition of the unit varies across the project area and is largely dependent on the nearby lithology and mechanical processes. The unit mainly comprises red sand, with variable proportions of clay, coarse white quartz grains, dark magnetic fragments, and lag. Dune sands tend to be finer and better sorted than those encountered in the swales, and typically lack clay and lag content. Site observations and Landsat data suggest the unit is fine-grained and quartz-rich in the central south, and tends to be more mixed (including greater portions of iron-rich fragments and clay) north of the Cornelia Range.

Sampling and new analytical techniques

Twenty programs at 1:250 000-scale have been completed in the GSWA regional regolith and geochemical mapping program. This program has been responsible for stimulating a diverse range of exploration in Western Australia, such as in the Byro Group on GLENBURGH (1:250 000; Sanders et al., 1998), the Byro Group, Gearle Siltstone and Windalia Radiolarite on WINNING POOL – MINILYA (1:250 000; Sanders and McGuinness, 2001), and the Glenayle Dolerites of northwest STANLEY (1:250 000; Morris et al., 2000a). In most cases, the program has shown good correlation between bedrock type and regolith chemistry, and between known mineralization and regolith chemistry (Kojan et al., 1996; Butt and Scott, 2001; Morris and Sanders, 2001). An exception to this is the suppression in trace element response in certain regolith types, particularly those dominated by sand of eolian, fluvial or colluvial origin such as on central AJANA (1:250 000; Sanders and McGuinness, 2000), central WINNING POOL – MINILYA (1:250 000; Sanders and McGuinness, 2001), the eastern Fraser Range region (Morris et al., 2000b), and north-eastern STANLEY (1:250 000; Morris et al., 2000a). Large areas of Western Australia are covered with such regolith, so GSWA has considered ways of modifying the approach to regolith sampling in such areas to overcome this problem.

New methods trialled by GSWA for regional-scale sampling in sand-dominated environments include shallow augering and targeting of 'windows' in the sand environments to sample more geochemically responsive regolith types such as iron-rich duricrust material. These units concentrate trace elements from surrounding sources and are thereby useful for regional-scale work (Butt et al., 2000; Cornelius et al., 2001). Remotely sensed data including Landsat TM ratios and digital elevation models are useful in targeting these 'windows'. However, this approach is not suitable in all areas, and augering is significantly more time consuming than simple surface sampling.

Although a nominal 4 × 4 km grid may not always produce the best type of sample, consistent sampling across the area produces a complete gravity dataset, and a complete set of regolith samples across the project area. Although some of these samples may not be ideal for a total digest analytical approach, they may be suitable for new geochemical techniques, such as partial and selective extraction, now being used to explore in deeply covered terrains.

To test the effectiveness of such techniques, a partial extraction approach was applied to samples collected on NICHOLLS, using Genalysis Laboratory Services' Terra-Leach™ (Genalysis code: TL1) partial extraction technique (see **Partial extraction techniques** below) to gather additional geochemical information. The little-explored map sheet with its combination of sand (Little Sandy Desert), outcrop (Oldham Inlier), recent GSWA information (drilling and gravity), and discovery of barite–hematite mineralization with anomalous gold levels provided a suitable test environment. Partial extraction results were compared to those derived from total analysis.

Expanded element suite, analytical methods, and level of detection

In an attempt to improve the information collected in sand-dominated areas, an expanded suite of elements was trialled, along with new analytical methods (total and partial digest techniques), and lower detection levels than previously employed in the regional regolith and geochemical mapping programs. NICHOLLS data includes an element suite of up to 66 elements (raw Batch 1), compared to the typical 48 reported in previous Explanatory Notes (e.g. Sanders and McGuinness, 2001). After ascertaining the effectiveness of certain elements in identifying bedrock and the mineralization at Quadrio Lake, their detection level, and cost, a suite of 57 elements for total analysis and 53 elements for partial analysis was identified. All data in NICHTOT.CSV (results after total digest analysis) have been normalized to the highest detection level in the three batches and recalculated to the same units. The units and detection levels in NICHPART.CSV (results after partial digest analysis) are consistent throughout. The analytical methods, detection level, and units for each batch and method are outlined in Appendix 3.

Sampling

Two size fractions (<2 mm to >0.45 mm and the whole fraction smaller than 2 mm) of a number of samples from the Quadrio Lake – Phenoclast Hill area (Plate 1) were analysed by the total approach to determine which fraction had the greatest discriminating power. Although not included in these notes, the results indicate that for most elements the <2 mm to >0.45 mm fraction had higher metal loadings than the whole fraction, which can largely be attributed to dilution by quartz sand in the <0.45 mm part of the fraction. For the total approach, the analysed size fraction in the three batches presented in NICHTOT.CSV is <2 mm to >0.45 mm, consistent with all GSWA regional geochemical mapping programs except on AJANA (1:250 000; Sanders and McGuinness, 2000) where the whole fraction was analysed.

Some mineral exploration case studies, using Genalysis Laboratories Services' partial extraction technique (Terra-Leach™), have determined that fine-grained material may be the preferred sample fraction in sand-dominated terrain and recommended the <0.075 mm grain size (Genalysis Laboratory Services, 2000). The fines can carry disproportionately higher levels of Fe–Mn oxides and hydroxide species, clay minerals, and organic compounds that can host target sites for weakly bound ions. However, this fraction is typically a small percantage of sand-dominated regolith on NICHOLLS, and in order to balance the need for a fine grain-size against the time required for its recovery, the <0.2 mm fraction (i.e. fine-grained sand, silt, and clay) was sieved out for analysis. Sieving of all samples to obtain the <0.2 mm fraction was undertaken at GSWA's Carlisle depot and the resulting fraction was analysed by Genalysis Laboratory Services' Terra-Leach™ method.

Partial extraction techniques

The application of partial and selective extraction techniques to mineral exploration has been discussed by Mann et al. (1998), Xuequi (1998), Yeager et al. (1998), and Bajc (1998), amongst others. Interest in selective leaches in geochemistry has gained increasing popularity following reported success in locating deeply buried mineralization in Russia (Antropova et al., 1992). Hall (1998) reported that, until recently, few programs had been carried out outside of Russia, probably due to inadequate detection limits and high analytical costs. Both problems have been minimized by the availability of high sensitivity inductively coupled plasma mass spectrometry (ICP-MS) techniques in commercial laboratories, and a number of selective or partial leach approaches have been discussed in the literature including Enzyme Leach (Clarke, 1993) and MMI (Mobile Metal Ion; Mann et al., 1998).

The basis of the selective leaching approach in mineral exploration is to measure the mobile forms of an element that may have migrated from mineralization at depth and become immobilized in the surface environment. Methods for transporting ions from buried mineralization may include diffusion, 'fast-ion migration' (Goldberg, 1998), or rising by action of water or gas (Hall, 1998). There is evidence to suggest that mobile forms of an element may travel through hundreds of metres of overburden, from buried mineralization to the surface (Goldberg, 1998).

In the surface environment, the free ions are attracted to particular host sites, including hydrous Fe and Mn oxides, humic and fulvic components, and clay minerals, often found as colloids (Hall, 1998). The binding mechanisms for elements onto these phases are complex and include adsorption, chelation, occlusion, complexation, and coprecipitation. Certain soil types and horizons have greater metal adsorption capabilities, and this is called the Cation Exchange Capacity of the soil (Hall, 1998).

Although a number of case studies in the literature discuss the successful application of the partial or selective leach approach in identifying buried mineralization, the results tend to be site-specific (Grey et al., 1999), and hence the appropriateness of wide-scale application is in doubt. In general, the techniques suffer from a number of inherent problems arising from the complex nature of host phases, and the varying speciation of mobile elements

(Hall, 1998). The effectiveness of various leachants used by the Geological Survey of Canada and several commercial laboratories has been discussed by Hall et al. (1996a,b). Hall (1998) also discussed the reproducibility of results, and concluded that accuracy was of prime importance in evaluating exploration data, and evaluation of precision should be undertaken from both a field sampling and analytical method perspective.

Problems with selective extraction, such as the readsorption of gold and the related issue of poor precision, are discussed by Hall et al. (1995) and Gray et al. (1998). Both studies point out that the readsorption effects varied for different regolith types, which could result in incorrect interpretation if traverses took in several soil types.

Gray et al. (1999), after comparing a number of selective extraction techniques, suggested they were of limited value over a total approach in work carried out from seven sites in the Yilgarn Craton. Selective extraction results were site-specific, with variations due to regolith type, groundwater conditions, effects of soil matrix, and relative abundance of carbonates, and Mn- and Fe-oxides. Gray et al. (1999) point out that a selective extraction approach may be useful for refining anomalies expressed in the total digest results.

Cheng et al. (1997) compared till from the Sudbury Basin data analyzed by both conventional total digest and selective partial leaching, the latter designed to extract the metals bound to the soluble organic fraction of humus and the amorphous Fe and Mn oxides. Statistical comparisons showed that the selective leaching method has advantages when used in conjunction with total digest results for refining interpretations of the geology and mineralization.

Dronseika and Evers (2000) argued that partial digest solutions are useful to enhance anomaly contrast in areas of surface or near surface mineralization, and to identify surface anomalies over areas of buried mineralization that may not be apparent using conventional techniques. They pointed out that selective digests have an optimal operating pH range, and that the recovery of targeted elements may be adversely affected by changing acidity–alkalinity of various soil types. They advocated measuring the pH of each soil solution and adjusting the solution into the target pH range of the selective digest.

Terra-Leach™

Two proprietary Genalysis Laboratory Services Terra-Leach™ extractants were tested (weak acid and weak alkaline) on a number of samples from the Quadrio Lake – Phenoclast Hill area (Plate 1) to determine which produced the greatest geochemical discrimination. Although not included in these notes, the results indicate that the alkaline extractant produced higher metal loadings in a greater number of elements than the acid extractant. However, weak acid digest, although not as consistently responsive, did show sharp discrimination close to barite–hematite mineralization for elements such as As, Au, Pt, and Ni. Due to cost constraints, only the weak alkaline digest (Genalysis code: TL1) was used for the regional 4 × 4 km samples collected across the project area. This TL1 digest is a weak alkaline/cyanide digest with an ICP-MS, inductively coupled plasma optical emission spectrometry (ICP-OES), or atomic absorption spectrometry (AAS) finish and has three main targeted functions, namely:

- to desorb negatively charged species (anions, oxy-anions) by anion exchange with hydroxyl ions;
- to dissolve the humic acid phase; and
- to release precious metals (cyanide complexing).

In most cases the organic phase is a key host for mobile ions, which are released in the digestion of the humic components and measured in solution. Furthermore, soil particles may have a net negative charge, to which cations will be attracted. Above the cation layer another layer composed of anions and oxyanions (e.g. MoO_4^-) may form, and these weakly adsorbed species are exchanged with hydroxyl ions and measured in solution (Genalysis Laboratory Services, 2001, written comm.).

Quality control and analysis

One hundred and seventy-five regolith samples from NICHOLLS were analysed for inclusion in these notes. These samples were analysed after both total* and partial digestion, in three separate batches each, by Genalysis Laboratory Services. These batches consisted of 28 sheetwash samples, 91 stream-sediment samples, 18 soil samples, 37 sandplain samples, and one lake-sediment sample. In addition, 24 laboratory replicates (i.e. aliquot of the same pulp or sample) and 16 analyses of three GSWA standards were made through the three batches.

The results from the quality control samples are presented as a series of digital tables (in .CSV format) in Appendix 3. A discussion of sample preparation, analytical techniques, and quality-control procedures is presented in Appendix 2. Final analytical data are presented as two digital files: total digest results (NICHTOT.CSV) and partial digest results (NICHPART.CSV). Selected elements are displayed as spot-concentration plots (Figs 4–61) and all elements are presented as spot concentration plots (.pdf format) in Figures 4–61 and 70–119 on the disk accompanying these notes.

Standard and replicate analysis

For the total digest analytical techniques, a total of three blank analyses, 60 analyses of both Genalysis Laboratory in-house standards and international standards, nine GSWA reference materials (three types), and 13 repeats of GSWA samples were carried out, spread across the three batches. These data and comments on precision and accuracy are supplied as digital tables on the disk accompanying these notes (App3_2.csv).

* Throughout these notes the term ‘total digestion’ implies near total dissolution.

For the partial digest analytical techniques, a total of four blank analyses, 14 analyses of Genalysis and international standards, seven GSWA reference materials (three types), and 11 repeats of GSWA samples were carried out, spread across the three batches. These data and comments on precision and accuracy are supplied as digital tables on the disk accompanying these notes (App3_3.csv).

Analyses of blanks, GSWA standards, Genalysis standards, and replicates generally complied with the quality-control requirements set out in Appendix 2. Two of the three GSWA standards (IQC45 and IQC47) were acceptable in terms of both precision and (for most components) accuracy, compared to consensus values reported by Morris (2000). No consensus values are currently available for one of the GSWA standards (Bunbury Basalt).

Repeat analysis of samples with high analyte concentrations

Seven sample pulps showing relatively high total digest concentrations of one or more analytes and eighteen samples with relatively high partial digest concentrations of one or more analytes were re-analysed by Genalysis Laboratory Services. The relative differences between the two determinations (HRD: Appendix 2) were generally acceptable except for the inability to reproduce a high partial Ag value (GSWA 152140: 124.6 ppb, 2.5 ppb), elevated partial Au value (GSWA 152162: 1.58 ppb, 0.03 ppb) and an elevated partial Zn value (GSWA 176957: 5139 ppb, 790 ppb). The latter analysis is that included in the final datafile (NICHPART.CSV) as the initial high concentration was not repeatable on further testing. The large discrepancy in the Ag after value for GSWA 152140 is probably due to contamination, although the sample is from the northeast of the project area, which shows elevated concentrations of elements for both total and partial determinations (see **Discussion of data**). Results and comments for all repeat analyses are presented as digital tables in Appendix 3 (App3_4.csv).

Partial digest further work

Checks on high values recorded from the partial digest technique were largely reproducible with the exception of the high Ag, Au, and Zn values discussed above. A group of samples (GSWA 152174, 152190, 176925, 176966, and 176967; Table 3) returned high concentrations for most elements. Re-analysis of these samples replicated the elevated values, suggesting the high concentrations cannot be assigned to analytical error. One explanation for the high concentrations is the effect of rainfall and organic content. Samples 176925, 176966, and 176967 were all collected in the early morning following brief overnight rainfall, and were not sieved on site due to the dampness of the sample. Thus, the rainfall event or lack of sieving may have some influence on the partial extraction results, although other unsieved samples collected after brief overnight rainfall in other areas of the map sheet appear unaffected. Another factor may be the organic content of the samples, as these sites are well vegetated, which may lead to an enhanced humic component, although other well-vegetated sites do not have such elevated analyte concentrations. Alternatively, the increased vegetation cover could indicate a higher watertable, facilitating the movement and concentration of mobile ions in the surface environment. A further consideration is that a change of speciation has occurred in the environment or in the sample bag (anaerobic conditions) to forms easily desorbed by the alkaline digest. From pH measurements of the samples there is no evidence to suggest the high recoveries in these samples are related to unusual acidity–alkalinity conditions. Whatever the cause, it seems prudent to treat these samples separately when interpreting the data, either omitting them from the dataset or using ratios to minimize their anomalous effect (see **Element-index and ratio maps**). To better understand these problems a series of checks would be required. These would include compositing a number of samples from an area yielding higher than usual metal loadings before and after rainfall, to ascertain what effect the rainfall and following capillary rise or biological activity may have on elemental concentrations. In addition, organic carbon levels could be used as a normalizing factor for broad-scale comparisons or analysis after pyrophosphate digest to target only the organic phases in the sample.

The acidity–alkalinity of regolith seems to have an influence on the effectiveness of the partial extraction. Correlations of partial digest results (Spearmans rank correlation coefficient — r: App3_5.csv) show that most elements are moderately correlated, in that when any single element is in high concentration, many other elements are also efficiently extracted. The exception is partial digest Ca and measurements of pH, which both have moderately negative correlation with most partial digest elements. The strongest negative correlation is with partial digest Pb (pH spearmans r = –0.64, Ca spearmans r = –0.79). It seems probable that in the higher pH environments (more alkaline), metals are more efficiently 'locked up' in the substrate (e.g. as carbonates or phosphates) and are thereby not as readily available for extraction by the weak TL1 digest, although these metals may be more easily detectable after total extraction. As conditions become more acidic, species may become more mobile (i.e. less well bound to the substrate), and are therefore more readily available for extraction by a weak leachant. It is unclear what form of Ca is being extracted by the TL1 digest in the higher pH samples. Like the other metals, Ca extracted by the weak digest should be an ionic species, although its behaviour is contrary to the other metals, which tend to be at lower concentrations at higher pH. At higher pH levels, Ca should have a greater susceptibilty to being bound, for instance as a carbonate. One explanation is a speciation effect related to the general acidic to neutral soils on NICHOLLS, whereby the carbonate-dominated areas (e.g. calcrete-rich drainages), although still slightly acidic due to subsurface lithologies and mobile sands, have a higher proportion of available Ca . Whatever the cause, it is necessary to account for the influence of pH (or the correlated Ca concentration) when displaying the partial digest results (see **Element-index and ratio maps**), and further work is required on the relationship of regolith, pH, and the efficiency of extractions.

Other trials that may improve future data would be further size-fraction analysis to determine the best compromise fraction for regional-scale partial digest geochemistry. In some trial test cases the coarser fractions carried higher mobile-ion contents (Genalysis Laboratory Services, 2000).

The weak acid digest, although not as consistently responsive as the weak alkaline digest, did show sharp discrimination in some elements in close proximity to barite–hematite mineralization near Quadrio Lake. To this end, further work on the application of the weak acid extractant on NICHOLLS could be warranted.

Differences between batches

Although standard and blank values are acceptable for each batch of data, some between-batch differences are evident for analytes at low concentrations, and those resistant to dissolution. These include the total digest values for Ag, Nb, and Ta, where background concentrations for batch two, largely in the west of the sheet, appear marginally higher than other batches.

Regolith geochemical and geophysical maps

Data presentation styles

Geochemical data collected in the regional regolith and geochemical mapping program has traditionally been displayed as spot-concentration maps where the diameter of the spot is proportional to the measured concentration. However, in areas where subtle differences in concentration may be important (such as sand-dominated environments), different ways of processing and presenting both partial and total data are required.

Cheng et al. (1997), in a comparative study of total and partial data of till collected from the Sudbury Basin, used spot maps, but noted that many partial digest trends are subtle and that spot maps may obscure important trends. The authors described the effectiveness of residual plots, where partial digest data are presented after taking account of the geochemical trends apparent in the total digest results.

Smith and Perdrix (1983) and Smith et al. (1989) have shown how additive indices can be used to highlight areas of mineralization in arid terrains of the Yilgarn Craton. The use of additive indices has been adapted and extended by GSWA for use in the regional regolith and geochemical mapping program and is one way of weighting elements of significance which may be distributed at uniformly low concentration. For example, Kojan et al. (1996) have shown how a greenstone chalcophile index can be used to identify areas of known and potential gold mineralization on SIR SAMUEL (1:250 000). Indices are usually additive (e.g. element a + element b + element c, etc.), but account must be taken of the relative concentration and concentration range of each element. The first step is to log-transform the data, which reduces the effect of extremely high or low values. The transformed data are then standardized, which involves expressing each value as a standard normal deviate, thus allowing direct comparison of elements regardless of concentration (Rock, 1988). The standardized scores are then summed to create an elemental association suite (see **Element index and ratio maps**).

Mann et al. (1998) expressed selective leach data in terms of the element concentration relative to background (response ratio). The background is calculated as the average concentration of the lowest quartile of the data. The advantage of response ratios and standard scores is that data can be compared regardless of concentration. Mann et al. (1998, fig. 2) commonly show their selective leach response ratio results as multi-element stacked bar charts which, like the plotting of element indices, can show multi-element responses in a single figure. For the NICHOLLS partial digest data, additive element indices have been calculated after conversion to response ratios. In addition, the NICHOLLS partial digest data has been normalized to take account of varying organic levels in the sample and effects of soil acidity–alkalinity. For instance, GSWA samples 152174, 152190, 176925, 176966, and 176967 have high concentrations of most analytes. This unusual geochemical signature is unlikely to be controlled by either lithology or mineralization, but may be linked to high levels of organic acid in the sample (see **Partial digest further work** above). A measurement of organic carbon may provide a normalization factor for these effects; however, in its absence it is proposed that another element (typically correlated with organic acid levels) be invoked to normalize the data. If certain element species that are difficult to extract with a weak leachant are elevated, the concentrations present may reflect the scavenging effect of organic acids. Subtracting the response ratio scores of a component thought to be primarily associated with elevated organic acid levels from the response ratio scores of the element of interest may produce more interpretable maps. Furthermore, to minimize the effect of the generally negative correlation between most elements and pH (and Ca), the data can be presented as a ratio to an inverted pH value or Ca concentration (see **Partial digest further work** above).

Selected spot-concentration maps

In light of the above comments, use of spot-concentration maps may not be optimal, especially for partial digest data, but such maps provide a simple illustration of regolith chemistry in relation to geology without too much numerical manipulation. The concentration of 58 total and partial digest components of interest are shown as a series of spot-concentration maps in relation to simplified geology (Figs 4–61). Total and partial digest results are presented together where possible, ordered in terms of total digest major element oxides, then alphabetically by trace element. One-hundred and eight of the 110 analysed elements are also available on the disk accompanying these notes as .pdf files (Figs. 4–61 and Figs. 70–119). Partial digest results for Pd and Pt are not presented because all values are below detection level.

On the spot-concentration maps, the circle diameter is proportional to concentration, with star symbols indicating concentrations at or greater than the 97th percentile. Thus, stars correspond to values that lie either at the end of, or beyond, a normal distribution curve and are designated as anomalous.

For quick reference, samples with an analyte (or analytes) in the top ten concentration range for the map sheet are listed in Table 3 (partial) and Table 4 (total). Data in this table include a simplified geological code, locational data, regolith code, type of sample media, and list of high elements.

Exact element concentrations can be obtained by identifying the GSWA number from the sample-site location plan (Plate 1) and then referring to the digital datafiles (NICHTOT.CSV; NICHPART.CSV). Copies of the 1:100 000-scale element-concentration maps are available from the Department of Mineral and Petroleum Resources' (MPR) Information Centre.

Discussion of data

Regolith pH and regolith conductivity

Regolith over much of NICHOLLS has an acidic to neutral pH, with the exception of some isolated alkaline areas largely associated with calcrete-rich drainages or carbonate units of the Skates Hills Formation (Fig. 62). The most acidic regolith is in the north and south of the sheet, seperated by a band of less acidic regolith, which largely corresponds to the trend of the Oldham Sandstone.

The acidity–alkalinity has a clear effect on the partial digest values and hence an understanding of pH distribution is of fundamental importance in interpreting analytical data (see **Partial digest further work** above and **Element-index and ratio maps** below).

Conductivity values for the project area are below detection level apart from a few values near salt lakes in the southwest, central north, and east.

Gravity and magnetic map

A combined gravity and magnetic image with interpreted structure (Morris et al., in press) is presented as Figure 63. A series of northwesterly trending elongate positive and negative gravity anomalies (colour on Fig. 63) may represent fault-bounded blocks of differing lithology (Shevchenko, S. I., 2002, written comm.). Two low-density, circular features outlined by gravity data are centred just south of Phenoclast Hill (5 km in diameter) and southwest of the Oldham Range (9 km in diameter). These features may represent either low-density felsic intrusions or disaggregated rock from multiple faulting and fracturing, or (more likely) they are salt diapirs ((Shevchenko, S. I., 2000, written comm.). Gravity modelling by Shevchenko (2002, written comm.) suggests that if the southwestern gravity low represents a diapir, the body may be up to several kilometres in width and extend from several hundred metres beneath the surface to a depth of up to 5 km. If the gravity low represents faulting, fracturing or the weathered top of an intrusion, it may be up to 6 km wide and extend from near surface to a depth of nearly 1 km. The outcrop and regolith pattern in the vicinity of the southwestern gravity low (Plate 2) is broadly circular with a central salt lake, supporting the inference that the body may have some near-surface expression.

Total magnetic intensity data (greyscale on Fig. 63) reveal a series of northwesterly trending high-frequency anomalies in the south of the map sheet, previously described by Hocking et al. (2000b). They probably represent dolerite sills in the Oldham Sandstone and Brassey Range Formation, with their absence in the north demarcating the Oldham Sandstone from the Cornelia Sandstone.

Element-index and ratio maps

Three element-index plots have been compiled for total digest data on NICHOLLS. These comprise a chalcophile index (summed standard scores of As, Bi, Mo, Sb, Sn, and W; Fig. 64); base metals index (summed standard scores of As, Cu, Pb, Sb, and Zn; Fig. 65); and a ferro-alloy index (summed standard scores of Co, Cr, Ni, Pd, Pt, and V; Fig. 66).

Two normalized response-ratio plots have been produced for As (Fig. 67) and Sb (Fig. 68) using partial digest data. A chalcophile index (summed normalized response-ratio scores of As, Bi, Mo, Sb, Sn, and W; Fig. 69) has also been generated from partial digest data. Normalized values were generated by subtracting the response-ratio value for Cr (a typically poorly extractable component possibly correlated with organic acid levels; Fig. 33) from the response-ratio value of the element of interest (As and Sb) and dividing by the sample's inverted pH (i.e. a pH of 1 would become 13 and vice-versa).

Chalcophile index

Areas of relatively high chalcophile-index scores include the central north, the northwest, and the northeast of the project area (Fig. 64). Elevated values in the central north relate primarily to anomalous levels of Sb and As in the barite–hematite vein systems in the Quadrio Lake – Phenoclast Hill area (Hocking et al., 2000c). The chalcophile index plot suggests the barite–hematite stockwork may be of greater extent than that recognized in outcrop (Ba occurrence: Plate 1). The elevated chalcophile scores show a northerly trending band that coincides with a gravity corridor extending from the circular gravity low south of Phenoclast Hill to the northern boundary of the map sheet (see **Gravity and magnetic map** above; Fig. 63).

In the northeast, elevated chalcophile scores surround outcrops of the Cornelia Sandstone and Quadrio Formation, suggesting either lithological control on regolith chemistry or mineralization, possibly associated with faulting in the area. Scattered high chalcophile scores

Table 3. Samples with individual or multiple elements with the top ten concentrations after partial extraction

GSWA sample no.	*Easting*	*Northing*	*Regolith*	*Geology*	*Media*	*High analytes*
152102	462566	7259764	A_c	*PMCo*	stream	Ag, Ce, Cr, Cu, La, Ni, Sc, Te, Y, Ca, Dy, Eu, Gd, Nd, Sm
152104	456744	7259284	*Wd*	*PMCo*	sheetwash	Cu, La, Th, Eu, Nd, Sm
152127	451024	7287273	A_c	*PMEq*	stream	Ba, Sb
152129	453656	7282387	*Rf*	*PMEq*	soil	W
152136	481649	7283108	*Sd*	*PMEq*	sandplain	Mo, Y, Dy, Er, Gd, Lu, Yb
152137	483964	7282011	*Cl*	*PSs*	sandplain	U
152138	487194	7280100	*Sk*	*PMEq*	sheetwash	Li, Mg
152141	488629	7277778	*Wd*	*PMEn*	sheetwash	As, Au, Bi, Cr, Cu, Ga, In, Pb, Sc, U, Zn, Zr, Fe, Ge, Lu, P, Si, Yb
152144	470786	7280159	A_d	*PMEq*	sheetwash	Au, Mo, Mg
152151	481972	7273660	*Sd*	*PMEq*	sandplain	Au, Sn
152155	494069	7281403	*Cl*	*PMEq*	stream	Cd
152156	494173	7283251	A_c	*PMEq*	stream	Ag
152159	488382	7287852	*Sk*	*PSs*	sandplain	Li
152165	498628	7283593	A_c	*PMEq*	stream	Mn, P
152167	496767	7284210	A_c	*PMEq*	stream	Mn, P
152170	496960	7275449	*Sf*	*PMEq*	sandplain	Bi, Nb, Sb, Sc, Sn, Ta, W, Zr, Fe, Ti
152171	491275	7275725	*Ck*	*PSs*	sheetwash	Ag, Ca
152173	487964	7272140	L_l	*PMEq*	soil	S
152174	492595	7270770	*Xls*	*PSs*	soil	Be, Bi, Cr, Ga, In, Li, Nb, Sb, Sc, Sn, Ta, U, W, Zr, Al, Fe, Ge, Mg, Si, Ti
152176	495061	7267017	*Xkc*	*PSs*	stream	P
152177	499529	7266383	*Rf*	*PSs*	soil	Sn
152180	487617	7265212	*Sk*	*PMEq*	soil	Ag
152182	496115	7262591	*Xkc*	*PSs*	stream	Bi, Cr, Sn, Zr, Al, Fe, Ge, Si
152185	495372	7253148	L_m	*PMEq*	stream	Mg
152189	493650	7255086	*Wd*	*PMEq*	sheetwash	Au, Co, Tl
152190	492554	7257831	*Wd*	*PMEq*	sheetwash	Ag, Be, Bi, Cr, Cu, Ga, In, Nb, Pb, Sb, Sc, Sn, Ta, U, V, W, Zn, Zr, Al, Fe, Ge, P, Si, Ti, Tl
152191	488931	7259570	*Sk*	*PMEq*	sandplain	Ag, Au
152195	482669	7268690	*Sk*	*PMEq*	sandplain	As, Li
152196	450271	7239474	*Sf*	*PVb*	sandplain	V
152197	453780	7240809	*Sf*	*PVb*	sandplain	Ag
152199	458824	7235553	*Xqs*	*PVb*	stream	Ba
152200	457684	7238735	A_v	*PVb*	sheetwash	As, Ba, Be, Ce, Co, La, Th, V, Y, Zn, Dy, Er, Eu, Gd, Lu, Nd, Sm, Tl, Yb
171409	465444	7281840	*Cl*	*PMEq*	sheetwash	As, Ba
171417	466612	7278804	Xls_m	*PMEq*	stream	Mo, W
171429	464181	7285425	*Cf*	*PMEq*	sandplain	As, Au, Ni, Te, V, Y, Dy, Er, Lu, Yb
171476	468470	7278311	*Cl*	*PMEq*	stream	Cd, Co, S, Zn, Mn
171491	453173	7268498	A_c	*PMCo*	stream	Cd, Ce, La, Y, Dy, Er, Eu, Gd, Nd, P, Sm
171492	453482	7270999	*Xqz2*	*PMEn*	stream	Ce
171493	456957	7273673	L_l	*PSs*	sheetwash	S, Ca, K
171542	478974	7284541	Xls_m	*PMEq*	stream	Be, Bi, Ce, Co, Cr, Ga, In, La, Li, Nb, Ni, Sb, Sc, Sn, Ta, Th, U, W, Zn, Zr, Al, Fe, Ge, K, Mg, Nd, Si, Sm, Ti, Tl
171546	468114	7281889	L_m	*PMEq*	lake	S, Ca, K
171547	470969	7282706	*Wd*	*PSs*	stream	Ca, Mg
171548	473845	7282417	A_c	*PSs*	stream	Cd
171552	478076	7278659	Xls_s	*PMEn*	stream	Pb, Sb
171553	474620	7278561	Xls_m	*PMEq*	sheetwash	S, K
171554	472077	7277664	A_c	*PMEq*	stream	As, Be, Cd, Ce, Cu, La, Mo, Ni, Th, Y, Ca, Dy, Er, Eu, Gd, Nd, P, Sm
171555	469458	7275015	Xls_m	*PMEq*	sheetwash	Au, S, K
171558	458631	7283495	*Sf*	*PMEq*	sandplain	Zn, K, Mg, Tl
171562	452795	7280428	*Sd*	*PSs*	sandplain	Er, Lu, Yb
171563	451187	7278878	*Cl*	*PSs*	sandplain	Ag, Cd, Cu, Ca
171564	455038	7277752	*Sd*	*PMEn*	sandplain	Ba, Lu, Yb
171565	457307	7278676	*Sd*	*PMEq*	sandplain	Be, Li, Zn, Mg, Mn, Tl
171568	462447	7272812	*Xqz2*	*PMEn*	stream	Pb, Mn
171574	477113	7271275	*Wd*	*PMEq*	sheetwash	Pb
171575	475595	7273645	Xls_m	*PMEq*	sheetwash	Ba, Pb
171579	467228	7274146	*Cl*	*PMEn*	sheetwash	As, Cd, Mo
171580	458782	7271818	*Rf*	*PSs*	soil	Mo
171584	463519	7267928	A_c	*PMEn*	stream	Cd, Co, Mn
171586	468294	7263768	*Cq*	*PMEn*	stream	Pb
171589	449895	7273581	*Xqz1*	*PMCo*	stream	Sn
171598	457175	7252983	A_c	*PMCo*	stream	Ni

Table 3. (continued)

GSWA sample no.	Easting	Northing	Regolith	Geology	Media	High analytes
176903	467847	7237978	A_c	*EVb*	stream	W
176911	489910	7238652	*Sd*	*EMCo*	stream	Bi, Ce, Cr, Ga, In, La, Nb, Pb, Sb, Ta, Th, Y, Zr, Al, Dy, Er, Eu, Gd, Ge, Lu, Mn, Nd, Sm, Ti, Yb
176913	493235	7237713	A_c	*EMCo*	stream	Ca
176914	486588	7242599	*Wd*	*EMCo*	sheetwash	Ce, Co, Cu, Ga, In, La, Mo, Nb, Pb, Sc, Ta, Th, U, V, Y, Zn, Zr, Al, Dy, Er, Eu, Fe, Gd, Lu, Nd, P, Si, Sm, Ti, Yb
176917	496307	7241718	Xls_m	*EMCo*	stream	Ba, Mn
176919	497749	7241286	A_c	*EMCo*	stream	Ni, V
176920	482867	7244201	*Wd*	*EMCo*	sheetwash	As, Mo, Te, Ca
176925	467162	7245319	*Xqz1*	*EMCo*	stream	Ba, Be, Bi, Co, Cr, Ga, In, Li, Nb, Ni, Sb, Sc, Sn, Ta, Te, Th, Zr, Al, Fe, Ge, K, Mg, Si, Ti, Tl
176926	463776	7244923	*Sk*	*EMCo*	soil	Ag, Au
176927	462405	7246508	*Sk*	*EMCo*	sheetwash	Ba, Be, Co, Te, U, P, Tl
176928	460274	7245226	*Rf*	*EVb*	sandplain	Au, Ga, In, Li, Nb, S, Ta, Te, V, Al, Ge, Mn, Si, Ti, Tl
176932	452166	7244571	*Cl*	*EVb*	sheetwash	Cu, Th, U
176933	454359	7247044	A_c	*EMCo*	stream	Ba, Y, Dy, Er, Eu, Gd, Lu, Yb
176939	457593	7247542	*Rf*	*EMCo*	sheetwash	S, Te
176940	459374	7249182	L_l	*EMCo*	soil	S, V, K
176943	458572	7251150	*Sf*	*EMCo*	stream	Pb
176944	455874	7249727	*Sd*	*EMCo*	stream	S, W, K
176948	477563	7262487	A_c	*EMEn*	stream	Au
176950	480740	7259821	*Sk*	*EMEq*	soil	Te
176954	479188	7253685	A_c	*EMCo*	stream	W
176957	487627	7250356	*Cl*	*EMCo*	stream	Cd
176962	483487	7247473	*Sd*	*EMCo*	stream	Mn
176964	472170	7250626	A_c	*EMCo*	stream	Ni
176966	462868	7255110	A_c	*EMCo*	sheetwash	As, Be, Bi, Ce, Co, Cr, Cu, Ga, In, La, Li, Mo, Nb, Ni, Sb, Sc, Ta, Te, Th, U, V, Al, Eu, Fe, Gd, Ge, Nd, Si, Sm, Ti
176967	451069	7252332	*Sd*	*EVb*	sheetwash	Ag, As, Be, Bi, Cd, Ce, Co, Cr, Cu, Ga, In, La, Li, Mo, Nb, Ni, Sb, Sc, Sn, Ta, Te, Th, U, V, W, Y, Zn, Zr, Al, Ca, Dy, Er, Eu, Fe, Gd, Ge, K, Lu, Mg, Nd, P, Si, Sm, Ti, Tl, Yb

in the northwest can be attributed to high concentrations of As and Sb in the regolith (Figs 21 and 49). These features are also weakly coincident with a northwesterly trending gravity anomaly (Fig. 63).

Base metal index

High base metal index scores are similar to those of the chalcophile index, although there appears to be an extension of elevated base metal scores on the northern flank of the Cornelia Range, towards the southeast (Fig. 65). This area coincides with the southern flank of an elongate, northwesterly trending gravity anomaly (Fig. 63). The high base metal scores can be largely assigned to the high Pb and As concentrations recorded in regolith along this trend (Figs 42 and 21). Other areas of elevated scores include the northeast of the project area and in the southwest, along the northeast flank of the southern gravity low and in the mixed dolerite and sandstone hills of the Oldham Range.

Ferro-alloy index

The ferro-alloy index (Fig. 66) highlights the southwest of the map sheet and probably reflects exposed and near-surface dolerite intrusions. Another group of less elevated scores is in the southeast of the map sheet, largely associated with mudstone and iron-rich duricrust units along the footslopes of the Oldham Range (Plate 2). Scattered higher ferro-alloy index scores are also in the northeast, central north, and northwest of the project area, but these areas are typically better defined by chalcophile or base metal scores.

Normalized response-ratio plot of arsenic and antimony

Normalized partial digest As (Fig. 67) highlights three main areas, including the faulted Quadrio Formation – Cornelia Sandstone area in the northeast of the map sheet, around the southeastern margin of the gravity low in the southwest of the map sheet, and most prominently around the flanks of the central north gravity low, extending through to the Quadrio Lake area. Another group of scattered high values are at the eastern end of the Cornelia Range, and like the base metals index, may represent a southeasterly extension of elevated values along the northern margin of the ranges. Alternatively, these high values may be a regolith effect, the data normalization not fully compensating for the calcrete-rich, sand-filled palaeodrainages of the area (*Sk*).

Normalized partial digest Sb (Fig. 68) highlights the northeast and northwest of the project area, and

Table 4. Samples with individual or multiple elements with the top ten concentrations after total extraction

GSWA sample no.	*Easting*	*Northing*	*Regolith*	*Geology*	*Media*	*High analytes*
152101	459475	7261725	A_c	*PMCo*	stream	Ag
152102	462566	7259764	A_c	*PMCo*	stream	Al_2O_3, CaO, Ce, Co, Cu, La, Li, Ni, Pd, Pt, Sn, Ta, Y, Dy, Er, Eu, Gd, Nd, Sm, Tl, Yb
152103	460512	7257950	A_c	*PMCo*	stream	TiO_2, Fe_2O_3, MnO, MgO, CaO, Na_2O, K_2O, P_2O_5, Ag, Be, Cd, Ce, Co, Cr, Cu, La, Ni, Pb, Pd, Pt, Rb, Sc, U, Y, Zn, Dy, Er, Eu, Gd, Lu, Nd, Sm, Tl, Yb
152124	461999	7288197	*Rf*	*PMEq*	sandplain	Pt
152125	458543	7286994	*Xls*	*PMEq*	soil	Ag, Au, Pd, Pt
152126	455085	7288447	*Rf*	*PMEq*	soil	Au, Pd
152127	451024	7287273	A_c	*PMEq*	stream	Ag, As, Ba, Li, Pt, Sb, Sr, Te, W, Ge
152128	450041	7285189	*Rf*	*PMEq*	stream	Sb, Sr
152130	458814	7281534	*Rf*	*PMEq*	soil	Zr
152135	481867	7285975	*Sd*	*PDf*	sandplain	SiO_2
152140	496300	7279572	A_c	*PMEq*	stream	Mo, Sb
152141	488629	7277778	*Wd*	*PMEn*	sheetwash	Au, Bi, Sn
152143	480197	7280373	*Sd*	*PSs*	sandplain	B
152152	484845	7275569	Xls_s	*PMEn*	sheetwash	Au
152155	494069	7281403	*Cl*	*PMEq*	stream	TiO_2, MnO, MgO, K_2O, P_2O_5, Ba, Be, Cd, Ce, Co, Ga, In, La, Li, Ni, Rb, Sb, Sn, Te, Y, Zn, B, Dy, Er, Eu, Gd, Ge, Lu, Nd, Sm, Tl, Yb
152156	494173	7283251	A_c	*PMEq*	stream	TiO_2, Al_2O_3, K_2O, P_2O_5, As, Au, Be, Cu, Ga, In, La, Li, Mo, Nb, Rb, Sb, Sc, Sr, Te, U, V, Y, B, Dy, Er, Eu, Gd, Ge, Lu, Tl, Yb
152158	491052	7286380	*Sk*	*PSs*	soil	SiO_2
152159	488382	7287852	*Sk*	*PSs*	sandplain	SiO_2
152162	492708	7288091	*Cl*	*PSs*	stream	CaO
152165	498628	7283593	A_c	*PMEq*	stream	As, Mo, Rb, Sb, Te, Ge
152167	496767	7284210	A_c	*PMEq*	stream	K_2O, Mo, Rb, B, Ge
152170	496960	7275449	*Sf*	*PMEq*	sandplain	SiO_2
152171	491275	7275725	*Ck*	*PSs*	sheetwash	CaO
152173	487964	7272140	L_l	*PMEq*	soil	SiO_2, CaO, S
152174	492595	7270770	*Xls*	*PSs*	soil	Nb
152175	496887	7270348	*Rf*	*PSs*	soil	Nb, Zr
152176	495061	7267017	*Xkc*	*PSs*	stream	MnO, U
152177	499529	7266383	*Rf*	*PSs*	soil	Pd, Pt
152179	489580	7266928	*Sk*	*PMEq*	sandplain	SiO_2
152181	493014	7263334	*Wd*	*PSs*	sheetwash	Ta
152183	496463	7257803	*Ck*	*PSs*	stream	K_2O, Ce, La, Nb, U, Gd, Lu, Nd, Sm, Tl
152185	495372	7253148	L_m	*PMEq*	stream	Ba,Te,Th
152189	493650	7255086	*Wd*	*PMEq*	sheetwash	Au
152190	492554	7257831	*Wd*	*PMEq*	sheetwash	Au
152193	482263	7264216	*Rl*	*PMEn*	stream	As, Au, Cr, Th, U
152194	479283	7266344	Xls_m	*PMEn*	stream	MnO, Nb, Pb
152196	450271	7239474	*Sf*	*PVb*	sandplain	TiO_2, Fe_2O_3, Ag, Au, Cr, Cu, Ga, In, Nb, Pt, Sc, Th, V, W
152197	453780	7240809	*Sf*	*PVb*	sandplain	TiO_2, Fe_2O_3, Ag, In, V
152200	457684	7238735	A_v	*PVb*	sheetwash	TiO_2, Fe_2O_3, Cr, Ga, In, Ta, Te, Th, V
171409	465444	7281840	*Cl*	*PMEq*	sheetwash	Fe_2O_3, P_2O_5, As, Ba, Bi, Ga, In, Pd, S, Sb, Sr, Te, Th, U, W, B, Eu, Ge, Sm
171417	466612	7278804	Xls_m	*PMEq*	stream	P_2O_5, La, S, Sr, Nd, Sm
171429	464181	7285425	*Cf*	*PMEq*	sandplain	Fe_2O_3, P_2O_5, As, Ba, Bi, Mo, Nb, S, Sb, Ta, Te
171476	468470	7278311	*Cl*	*PMEq*	stream	MgO, K_2O, P_2O_5, Ba, Be, Ce, La, Mo, Pb, Rb, S, Sr, W, Y, Zn, B, Dy, Er, Eu, Gd, Lu, Nd, Sm, Tl, Yb
171487	452319	7258967	A_c	*PMCo*	stream	Ag, Co, Cu, Y, Zn, Dy, Er, Lu, Yb
171488	453026	7261305	A_c	*PMCo*	stream	Fe_2O_3, As, Bi, Cr, Ga, In, Mo, Pd, Pt, Sc, Sn, Ta, Te, Th, V, W, Ge
171489	454370	7263930	*Xqz1*	*PMCo*	stream	Al_2O_3, Cr
171490	453088	7266640	*Cq*	*PMCo*	stream	TiO_2, P_2O_5
171491	453173	7268498	A_c	*PMCo*	stream	Sr
171493	456957	7273673	L_l	*PSs*	sheetwash	MgO, Na_2O, S
171541	476404	7286003	*Sf*	*PMEq*	soil	Zr
171542	478974	7284541	Xls_m	*PMEq*	stream	Be, U, W, Y, Zn, Dy, Er, Gd, Lu, Nd, Yb
171543	471428	7286426	*Xls*	*PSs*	stream	Zr
171544	468995	7286947	*Sf*	*PSs*	stream	SiO_2
171545	467835	7284163	*Rf*	*PMEq*	sheetwash	Sb, Zr
171546	468114	7281889	L_m	*PMEq*	lake	Al_2O_3, MgO, CaO, Na_2O, P_2O_5, Ba, Li, S, Sb, Sn, Sr, Sm
171547	470969	7282706	*Wd*	*PSs*	stream	MnO, Ce, Nb, Pb, Pt, Y, Dy, Er
171548	473845	7282417	A_c	*PSs*	stream	Ce

Table 4. (continued)

GSWA sample no.	Easting	Northing	Regolith	Geology	Media	High analytes
171552	478076	7278659	Xls_s	*EMEn*	stream	MgO, K_2O, Cd, La, Rb, Nd
171553	474620	7278561	Xls_m	*EMEq*	sheetwash	MgO, Na_2O, Ba, Bi, Cd, S, Sr
171554	472077	7277664	A_c	*EMEq*	stream	Li
171555	469458	7275015	Xls_m	*EMEq*	sheetwash	Al_2O_3, MnO, MgO, Na_2O, K_2O, Au, Ba, Be, Bi, Ce, Co, Cu, Ga, La, Li, Ni, Rb, S, Sc, Sn, Sr, Ta, U, W, Y, Zn, B, Dy, Er, Eu, Gd, Ge, Lu, Nd, Sm, Tl, Yb
171560	456776	7284240	*Rf*	*EMEq*	soil	Al_2O_3, Ag, As, Bi, Cr, Ga, In, Mo, Pd, Sc, Sn, Th, V, W
171561	455934	7281582	*Rf*	*EMEq*	sandplain	Al_2O_3, Fe_2O_3, As, Bi, Cr, Ga, In, Mo, Sc, Sn, Te, Th, V
171562	452795	7280428	*Sd*	*ESs*	sandplain	Cd
171565	457307	7278676	*Sd*	*EMEq*	sandplain	Cd
171567	461920	7279527	*Sk*	*EMEq*	sandplain	SiO_2, Cd
171569	465939	7270490	*Cq*	*EMEn*	stream	Cd, Zr
171570	468940	7268035	*Cq*	*EMEn*	stream	Zr
171571	472147	7266578	*Cq*	*EMEn*	stream	Pb
171573	475934	7268119	A_c	*EMEn*	stream	Pb
171575	475595	7273645	Xls_m	*EMEq*	sheetwash	K_2O, As, Bi, Pb, Rb, W, B, Ge, Tl
171577	473423	7269566	A_c	*EMEn*	stream	Pb
171578	470707	7271747	A_c	*EMEn*	stream	MnO, Be, Pb, U, Tl
171579	467228	7274146	*Cl*	*EMEn*	sheetwash	Ag
171580	458782	7271818	*Rf*	*ESs*	soil	Bi, Mo, Ta, Th, Zr
171582	461373	7270370	*Sd*	*ESs*	sandplain	SiO_2
171585	465574	7264464	A_c	*EMEn*	stream	Ag, Nb
171586	468294	7263768	*Cq*	*EMEn*	stream	Cd
171598	457175	7252983	A_c	*EMCo*	stream	TiO_2, Fe_2O_3, MnO, Na_2O, Be, Cd, Co, Cr, Cu, Ni, Pd, Pt, Sc, V, Y, Zn, Dy, Er, Eu, Gd, Lu, Yb
176901	460100	7240692	A_c	*EVb*	stream	Ce
176908	475776	7236356	*Xqs*	*EVb*	stream	Ta
176913	493235	7237713	A_c	*EMCo*	stream	TiO_2, CaO, Li, Nb, Pd, Sn, Ta, W
176915	492639	7242001	*Xqz1*	*EMCo*	stream	MnO, Co, Ni
176917	496307	7241718	Xls_m	*EMCo*	stream	Al_2O_3, K_2O, Be, Ce, La, Rb, Sc, Eu, Gd, Ge, Nd, Sm, Tl
176919	497749	7241286	A_c	*EMCo*	stream	CaO, Na_2O, Co, Cu, Ni, Zn, Eu
176920	482867	7244201	*Wd*	*EMCo*	sheetwash	V
176923	475512	7244141	*Xqz1*	*EMCo*	stream	Na_2O, Co, Cu, Ni, Zn
176924	471971	7245064	A_c	*EMCo*	stream	Co, Cu, Ni
176926	463776	7244923	*Sk*	*EMCo*	soil	CaO
176932	452166	7244571	*Cl*	*EVb*	sheetwash	B
176933	454359	7247044	A_c	*EMCo*	stream	Al_2O_3, Ba, Li, Ta
176940	459374	7249182	L_l	*EMCo*	soil	Al_2O_3, MgO, Na_2O, Be, Ga, Li, Ni, S, Sc, Sn, Th, U, Zn, B, Lu, Yb
176944	455874	7249727	*Sd*	*EMCo*	stream	TiO_2, Fe_2O_3, Na_2O, Cr, In, V
176946	455144	7251942	*Rf*	*EMCo*	soil	Zr
176947	473560	7263847	A_c	*EMEn*	stream	SiO_2
176948	477563	7262487	A_c	*EMEn*	stream	Pb
176950	480740	7259821	*Sk*	*EMEq*	soil	MgO, CaO
176957	487627	7250356	*Cl*	*EMCo*	stream	P_2O_5
176958	490667	7247729	*Xmh*	*Ed*	sheetwash	MnO
176965	467881	7252635	*Sd*	*EMCo*	sheetwash	Zr

the northerly trending corridor of the Quadrio Lake–Phenoclast Hill area, also highlighted in the partial As, and total chalcophile- and base metal-index plots.

The plots of normalized partial digest As and Sb are easier to interpret compared to their raw counterparts (Figs 22 and 50). The normalized data in particular bring the partial digest Sb patterns in line with Sb patterns expressed in the total digest data (Fig. 49). Thus properly normalized partial digest chemistry is a useful tool for refining anomalies detected by a total approach, as well as identifying anomalous areas, possibly not expressed in the total data.

Normalized response-ratio plot of chalcophile index

The summed normalized partial digest chalcophile elements (Fig. 69) appear to give a less well-defined picture than the chalcophile index based on total digest data. Nevertheless, some basic similarities still exist, including the high value corridor in the Quadrio Lake – Phenoclast Hill area, and some elevated values in the northeast and northwest of the project area. Further work is required to fully ascertain the significance of the scattered highs on the normalized plot and their relationships to lithology, regolith, and mineralization.

Mineralization potential

Hocking et al. (2000c) proposed that the barite–hematite stockwork at Quadrio Lake could represent the distal facies of sedex-style mineralization, based on the sedex-style sulfide deposits described by Goodfellow et al. (1993). In this model, sulfide deposition takes place close to a feeder vent with progressive depletion and metal zonation outwards. Hocking et al. (2000c) suggested the barite–hematite veins with anomalous concentrations of gold, manganese, arsenic, and antimony at Quadrio Lake could represent a distal zonation away from the primary sulfides. Large northwesterly trending faults interpreted from gravity data, and by surface mapping in the project area, could be the controlling structures, providing pathways for fluid migration (Hocking et al., 2000c).

A series of northerly and northwesterly trending elongate gravity corridors through the centre and north of the map sheet (Fig. 63) probably represent a series of fault-bounded lithologies of contrasting composition (Shevchenko, S. I., 2002, written comm.). There appears to be some overlap between these features and geochemical anomalies in the regolith, such as the zones of high values in the total digest base metals index along the northern flank of the Cornelia Range and stretching up through the Phenoclast Hill – Quadrio Lake area. The elevated total Pb values (Fig. 42) in the Cornelia Range, above the trace of the elongate gravity corridor (inferred fault), are consistent with the proximal- and distal-mineralization zones as suggested by Hocking et al. (2000c).

Other possible mineralization styles include that centred on a buried intrusion, inferred from gravity data, immediately south of Phenoclast Hill (Hocking et al., 2000c; Fig. 63). Whatever the nature of this gravity low (felsic intrusive, a faulted and fractured package of rocks, or a salt diapir), it may act as a source or as a focus of fluids or provide ligands to dissolve metals.

The Quadrio Lake – Phenoclast Hill area is well defined by high total As, Ba, Sb, and W concentrations in regolith. This pattern is repeated in the far northwest of the map sheet along the continuation of the gravity corridor, suggesting that there may be similar barite–hematite mineralization elsewhere in the area.

Elevated total Ba is recorded in the southwest of the map sheet, in the vicinity of the large southwestern gravity low. In this area, and extending north through the Oldham Range, are many of the highest total and some of the highest partial Cr, Cu, Ni, V, and Zn values for the map sheet. It is unclear whether this represents mineralization or simply the abundance of exposed and near-surface dolerite in the area. Ferruginous duricrust material from a stream at the northern end of the salt lake (near GSWA 176944: Plate 1) returned elevated levels of Cu (255 ppm), Ni (575 ppm) and Zn (848 ppm). It is uncertain whether or not these relatively high concentrations are directly related to dolerite.

In the northeast of the map sheet, the wide range of elements with high concentrations suggest a lithological influence on regolith geochemistry. In particular, the elevated total K_2O, Rb, and REE suggest a higher felsic component to the sedimentary rocks, consistent with field observations of abundant wacke (exposed-regime regolith type — *Xls*$_s$) in the area. However, elevated concentrations of a number of total and some partial elements, including MnO, Mn, As, Cd, Cu, Mo, Sb, and Zn, in regolith suggest there may also be mineralization in the area.

In summary, areas with potential mineralization based on the regolith geochemistry include:

- the Quadrio Lake – Phenoclast Hill area and extensions towards the north;
- the area around the northern gravity low, extending southeast and northwest along the trend of the Cornelia Range and elongate gravity anomalies;
- the far northwest of the map sheet;
- the area around the southwestern gravity low extending into the Oldham Range; and
- the northeast of the map sheet.

Summary and conclusions

Regional-scale regolith and geochemical mapping on NICHOLLS involved the collection of 175 regolith samples (28 sheetwash, 91 stream-sediment, 18 soil, 37 sandplain, and one lake sample), representing a nominal sample density of one sample per 16 km^2. Each sample has been divided into two size fractions, <2 mm – >0.45 mm and <0.2 mm, the former fraction analysed for 57 major and trace elements after total digest, and the latter fraction analysed for 53 major and trace elements after partial digest. Acidity–alkalinity (pH) and conductivity were also measured for each sample.

Regolith-materials mapping of NICHOLLS has used the new GSWA regolith-classification scheme, which allows a wide range of regolith types and compositions to be defined (Hocking et al., 2001). The project area consists of a broad range of regolith types overlying Proterozoic sedimentary rocks and dolerites of the northwest Officer Basin. The map has been compiled from Landsat imagery, Aster imagery, aerial photography, sample-site descriptions, and previous geological mapping (Williams, 1995). Sandplain (*S*) is the dominant regolith type on NICHOLLS and occupies 56% of the map sheet. Exposed-regime regolith (*X*) occupies the second greatest area (21%) and is dominated by rocks of the northwesterly trending Oldham and Cornelia ranges.

Quality-control procedures have shown that precision and accuracy of laboratory and GSWA standard analyses are satisfactory, although some small batch variation occurs in analytes at low concentrations or in elements that are typically resistant to dissolution. There was difficulty in reproducing three elevated Ag, Au, and Zn partial analysis values, the initial high values possibly representing some form of contamination.

Both partial and total regolith chemical data are presented as a series of spot-concentration maps, or index and ratio plots, against a background of simplified geology. The data shows that there are four main areas of

significant regolith chemistry on the map sheet, including in the northwest and northeast corners, southwest in the vicinity of the large gravity low extending into the Oldham Range, and in the central north around Quadrio Lake and its extensions to the southeast and north.

A total analytical approach has been used to construct three additive element-index maps, including chalcophile, base metal, and ferro-alloy index plots. These plots efficiently highlight the main geochemical areas of interest on the sheet, and suggest extensions to mineralization, such as along the northern flank of the Cornelia Range.

Partial digest chemistry is shown to provide meaningful data when adequately normalized to account for variations in pH and the abundance of organic material. Normalization of the partial digest data provides significant improvement in terms of data clarity and the ability to interpret data. In this regard, significant attention must be paid to establishing the pH and organic content of each sample. These techniques may be applied in future to other areas of transported regolith, where total digest responses are typically suppressed.

Comparisons of anomalous regolith chemistry with gravity and magnetic data reveal that regolith chemistry may be influenced by subsurface features. Elongate gravity anomalies on the sheet may be fault bounded, and these faults may act as fluid pathways controlling regolith composition and mineralization. Two circular gravity lows on the sheet may also have influence on the surface chemistry, with both areas containing a number of elevated elements along their flank.

Mineralization potential on NICHOLLS includes the Quadrio Lake – Phenoclast Hill area and extensions to the north, northwest, and southeast. Of principal significance are the Pb anomalies to the southeast along the trend of the Cornelia Range. Their proximity to inferred major faults and to the barite–hematite mineralization at Quadrio Lake is consistent with the mineralization model proposed by Hocking et al. (2000c). There is an apparent metal zonation (from base metals to chalcophile elements; Figs 64 and 65) from the flanks of the Cornelia Range, northwards along the margin of the gravity low to the Quadrio Lake area and beyond. Other areas on the map sheet with mineralization potential include the northwest, northeast, and southwest of the project area.

References

ANTROPOVA, L. V., GOLDBERG, I. S., VOROSHILOV, N. A., and RYSS, Ju. S., 1992, New methods of regional exploration for blind mineralization: application in the USSR: Journal of Geochemical Exploration, v. 43, p. 157–166.

BAGAS, L., GREY, K., HOCKING, R. M., and WILLIAMS, I. R., 1999, Neoproterozoic successions of the northwestern Officer Basin: a reappraisal: Western Australia Geological Survey, Annual Review 1998–99, p. 39–43

BAGAS, L., GREY, K., and WILLIAMS, I. R., 1995, Reappraisal of the Paterson Orogen and Savory Basin: Western Australia Geological Survey, Annual Review 1994–95, p. 55–63.

BAJC, A. F., 1998, A comparative analysis of enzyme leach and mobile metal ion selective extractions; case studies from glaciated terrain, northern Ontario: Journal of Geochemical Exploration, v. 61, p. 113–148.

BEARD, J. S., 1974, Great Victoria Desert, explanatory notes to sheet 3: University of Western Australia Press, Vegetation Survey of Western Australia, 1:1 000 000 series, 50p.

BEARD, J. S., 1990, Plant life of Western Australia: Kenthurst, New South Wales, Kangaroo Press, 319p.

BRAKEL, A. T., and LEECH, R. E. J., 1980, Trainor,W.A.: Western Australia Geological Survey, 1:250 000 Geological Series Explanatory Notes, 13p.

BUTT, C. R. M., LINTERN, M. J., and ANAND, R. R., 2000, Evolution of regoliths and landscapes in deeply weathered terrain — implications for geochemical exploration: Ore Geology Reviews, v. 16, p. 167–183.

BUTT, C. R. M., and SCOTT, K. M., 2001, Geochemical exploration for gold and nickel in the Yilgarn Craton, Western Australia — an introduction: Geochemistry: Exploration, Environment, Analysis, v. 1, p. 179–182.

CHENG, Q., BONHAM-CARTER, G. F., HALL, G. E. M., and BAJC, A., 1997, Statistical study of trace elements in the soluble organic and amorphous Fe–Mn phases of surficial sediments, Sudbury Basin. 1. Multivariate and spatial analysis: Journal of Geochemical Exploration, v. 59, p. 27–46.

CLARKE, J. R., 1993, Enzyme-induced leaching of B-horizon soils for mineral exploration in areas of glacial overburden: Transactions of the Institution of Mining and Metallurgy, Section B, v. 102, p. 19–29.

CORNELIUS, M., SMITH, R. E., and COX, A. J., 2001, Laterite geochemistry for regional exploration surveys — a review, and sampling strategies: Geochemistry, Exploration, Environment, Analysis, v. 1, p. 211–220.

DAISHSAT PROPRIETARY LIMITED, 1995, Savory Basin gravity survey, operational and processing report: Western Australia Geological Survey, Statutory petroleum exploration report, S10312 (unpublished).

DANIELS, J. L., 1975, Bangemall Basin, *in* Geology of Western Australia: Western Australia Geological Survey, Memoir 2, p. 147–159.

DRONSEIKA, E., and EVERS, A., 2000, Aspects of EDTA Partial Digest Extractions in Variable pH Terrains — the Vunerability of Unbuffered Digests: Explore, Newsletter for the Association of Exploration Geochemists, Number 109, p. 10–14.

GENALYSIS LABORATORY SERVICES PROPRIETARY LIMITED, 2000, Terra-Leach™ partial digest geochemistry — cost effective geochemistry for the new millennia: Product Brochure, 2000.

GOLDBERG, I. S., 1998, Vertical migration of elements from mineral deposits: Journal of Geochemical Exploration, v. 61, p. 191–202.

GOODFELLOW, W. D., LYNDON, J. W., and TURNER, R. J. W., 1993, Geology and genesis of stratiform sediment-hosted (SEDEX) zinc–lead–silver sulphide deposits: Geological Association of Canada, Special Paper 40, p. 201–252.

GRAY, D. J., LINTERN, M. J., and LONGMAN, G. D., 1998, Readsorption of gold during selective extraction — observations and potential solutions: Journal of Geochemical Exploration, v. 61, p. 21–37.

GRAY, D. J., WILDMAN, J. E., and LONGMAN, G. D., 1999, Selective and partial extraction analyses of transported overburden for gold exploration in the Yilgarn Craton, Western Australia: Journal of Geochemical Exploration, v. 67, p. 51–66.

GREY, K., 1978, *Acaciella cf. Australica* from the Skates Hills Formation, eastern Bangemall Basin, Western Australia: Western Australian Geological Survey, Annual Report 1977, p. 71–73.

GREY, K., 1995, Neoproterozoic stromatolites from the Skates Hills Formation, Savory Basin, Western Australia, and a review of the distribution of *Acaciella australica*: Australia Journal of Earth Sciences, v. 42, p. 123–132.

GREY, K., and COTTER, K. L., 1996, Palynology in the search for Proterozoic hydrocarbons: Western Australia Geological Survey, Annual Review 1995–96, p. 70–80.

GREY, K., and STEVENS, M. K., 1997, Neoproterozoic palynomorphs of the Savory Sub-basin, Western Australia, and their relevance to petroleum exploration: Western Australia Geological Survey, Annual Review 1996–97, p. 49–54.

HALL, G. E. M., 1998, Analytical perspective on trace element species of interest in exploration: Journal of Geochemical Exploration, v. 61, p. 1–19.

HALL, G. E. M., MacLAURIN, A. I., and VAIVE, J. E., 1995, Readsorption of gold during the selective extraction of the 'soluble organic' phase of humus, soil and sediment samples: Journal of Geochemical Exploration, v. 54, p. 27–38.

HALL, G. E. M., VAIVE, J. E., BEER, R., and HOASHI, M., 1996a, Selective leaches revisited, with emphasis on the amorphous Fe oxyhydroxide phase extraction: Journal of Geochemical Exploration, v. 56, p. 59–78.

HALL, G. E. M., VAIVE, J. E., and MacLAURIN, A. I., 1996b, Analytical aspects of the application of sodium pyrophosphate reagent in the specific extraction of the labile organic component of humus and soils: Journal of Geochemical Exploration, v. 56, p. 23–36.

HOCKING, R. M., 1994, Subdivisions of Western Australian Neoproterozoic and Phanerozoic sedimentary basins: Western Australian Geological Survey, Record 1994/4, 84p.

HOCKING, R. M., and GREY, K., 2000, Stacked Proterozoic basins in central Western Australia: Geological Society of Australia; 15th Australian Geological Convention, Sydney, N.S.W., Abstract Series, no. 59, p. 231.

HOCKING, R. M., GREY, K., BAGAS, L., and STEVENS, M. K., 2000a, Mesoproterozoic stratigraphy in the Oldham Inlier, Little Sandy Desert, central Western Australia: Western Australia Geological Survey, Annual Review 1999–2000, p. 49–56.

HOCKING, R. M., and JONES, J. A., 2002, Geology of the Methwin 1:100 000 sheet: Western Australia Geological Survey, 1:100 000 Geological Series Explanatory Notes, 35p.

HOCKING, R. M., JONES, J. A., PIRAJNO, F., and GREY, K., 2000b, Revised lithostratigraphy for Proterozoic rocks in the Earaheedy Basin and nearby areas: Western Australia Geological Survey, Record 2000/16, 22p.

HOCKING, R. M., LANGFORD, R. L., THORNE, A. M., SANDERS, A. J., MORRIS, P. A., STRONG, C. A., and GOZZARD, J. R., 2001, A classification system for regolith in Western Australia: Western Australia Geological Survey, Record 2001/4, 22p.

HOCKING, R. M., PIRAJNO, F., IIZUMI, S., and MORRIS, P. A., 2000c, Barium–gold mineralization at Quadrio Lake, Oldham Inlier, Little Sandy Desert, Western Australia: Western Australia Geological Survey, Annual Review 1999–2000, p. 72–79.

KOJAN, C. J., BRADLEY, J. J., FAULKNER, J. A., and SANDERS, A. J., 1996, Targeting mineralization using a chalcophile index: results of regional and project-scale regolith geochemistry in the northern Eastern Goldfields: Western Australia Geological Survey, Annual Review 1995–96, p. 124–134.

MANN, A. W., BIRRELL, R. D., MANN, A. T., HUMPHREYS, D. B., and PERDRIX, J. L., 1998, Application of mobile metal ion technique to routine geochemical exploration: Journal of Geochemical Exploration, v. 61, p. 87–102.

MARTIN, D. McB., THORNE, A. M., and COPP, I. M., 1999, A provisional revised stratigraphy for the Bangemall Group on the Edmund 1: 250 000 sheet: Western Australia Geological Survey, Annual Review 1998–99, p. 51–55.

MORRIS, P. A., 2000, Composition of Geological Survey of Western Australia Geochemical Reference Materials: Western Australia Geological Survey, Record 2000/11, 33p.

MORRIS, P. A., McGUINNESS, S. A., SANDERS, A. J., and COKER, J., 2000a, Geochemical mapping of the Stanley 1:250 000 sheet: Western Australia Geological Survey, 1:250 000 Regolith Geochemistry Series Explanatory Notes, 53p.

MORRIS, P. A., PIRAJNO, F., and SHEVCHENKO, S., in press, Proterozoic mineralization identified by integrated regional geochemistry, geophysics and bedrock mapping in Western Australia: Geochemistry: Exploration, Environment, Analysis.

MORRIS, P. A., and SANDERS, A. J., 2001, The effect of sample medium on regolith chemistry over greenstone belts in northern Eastern Goldfields of Western Australia: Geochemistry: Exploration, Environment, Analysis, v. 1, p. 201–210.

MORRIS, P. A., SANDERS, A. J., McGUINNESS, S. A., COKER, J., and KING, J. D., 2000b, Geochemical mapping of the Fraser Range Region: Western Australia Geological Survey, 1:250 000 Regolith Geochemistry Series Explanatory Notes, 45p.

MUHLING, P. C., and BRAKEL, A. T., 1985, Geology of the Bangemall Group: Western Australia Geological Survey, Bulletin 128, 266p.

OCCHIPINTI, S. A., SHEPPARD, S., and TYLER, I. M., 1999, The Palaeoproterozoic tectonic evolution of the southern margin of the Capricorn Orogen, Western Australia: Geological Society of Australia, Abstract Series, no. 53, p. 173–174.

PERINCEK, D., 1996, The stratigraphy and structural development of the Officer Basin, Western Australia: a review: Western Australia Geological Survey, Annual Review 1995–96, p. 135–148.

ROCK, N. M. S., 1988, Numerical geology: Berlin, Springer-Verlag, 427p.

SANDERS, A. J., COKER, J., and FAULKNER, J. A., 1998, Geochemical mapping of the Glenburgh 1:250 000 sheet: Western Australia Geological Survey, 1:250 000 Regolith Geochemistry Series Explanatory Notes, 33p.

SANDERS, A. J., and McGUINNESS, S. A., 2000, Geochemical mapping of the Ajana 1:250 000 sheet: Western Australia Geological Survey, 1:250 000 Regolith Geochemistry Series Explanatory Notes, 55p.

SANDERS, A. J., and McGUINNESS, S. A., 2001, Geochemical mapping of the Winning Pool – Minilya 1:250 000 sheet: Western Australia Geological Survey, 1:250 000 Regolith Geochemistry Series Explanatory Notes, 57p.

SMITH, R. E., BIRRELL, R. D., and BRIGDEN, J. F., 1989, The implications to exploration of chalcophile corridors in the Archaean Yilgarn Block, Western Australia, as revealed by laterite geochemistry: Journal of Geochemical Exploration, v. 32, p. 169–184.

SMITH, R. E., and PERDRIX, J. L., 1983, Pisolitic laterite geochemistry in the Golden Grove massive sulphide district, Western Australia: Journal of Geochemical Exploration, v. 18, p. 131–164.

STEVENS, M. K., and ADAMIDES, N. G., 1998, GSWA Trainor 1 well completion report, Savory Sub-basin, Officer Basin, Western Australia with notes on petroleum and mineral potential: Western Australia Geological Survey, Record 1996/12, 69p.

STEVENS, M. K., and CARLSEN, G. M., 1998, A review of data pertaining to the hydrocarbon prospectivity of the Savory Sub-basin, Officer Basin, Western Australia: Western Australia Geological Survey, Record 1998/5, 65p.

STEVENS, M. K., and GREY, K., 1997, Skates Hills Formation and the Tarcunyah Group, Officer Basin — carbonate cycles, stratigraphic position, and hydrocarbon prospectivity: Western Australia Geological Survey, Annual Review 1996–97, p. 55–60.

TYLER, I. M., and HOCKING, R. M., 2001, Tectonic units of Western Australia (scale 1:2 500 000): Western Australia Geological Survey.

TYLER, I. M., PIRAJNO, F., BAGAS, L., MYERS, J. S., and PRESTON, W., 1998, The geology and mineral deposits of the Proterozoic in Western Australia: AGSO Journal of Geology and Geophysics, v. 17, p. 223–224.

van de GRAAFF, W. J. E., CROWE, R. W. A., BUNTING, J. A., and JACKSON, M. J., 1977, Relict early Cainozoic drainages in arid Western Australia: Zeitschrift fur Geomorphologie N.F., v. 21, p. 379–400.

WALTER, M. R., and GORTER, J. D., 1994, The Neoproterozoic Centralian Superbasin in Western Australia: the Savory and Officer Basins, *in* The sedimentary basins of Western Australia *edited by* P. G. PURCELL and R. R. PURCELL: Petroleum Exploration Society of Australia, West Australian Basins Symposium, Perth, W.A., 1994, Proceedings, p. 851–864.

WALTER, M. R., VEEVERS, J. J., CALVER, C. R., and GREY, K., 1995, Neoproterozoic stratigraphy of the Centralian Superbasin, Australia: Precambrian Research, v. 73, p. 173–195.

WILLIAMS, I. R., 1987, Late Proterozoic glacigene deposits in the Little Sandy Desert, Western Australia: Australian Journal of Earth Sciences, v. 34, p. 153–154.

WILLIAMS, I. R., 1990, Bangemall Basin, *in* Geology and mineral resources of Western Australia: Western Australia Geological Survey, Memoir 3, p. 308–329.

WILLIAMS, I. R., 1992, Geology of the Savory Basin, Western Australia: Western Australia Geological Survey, Bulletin 141, 115p.

WILLIAMS, I. R., 1995, Trainor, W.A. (2nd edition): Western Australia Geological Survey, 1:250 000 Geological Series Explanatory Notes, 31p.

WILLIAMS, I. R., BRAKEL, A. T., CHIN, R. J., and WILLIAMS, S. J., 1976, The stratigraphy of the eastern Bangemall Basin and Paterson Province: Western Australia Geological Survey, Annual Report 1975, p. 79–83.

WINGATE, M. T. D., 2002, Age and palaeomagnetism of dolerite sills intruded into the Bangemall Supergroup on the Edmund 1:250 000 map sheet, Western Australia: Western Australia Geological Survey, Record 2002/4, 48p.

XUEQIU, W., 1998, Leaching of mobile forms of metals in overburden: development and application: Journal of Geochemical Exploration, v. 61, p. 39–55.

YEAGER, J. R., CLARK, J. R., MITCHELL, W., and RENSHAW, R., 1998, Enzyme leach anomalies associated with deep Mississippi Valley-type zinc ore bodies at the Elmwood Mine, Tennessee: Journal of Geochemical Exploration, v. 61, p. 103–112.

Appendix 1

Gazetteer of localities

Name	Type	MGA coordinates Easting	Northing
Phenoclast Hill	Locality	467047	7279248
Quadrio Lake	Locality	464537	7283760
Trainor 1	Stratigraphic well	473777	7287560
TWB1	Water bore	473809	7287566
TWB2	Water bore	473331	7285926
TWB3	Water bore	473178	7286119
TWB4	Water bore	463363	7286302
TWB5	Water bore	463233	7277882
TWB6	Water bore	457149	7274512
TWB7	Water bore	453876	7264050

Appendix 2

Summary of sampling procedure, regolith classification, and analytical procedures

Regolith sampling

The aim of the Geological Survey of Western Australia's (GSWA's) regolith sampling program is to sample regolith from sites representative of the 4 × 4 km sampling polygon of interest. The preferred sampling medium is active stream sediment, sampled from lower order streams draining the sample polygon. In areas where drainage is absent or only weakly developed, sheetwash (colluvium), soil, sand, or lake sediment is sampled. Sampling sites are chosen using Landsat Thematic Mapper (TM) imagery and topographic maps, combined with a 4 × 4 km grid overlay. The site locations are digitized and assigned a unique site name made up of part of the relevant 1:100 000 map sheet name and a number. For example, GRA95 would correspond to site 95 on the GRANITE PEAK* 1:100 000 sheet (on the NABBERU 1:250 000 sheet).

The actual sampling site in the field is determined by the geologist, who can move the site from the designated position in order to facilitate access, or avoid areas of human or animal activity, or areas of standing water.

Stream sediments

Stream sediments in single, well-defined channels are sampled by trenching perpendicular to the flow direction. Narrow streams are sampled from pits excavated along their length, whereas braided stream systems are sampled from pits in several individual channels.

Sheetwash (colluvium) or soil

Sample sites are selected towards the centre of the 4 × 4 km polygon. Where a clear slope direction can be identified, regolith is composited from three pits excavated 30 m apart, perpendicular to the slope direction. Where no clear slope direction can be identified, regolith is sampled from three pits forming the apices of an equilateral triangle, whose sides are 30 m long.

Lake sediments

Lake sites are chosen to maximize ease of access. They are sampled as for sheetwash with no discernible slope.

Sandplain

In areas of active sand dunes, sandplain samples are taken from three pits along the swale. In sandplain areas lacking active dunes, sampling is carried out as for sheetwash sites.

Prior to excavating pits or trenches, the top 5–10 cm of material is removed to minimize any surface-related contamination. Pits and trenches are excavated to a depth of 30 cm. If the excavated material is sufficiently dry, it is sieved at the site to –6 mm through a plastic sieve into a graduated sieve pan, then thoroughly mixed using a small shovel. Regolith, either sieved or unsieved, is divided into an archive sample (weighing about 3 kg) and an analytical sample (weighing about 2 kg) using graduated rings in the sieve pan. Information such as the unique GSWA sample number, site number, a map sheet identifier, and the relevant geologist's initials are recorded on each bag. A soft aluminium tag, on which the GSWA number is written, is included with the analytical sample. Analytical and archive samples are distinguished by the use of different-coloured nylon bag ties.

Sample-recording form

An example of the sample-recording form is shown in Figure 2.1. At each sampling site, the sample's MGA coordinates (GDA94 grid, read from a hand-held GPS), the sample-site number, GSWA number, sampling date, sampler's initials, and nature of sample (e.g. stream, sheetwash, channel, or pit) are recorded. The cross section is used to record the position of the sample in an idealized landform profile. The composition of the regolith is recorded in terms of iron-rich, lithic, and non-lithic components, using a series of letters signifying abundance (i.e. **A**bundant: >30%; **C**ommon: 5–30%; **R**are: 1–5%; **T**race: <1%). Within each category, the relative abundance of each component is recorded using a numerical system from 1 (most abundant) to >1 (least abundant), or the A, C, R, T designations. Fresh bedrock-fragment types (if present) are recorded in the same way. Fields also exist for recording the nature of the surrounding regolith, any grain coatings, nature of fine-grained material, nature and distribution of bedrock and secondary units, and characteristics of the stream site (if appropriate). A free-form section (Remarks) allows for specific entries pertinent to the site that are not covered in the preceding sections.

Regolith-materials classification

Three regolith-materials classification schemes have been used during the course of the GSWA regional regolith and geochemical mapping program. All three are based on the regolith–landform RED scheme of Anand et al. (1993) and Anand and Smith (1994), where regolith is classified

* Capitalized names refer to standard 1:100 000 and 1:250 000 map sheets.

Sheet 3448 **Zone** 51	**Loc/n No**_____	**GSWA No**_____	**Date**_____
Site Ref_____	_____ **E**	_____ **N**	**Sampler**_____

☐ Channel ☐ Pit/hole | ☐ Single Point ☐ Multipoint | ☐ Shtwash ☐ Creek ☐ Soil ☐ Lake ☐ Sandplain

Site description

Drainage heading_____ Width _____m
☐ Single ☐ Braided ☐ Incised

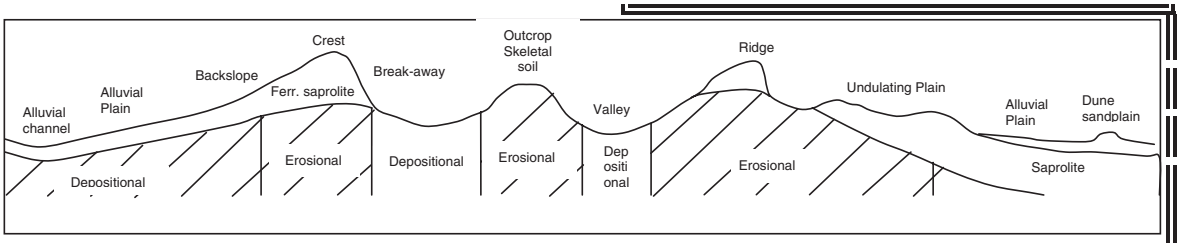

Surrounding (200m) regolith code Left_____ Right _____(facing downstream/slope).
Regolith material description:

Surface regolith material: ___%clasts ___%Sand ___%Clay ___%Other_____ Colour _____

Downhole regolith material: ___%clasts ___%Sand ___%Clay ___ %Other_____ Colour _____

Sieved to size Y/N %Osize____ Depth: _____

SURFACE CLASTS ☐ Gravel (2-5mm) ☐ Stones (5-64mm) ☐ Cobbles (64-256mm) ☐ Boulders(>256mm)
Abundant : >30% Common : 5-30% Rare : 1-5% Trace : <1%

Iron-rich Abnt/Comn/Rare/Tr ☐	**Lithic Abnt/ Comn / Rare/ Tr** ☐	**Non-Lith Abnt/Comn/Rare/Tr** ☐
☐ Pisoliths	☐ Saprolite fragments	☐ Feldspar ☐ Quartz (sand)
☐ Nodules ☐ Ferrug. Granules 2-4mm	☐ Saprock Fragments (below)	☐ Calcrete ☐ Other_____
☐ Ferrug. duricrust	☐ Fresh B'rock frag's (below)	☐ Hardpan _____
☐ Gossan fragments	☐ Vein quartz	☐ MnO_2 _____
☐ Ferrug lithic fragments	☐ Other Silica	☐ Silcrete _____

Clast Lithology (F= Fresh, S= Saprock)

☐ *M*afic	☐ *G*ranitic	☐ *S*andstone	☐ *C*hert	_____
☐ *U*ltramafic	☐ *Q*uartzite	☐ *A*rk / Gwk	☐ *C*arbonate	_____
☐ *F*elsic	☐ *B*IF	☐ *S*hale/Siltstone	☐ Other	_____

Secondary coating on ☐ clasts and/or ☐ grains: ☐ Fe ☐ Mn ☐ Silica ☐ Carbonate ☐ Clay ☐ Salt

Primary and Secondary Lithological Units

Rock O/c Dist. Dir. 1._____ ____ m _____ 2._____ ____ m _____
3._____ ____ m _____ 4._____ ____ m _____

Secondary Units Nearby ☐ Hardpan ☐ Consolidated Colluvium ☐ Calcrete ☐ Silcrete ☐ Duricrust
☐ Mottled Zone ☐ Saprolite ☐ Saprock ☐ Gyps Dune ☐ Sand Dune ☐ Salt

REMARKS (photos, contamination, anthropogenic influence etc)

_____
_____
_____

Figure 2.1. Sample recording form for NICHOLLS

according to its position in an idealized landform profile as relict (R), erosional (E), or depositional (D). Relict-regime regolith is commonly in areas of higher topographic elevation (e.g. upland surfaces and plateaus), and includes areas of siliceous and ferruginous duricrust ('laterite'). The erosional regime includes areas of outcrop and subcrop where there is a net loss of material caused by downslope transport. Areas of net material gain comprise the depositional regime, including active alluvial channels, areas of sheetwash, overbank deposits, sandplain, and lakes.

The three schemes reflect an ongoing change in the focus of the GSWA's regolith geochemistry program, from relatively simple granite–greenstone associations of the Yilgarn Craton to more complex associations such as the Capricorn and Albany–Fraser Orogens.

Maps produced early in the GSWA regional regolith and geochemical mapping program focused on Archaean granite–greenstone associations of the Yilgarn Craton (e.g. MENZIES 1:250 000: Kojan and Faulkner, 1994; LEONORA 1:250 000: Bradley et al., 1995), which had few regolith–landform divisions, reflecting the lack of relief and limited number of lithologies. Regolith was subdivided according to its landform position (using R, E, D), slope position, and lithology. For example, in the erosional regime, E2v corresponded to erosional-regime regolith (E) derived from mafic igneous rock (v) that was upslope (2) from lithologically similar material that would be termed E4v. Alluvium of the depositional regime was separated using numerical qualifiers, such as DA4 (alluvium in active alluvial channels), DA5 (overbank deposits), DA7 (playa lake and associated deposits), and DA8 (calcrete). Sandplain was denoted as D9. This system has drawbacks, in that it only works well for lithologically simple map sheets, relies on a qualitative determination of slope position, and requires identification of the parent rock type to indicate the composition of regolith — the latter was commonly difficult for fine-grained, better sorted regolith, such as that of the depositional regime.

The shift in focus of the GSWA's regolith geochemistry program to Proterozoic successions of the Capricorn Orogen involved a change to map sheets with a relatively diverse lithology and physiography, combined with a less arid climate. This resulted in an increase in the number of regolith–landform divisions and increasingly complex regolith–landform maps. Several factors prompted a revision of the regolith-classification scheme. These included a need to simplify the regolith–landform maps, produce a more objective classification scheme, and introduce criteria that would enable the compositional classification of regolith independent of parent rock type. This change in scheme also coincided with the need for a universal regolith-classification scheme that could be used throughout GSWA.

The revised scheme retained the regolith–landform approach, and used a set of 11 primary codes for the subdivision of regolith in terms of landform position (Table 2.1). These codes aimed to satisfy a wide range of physiographic associations. The issue of regolith composition was addressed by a series of secondary codes, including some designations for common regolith types (e.g. h: hardpan; w: consolidated colluvium) that were not strictly compositionally based. These secondary codes highlighted the composition of the regolith rather than the parent rock type. In situations where the parent rock type was identifiable (usually in the erosional regime), this could be designated using a set of tertiary codes (Table 2.1)

This revised scheme relied on placing the regolith in an idealized landform profile, and making basic macroscopic and mesoscopic (hand lens) observations about regolith composition. The scheme did not rely on detailed knowledge of regolith-forming processes. The revised scheme resulted in a reduction in the number of regolith–landform types, and hence a more simple regolith–landform map. In addition, the revised scheme allowed a more rigorous approach to statistical analysis of regolith chemistry according to regolith type, as there were usually larger sample populations for each regolith–landform subdivision.

Following implementation of this revised regolith-classification scheme on several GSWA 1:250 000 regolith–landform maps (e.g. MOUNT EGERTON: Morris et al., 1998; TUREE CREEK: Coker et al., 1998), several improvements were made to the scheme, as discussed by Hocking et al. (2001). These changes included expansion and some modification of the primary (environment or process), secondary (compositional), and tertiary (parent rock or cement) code sets, and the optional use of subscripts to primary, secondary, and tertiary codes to allow further subdivision of regolith.

An example of this approach to describe a gravel bar in an alluvial channel derived from ferromagnesian volcanic rock (basalt) would result in the code $A_g mv_b$, where *A* is a primary code denoting an alluvial environment, and the subscript ($_g$) indicates a gravel bar. The secondary code (*m*) defines the composition as ferromagnesian material, whereas the tertiary code (*v*) indicates derivation from volcanic parent rock. The subscript ($_b$) denotes the parent lithology as basalt. Lists of primary codes, selected primary code qualifiers, secondary codes and qualifiers, and tertiary codes with common qualifiers are shown in Tables 2.2 to 2.5.

Quality control during the analysis of regolith

Quality control aims to assess the precision and accuracy of chemical analysis using a series of standards (for which compositions are known), replicate and duplicate samples, and blank determinations. Precision is the closeness of agreement of independent test results obtained under prescribed conditions, whereas accuracy is the closeness of agreement between the result of a measurement and the true value (Thompson and Ramsey, 1995). Both precision and accuracy can only be reliably assessed when the analyte concentration is sufficiently above the detection level, which is the lowest level at which the analyte can be reliably measured using the technique under consideration. Precision is assessed using a series of GSWA and laboratory reference standards for which there are

Table 2.1. Primary, secondary, and tertiary codes, prior to revision

Regolith code		*Description*
Primary codes — environment		
R	relict	Relicts of an ancient land surface, including overlying and proximal reworked material
E	erosional	Exposed rock, saprock, saprolite, with thin locally derived debris
C	colluvial	Proximal mass-wasting products grading into sheetwash. Noticeable slope
W	diluvial	Distal sheetwash; minimal gradient; poorly defined drainage
A	alluvial	Alluvium in fluvial channels, and distal floodplain deposits with recognizable drainage systems
O	overbank	Overbank alluvial deposits
L	lacustrine	Inland lakes, associated dunes, and playa deposits, and some coastal lakes (not formed by coastal barring). Includes saline and freshwater playas, and eolian deposits (e.g. gypsiferous dunes) associated with such lake systems
S	eolian	Eolian dunes and sandplains, including interdunes
B	beach	Deposits at or above high water mark, adjacent to marine and tidal-related areas
T	tidal	Deposits between high- and low-water marks
M	marine	Sea-bed deposits, extending from below wave base. Includes reefs
Secondary codes — composition		
b	black soil, gilgai	
c	clay-mineral rich	
e	evaporite	
f	iron rich (ferruginous)	
g	quartzofeldspathic	
h	hardpan	
k	carbonate rich (including calcrete)	
m	ferromagnesian	
q	quartz rich	
r	carbonaceous	
u	ultramafic	
w	compacted and/or weakly cemented material (includes consolidated colluvium)	
x	mineral-rich material	
y	gypsiferous	
z	siliceous (including silcrete)	
Tertiary codes — rock qualifiers and specified compositional qualifiers		
m	metamorphic	
p	plutonic	
v	volcanic	
s	sedimentary	
h	halite	
a	aluminous	
n	magnesite	

consensus or recommended values. In the GSWA regional regolith and geochemical mapping program, precision is deemed acceptable if the percent relative standard deviation (RSD% = (standard deviation/mean) × 100) is less than 20 for multiple analyses, provided the analyte concentration is more than 20 times (in some cases 10 times) the detection level. Measurement of a replicate sample (i.e. a second analysis of the same sample pulp) also assesses precision, as well as any change in analytical conditions during a sample run (machine drift), and any variation in analytical conditions between batches (batch effects). In future regolith programs carried out by GSWA, the Half Relative Difference (HRD) factor ((assay #1– assay #2)/(assay #1 + assay #2) × 100; Shaw et al., 1998) will be used to assess replication, with a value of 10% deemed acceptable.

Accuracy is assessed using GSWA and laboratory standard analyses, with an acceptable accuracy if the analyte concentration lies within 20% of the recommended or consensus value, provided the analyte concentration is greater than 10 or 20 times the detection level. These data can also be used to assess machine drift and batch effects.

Background levels are assessed by periodic analysis of blanks, with acceptable background levels in the GSWA program being less than three times the detection level.

For each analytical batch of between 120 and 200 samples (batch size depends on the laboratory), up to three GSWA standards are included as blind checks (i.e. with the GSWA number only), resulting in about 10 standard analyses per map sheet. These standards include a laterite (IQC47), a gossan (IQC45), and an amphibolite (IQC42), which span a wide SiO_2 interval of 42–88%.

Rigorous application of criteria for acceptability of results in terms of accuracy and precision assumes sample homogeneity and the suitability of the analytical technique to the analyte under consideration. With a wide range in composition — Morris et al. (1997) reported a SiO_2 range of 7% to 96% for regolith on NABBERU (1:250 000) — and

Table 2.2. Primary regolith codes for GSWA maps

Primary landform code	*Environment and process*	*Notes*
R	Residual or Relict	Remnant material overlying an ancient land surface. Residual material is derived by in situ weathering and shows no evidence of having undergone significant transport. Relict material comprises deposits of uncertain origin, either transported or residual, or a combination of both. The term relict should not be used if the original depositional process can be determined. In such cases the appropriate primary code (e.g. A, C, W), together with a relative age qualifier, should be used instead
X	Exposed	Used for rock (optional) and weathered rock. Includes subcrop and bouldery lag
C	Colluvial	Proximal mass wasting deposits grading into sheetwash with a significant to perceptible slope
W	Low-gradient slope	Distal slope deposits (sheetwash and sheet flood) where the gradient is minimal, and drainage is not clearly defined
A	Alluvial / fluvial	Alluvium in channels and floodplains. Includes deltaic deposits
L	Lacustrine	Inland lakes, dune and playa terrain, and some coastal lakes. Includes saline and fresh-water playas and claypans, and minor eolian deposits directly associated with the lake system (fringing gypsiferous dunes, etc.)
E	Eolian	Eolian dunes, interdune areas, and sandplain
S	Sandplain	Dominantly sandplain. May be of mixed origin, including residual, sheetwash and eolian sands
B	Coastal (wave-dominated)	Beaches, beach ridges, barrier bars and lagoons, and back-beach dunes, coastal cliffs and other erosional features e.g. blowouts
T	Coastal (tide-dominated)	Intertidal and supratidal flats and channels, estuaries, and mangrove flats
M	Marine	Subtidal, shoreface, and offshore marine deposits such as coralgal reefs, shell banks, and sea-grass banks
V	Valley	Higher level category; includes lacustrine, alluvial, floodplain, sheetwash, and colluvial
K	Coastal	Higher level category; includes wave- and tide-dominated coastal, and marine
D	Depositional	Includes all depositional systems

the concentration of resistate phases (e.g. rutile, chromite, and zircon) lower in the landform profile, it is unlikely that one preparation or analytical technique is suitable for all samples. Morris et al. (1998) discussed this problem with regard to analysis of niobium on MOUNT EGERTON and TUREE CREEK (1:250 000). They concluded that precise and accurate analysis of high field strength elements such as niobium is difficult, as these elements were common in resistate phases, such as rutile, which are difficult to dissolve prior to analysis by inductively coupled plasma (ICP) techniques. One approach to reducing these problems is to use different preparation or analytical techniques depending on analyte concentration. For example, Morris et al. (1998) reported chromium data for regolith on MOUNT EGERTON according to two techniques: for concentrations of less than 100 ppm, data are reported after mixed acid digestion and inductively coupled plasma mass spectrometric (ICP-MS) analysis; for values greater than 100 ppm, data are reported following fusion and mixed acid digest and inductively coupled plasma optical emission spectrometric (ICP-OES) analysis. Although this approach can produce more acceptable data, the niobium issue on MOUNT EGERTON and TUREE CREEK as discussed by Morris et al. (1998) was not resolved by using different preparation or analytical techniques. Another factor in this approach is that of cost, which increases with the number of sample digests or techniques employed.

Batch effects have been noted for gold in regolith on EDMUND (1:250 000; Pye et al., 1998) and GLENBURGH (1:250 000; Sanders et al., 1998). In both cases, gold at levels of less than 4 ppb (detection level of 1 ppb) were subject to batch control.

Quality-control data for regolith on NICHOLLS are presented as a series of digital datafiles on the accompanying compact disk. For GSWA standards, the consensus values are taken as averages of analyses carried out at individual laboratories during the course of the GSWA regolith program. Consensus values for laboratory standards have been provided by the respective laboratories.

Table 2.3. Landform (primary) code qualifiers

Primary landform /process	*Landform element or pattern*	*Suggested primary code*	*Suggested subscript code*
Residual or relict		*R*	
	In situ weathered (residual)		R_i
	Duricrust (residual or relict)		R_r
	Sand (residual or relict)		R_s
	Transported (relict)		R_t
Exposed		*X*	
	Deeply weathered		X_w
Colluvial (proximal slope)		*C*	
	Cliff-foot slope		C_c
	Footslope		C_f
	Landslide		C_l
	Scarp-foot slope		C_s
	Talus		C_t
Low gradient slope (sheet-flood, distal slope)		*W*	
	Sheet-flood fan		W_f
	Playa, pan		W_p
	Scarp-foot slope		W_s
Alluvial		*A*	
	Alluvial plain		A_a
	Stream bed		A_b
	Stream channel		A_c
	Drainage depression /swale		A_d
	Delta		A_e
	Floodplain		A_f
	Gravel bar		A_g
	Channel bench		A_h
	Stream bank		A_k
	Levee		A_l
	Meander plain		A_m
	Backplain		A_n
	Playa, pan		A_p
	Stream bar		A_r
	Sand bar		A_s
	Terrace		A_t
	Superficial channel		A_u
	Fan/ flood-out		A_v
	Swamp		A_w
	Ox-bow		A_x
Lacustrine		*L*	
	Fringing dunes		L_d
	Fringing bedded deposits		L_g
	Lake, excluding fringing deposits		L_l
	Dune and playa terrain		L_m
	Playa		L_p
	Saline lake		L_s
	Subcropping bedrock in lake		L_x
Eolian		*E*	
	Parabolic dunefield		E_a
	Blow-out		E_b
	Dunefield		E_d
	Dune		E_e
	Longitudinal dunefield		E_l
	Mobile dune		E_m
	Net-like dunefield		E_n
	Sand and playa terrain		E_p
	Lunette		E_u
	Interdune pavements		E_v
	Swampy swale		E_w
Sandplain; residual, uncertain, and mixed origin		*S*	
	Blow-out		S_b
	Dune		S_d
	Gravel deflation pavement		S_g
	Longitudinal dunefield		S_l

Table 2.3. (continued)

Primary landform /process	*Landform element or pattern*	*Suggested primary code*	*Suggested subscript code*
Sandplain; residual, uncertain, and mixed origin (cont.)	Net-like dunefield		S_n
	Sand and playa terrain		S_p
	Undulating		S_u
Coastal (wave-dominated)		*B*	
	Beach (foreshore and backshore)		B_b
	Cliffs		B_c
	Foredune		B_d
	Foreshore		B_f
	Backshore		B_k
	Back-barrier lagoon		B_l
	Mobile dunes		B_m
	Boulder beach		B_o
	Beach ridge plain		B_r
	Storm beach gravels		B_s
Tide-dominated		*T*	
	Tidal bar, in channel		T_b
	Tidal channel (subtidal base)		T_c
	Tidal delta		T_d
	Estuary		T_e
	Tidal flat (intertidal and supratidal)		T_f
	Chenier plain		T_h
	Intertidal flat		T_I
	Lagoon		T_l
	Mangrove flats		T_m
	Superficial channel (intertidal)		T_s
	Supratidal flat		T_u
Marine		*M*	
	Coral reef		M_c
	Shell bank		M_k
	Plain, nearshore		M_n
	Plain, offshore		M_p
	Reef flat / backreef/rock flat		M_r
	Shoreface		M_s
	Relict channel		M_v

NOTES: These combinations should be followed where possible, however, the list is not exhaustive. Landform elements and patterns largely follow McDonald et al. (1990)

Typical analytical schemes from three commercial laboratories are outlined below.

Genalysis Laboratory Services

All regolith samples were oven dried at GSWA's Carlisle base. Approximately 2 kg of each sample (either sieved to <2 mm or to <6 mm) was supplied to the laboratory. Following further drying, an aliquot of each sample was sieved to between 2 and 0.45 mm. This material was pulverized to <75 µm in a zirconia ring mill (for analysis of SiO_2, TiO_2, Fe_2O_3, Al_2O_3, MnO, MgO, K_2O, and Cr), or a chrome-steel jumbo ring mill (for analysis of CaO, Na_2O, P_2O_5, Ag As, Ba, Be, Bi, Cd, Ce, Co, Cu, Ga, In, La, Li, Mo, Nb, Ni, Pb, Rb, Sc, Se, Sn, Sr, Ta, Te, Th, U, V, W, Y, Zn, and Zr).

Seven different analytical methods were used:

1. Silver, As, Ba, Be, Bi, Cd, Ce, Co, Ga, In, La, Li, Mo, Pb, Rb, Sb, Sn, Sr, Te, Th, U, W, and Y were analysed by ICP-MS using a combined mixed acid digest (Genalysis code A/MS). The pulverized sample was digested in a hydrofluoric–perchloric–nitric acid mixture for at least 24 hours, evaporated to fume dryness and leached in hydrochloric acid.
2. Manganese oxide, Na_2O, P_2O_5, Cr, Cu, Ni, Sc, V, and Zn were analysed by ICP-OES using a mixed acid digest (Genalysis code A/OES). The pulverized sample was digested in a hydrofluoric–perchloric–nitric acid mixture for at least 24 hours, evaporated to fume dryness, and leached in hydrochloric acid.
3. SiO_2, TiO_2, Al_2O_3, Fe_2O_3, MgO, CaO, K_2O, and S were analysed by ICP-OES using an alkaline oxidative fusion with sodium peroxide in a nickel crucible followed by leaching with hydrochloric acid (Genalysis code DX/OES).
4. Niobium, Ta, and Zr were analysed by ICP-MS using an alkaline oxidative fusion with sodium peroxide in nickel crucibles followed by leaching with hydrochloric acid (Genalysis code DX/MS).

Table 2.4. Secondary codes and qualifiers for regolith composition

Code	*Composition*	*Qualifier*	*Composition*
c	clay	c_b	black soil/ gilgai
		c_c	chlorite
		c_g	glauconite
		c_k	kaolin
		c_i	illite
		c_m	montmorillonite
		c_s	smectite
d	undivided		
e	evaporite	e_a	anhydrite
		e_g	gypsum
		e_h	halite
f	ferruginous	f_g	gossan
		f_h	hematite
		f_l	limonite
		f_o	goethite
g	quartzofeldspathic		
h	heavy mineral	h_a	apatite
		h_g	garnet
		h_i	ilmenite
		h_l	leucoxene
		h_m	magnetite
		h_o	monazite
		h_r	rutile
		h_z	zircon
k	carbonate	k_a	aragonite
		k_c	calcite
		k_d	dolomite
		k_m	magnesite
l	heterogeneous		
m	ferromagnesian		
q	quartz		
r	carbonaceous/organic	r_c	coal
		r_h	humus
		r_p	peat
		r_y	pyritic
t	lithic (rock fragments)		
u	ultramafic		
x	other mineral	x_a	aluminous/bauxitic
		x_i	mica
		x_m	manganese
z	siliceous		

Table 2.5. Tertiary codes and qualifiers for parent rock or cement type

Parent rock or cement		*Parent rock qualifier*	
a	aluminous cement		
c	chemical /biochemical sedimentary deposit	c_c	chert
		c_d	dolomite
		c_i	iron-formation
		c_l	limestone
		c_t	diatomite
h	hypabyssal	h_d	dolerite
		h_p	porphyry
i	iron cement		
k	carbonate cement		
m	metamorphic	m_n	gneiss
		m_p	pelite
		m_m	psammite
		m_s	schist
o	fossiliferous	o_s	shells
		o_c	coral/coralgal
p	plutonic	p_a	alkali granite
		p_r	gabbro
		p_d	diorite
		p_g	granite
		p_m	monzogranite/monzonite
		p_o	granodiorite
		p_s	syenogranite/syenite
		p_t	tonalite
r	duricrust		
s	siliciclastic sedimentary rock	s_c	conglomerate
		s_m	mudstone, siltstone, shale
		s_s	sandstone, arenite, wacke
u	ultramafic	u_d	dunite
		u_k	komatiite
		u_p	peridotite
		u_y	pyroxenite
		u_s	serpentinite/talc rock
v	volcanic	v_a	andesite
		v_b	basalt
		v_d	dacite
		v_r	rhyolite
		v_t	trachyte
		v_v	volcaniclastic
z	silica cement		

5. The precious metals Au, Pd, and Pt were analysed by fire-assay lead collection and ICP-MS analysis (Genalysis code FA*MS).
6. Selenium was analysed by precipitation of selenium metal followed by aqua-regia digestion and ICP-MS analysis (Genalysis code A*MS)
7. Loss on ignition (LOI) was determined by gravimetric means (Genalysis code GRAV).

Analabs

The total sample was dried to 110°C, jaw crushed if necessary, split then milled in a chromium-free mill to a nominal particle size of 90% less than 75 µm. An analytical pulp of approximately 200 g was subsampled from the bulk and the milled residue and any split retained for future reference. All the preparation equipment was flushed with barren feldspar prior to the commencement of the job and after each batch.

The following analytical schemes were used:

1. Silica, TiO_2, Al_2O_3, Fe_2O_3, MnO, MgO, CaO, Na_2O, K_2O, and P_2O_5 were measured by X-ray fluorescence spectrometry (XRF) on a glass fusion disc (Analabs code X408).
2. Loss on ignition (LOI) was determined gravimetrically, by heating the sample to 1000°C (Analabs code V955).
3. A series of trace elements were measured by ICP-MS, following sample digestion with nitric, hydrochloric, hydrofluoric, and perchloric acids (Analabs code G104). Elements measured include: Ag, As, Ba, Be, Bi, Cd, Ce, Co, Ga, In, La, Li, Mo, Nb, Ni, Pb, Rb, Sb, Sc, Sn, Ta, Th, U, W, and Y (Analabs code M104).
4. The G104 digest (at 3. above) was used for the analysis of Sr, V, and Zr by ICP-OES (Analabs code I104).
5. An aliquot of the G104 digest (at 3. above) was analysed by atomic absorption spectrometry (AAS) for Cr, Cu, and Zn (Analabs code A104).
6. The volatile metals Se and Te were analysed by hydride generation AAS (Analabs code H109), from a chromate-enhanced hydrochloric and nitric acid digestion carried out at low temperature (Analabs code G109).
7. Sulfur (as S) was evolved at high temperature in a stream of oxygen, and the resultant gas was measured in an infrared cell (Analabs code V821).
8. A 50 g subsample of the assay pulp was fused in a lead collection fire assay. The prill was dissolved in aqua regia (i.e. hydrochloric and nitric acid) and the resultant solution presented to an ICP-MS (Analabs code F627) for analysis of Au, Pd, and Pt.

Amdel Laboratories

Following oven drying, an aliquot of each sample was sieved to between 2 and 0.45 mm. This material was pulverized to <75 µm in a chrome-free bowl pulverizer; imparted contamination during milling estimated by the manufacturer is 50 ppm Mn and 5000 ppm Fe, with no detectable contamination for Co, Cu, Mo, Ni, Pb, V, or Zn.

Six analytical methods were used:

1. Silica, TiO_2, Al_2O_3, Fe_2O_3, MnO, MgO, CaO, Na_2O, K_2O, and P_2O_5 were analysed by ICP-OES following a lithium metaborate fusion and dilute hydrochloric acid digestion (Amdel code IC4).
2. Silver, As, Bi, Cd, Ce, Co, Cu, Ga, In, La, Mo, Nb, Pb, Rb (up to 20 ppm; IC4M >20 ppm), Sb, Se, Sn, Sr (up to 500 ppm; IC3E >500 ppm), Te, Th, U, W, and Y were analysed by ICP-MS following mixed-acid sample digestion (hydrofluoric–perchloric–nitric–hydrochloric) for 24 hours. Samples were evaporated to fume dryness and dissolved in hydrochloric acid prior to analysis (Amdel code IC3M).
3. Barium, Be, Cr (up to 100 ppm; IC4E >100 ppm), Li, Ni, S (up to 5%; analysis by Leco (Amdel code VOL2) >5%), Sc, V, and Zn were analysed by ICP-OES (Amdel code IC3E). Samples were digested using a hydrofluoric–perchloric–nitric–hydrochloric acid mixture for 24 hours, then evaporated to fume dryness and dissolved in dilute hydrochloric acid.
4. Tantalum and Zr were analysed by ICP-MS following a lithium metaborate fusion and dilute hydrochloric acid digestion (Amdel code IC4M).
5. Gold, Pt, and Pd were collected in a lead collection fire-assay fusion. Following cupellation, the prill was dissolved in aqua regia (i.e. hydrochloric and nitric acids), then analysed by graphite furnace AAS (Amdel code FA3).
6. Loss on ignition (LOI) was determined by gravimetric means (Amdel code GRAV7).

Determination of regolith pH and total dissolved solids

The acidity–alkalinity (pH) and total dissolved solids (TDS) of all regolith samples were measured at the GSWA Carlisle base. For both types of measurements, a subsample was mixed with deionized water in the ratio of 1:5, then shaken vigorously. After standing overnight, the pH was measured using a portable Jenway pH meter, calibrated using standard solutions of pH=4 and pH=7. The electrode was rinsed in deionized water between each measurement of unknowns. The conductivity of each sample (i.e. a measure of the TDS) was made using a SCAN4 conductivity meter, calibrated using a buffer solution of 11.67 millisiemens/centimetre (mS/cm). Electrodes were rinsed between every measurement of unknowns.

References

ANAND, R. R., SMITH, R. E., PHANG, C., WILDMAN, J. E., ROBERTSON, I. D. M., and MUNDY, T. J., 1993, Geochemical exploration in complex lateritic environments of the Yilgarn Craton, Western Australia: Australia CSIRO, Division of Exploration and Mining, Report 442R, 297p.

ANAND, R. R., and SMITH, R. E., 1994, Classification, origin and geochemistry of laterites and ferruginous regolith materials in the Yilgarn Craton — implications for exploration: Geological Society of Australia; 12th Australian Geological Convention, Perth, W.A., 1994; Abstracts no. 37, p. 7–8.

BRADLEY, J. J., SANDERS, A. J., VARGA, Z. S., and STOREY, J. M., 1995, Geochemical mapping of the Leonora 1:250 000 sheet: Western Australia Geological Survey, 1:250 000 Regolith Geochemistry Series Explanatory Notes, 86p.

COKER, J., FAULKNER, J. A., and SANDERS, A. J., 1998, Geochemical mapping of the Turee Creek 1:250 000 sheet: Western Australia Geological Survey, 1:250 000 Regolith Geochemistry Series Explanatory Notes, 65p.

HOCKING, R. M., LANGFORD, R. L., THORNE, A. M., SANDERS, A. J., MORRIS, P. A., STRONG, C. A., and GOZZARD, J. R., 2001, A classification system for regolith in Western Australia: Western Australian Geological Survey, Record 2001/4, 22p.

KOJAN, C. J., and FAULKNER, J. A., 1994, Geochemical mapping of the Menzies 1:250 000 sheet: Western Australia Geological Survey, 1:250 000 Regolith Geochemistry Series Explanatory Notes, 55p.

MORRIS, P. A., SANDERS, A. J., and FAULKNER, J. A., 1997, Geochemical mapping of the Nabberu 1:250 000 sheet: Western Australia Geological Survey, 1:250 000 Regolith Geochemistry Series Explanatory Notes, 63p.

MORRIS, P. A., COKER, J., and FAULKNER, J. A.,1998, Geochemical mapping of the Mount Egerton 1:250 000 sheet: Western Australia Geological Survey, 1:250 000 Regolith Geochemistry Series Explanatory Notes, 63p.

PYE, K. J., COKER, J., FAULKNER, J. A., and SANDERS, A. J., 1998, Geochemical mapping of the Edmund 1:250 000 sheet: Western Australia Geological Survey, 1:250 000 Regolith Geochemistry Series Explanatory Notes, 51p.

SANDERS, A. J., FAULKNER, J. A., COKER, J., and MORRIS, P. A., 1998, Geochemical mapping of the Glenburgh 1:250 000 sheet: Western Australia Geological Survey, 1:250 000 Regolith Geochemistry Series Explanatory Notes, 33p.

SHAW, W. J., KHOSROWSHAHI, S., HORTON, J., and WALTHO, A., 1998, Predicting and monitoring variability in sampling, sample preparation, and assaying, *in* More meaningful sampling in the mining industry *edited by* B. DAVIS and S. E. HO: Australian Institute of Geoscientists, Bulletin 22, p. 11–19.

THOMPSON, M., and RAMSEY, M. H., 1995, Quality concepts and practices applied to sampling — an exploratory study: Analyst, v. 120, p. 261–270.

Figures

Speciality maps — hardcopy and digital

62. Acidity–alkalinity (pH) on NICHOLLS
63. Combined first vertical derivative Bouguer gravity (colour) and TMI image (intensity), and interpreted lineaments on NICHOLLS
64. Chalcophile index (total) on NICHOLLS
65. Base metal index (total) on NICHOLLS
66. Ferro-alloy index (total) on NICHOLLS
67. Normalized arsenic (partial) on NICHOLLS
68. Normalized antimony (partial) on NICHOLLS
69. Normalized chalcophile index (partial) on NICHOLLS

Element-distribution maps (pdfs) — digital only

70. SiO_2 (total)
71. Si (partial)
72. Ag (total)
73. Ag (partial)
74. Be (total)
75. Be (partial)
76. Bi (total)
77. Bi (partial)
78. Co (total)
79. Co (partial)
80. Dy (total)
81. Dy (partial)
82. Er (total)
83. Er (partial)
84. Ga (total)
85. Ga (partial)
86. Gd (total)
87. Gd (partial)
88. Ge (total)
89. Ge (partial)
90. In (total)
91. In (partial)
92. La (total)
93. La (partial)
94. Li (total)
95. Li (partial)
96. Lu (total)
97. Lu (partial)
98. Nb (total)
99. Nb (partial)
100. Nd (total)
101. Nd (partial)
102. Sc (total)
103. Sc (partial)
104. Sm (total)
105. Sm (partial)
106. Sn (total)
107. Sn (partial)
108. Ta (total)
109. Ta (partial)
110. Te (total)
111. Te (partial)
112. Tl (total)
113. Tl (partial)
114. Y (total)
115. Y (partial)
116. Yb (total)
117. Yb (partial)
118. Zr (total)
119. Zr (partial)

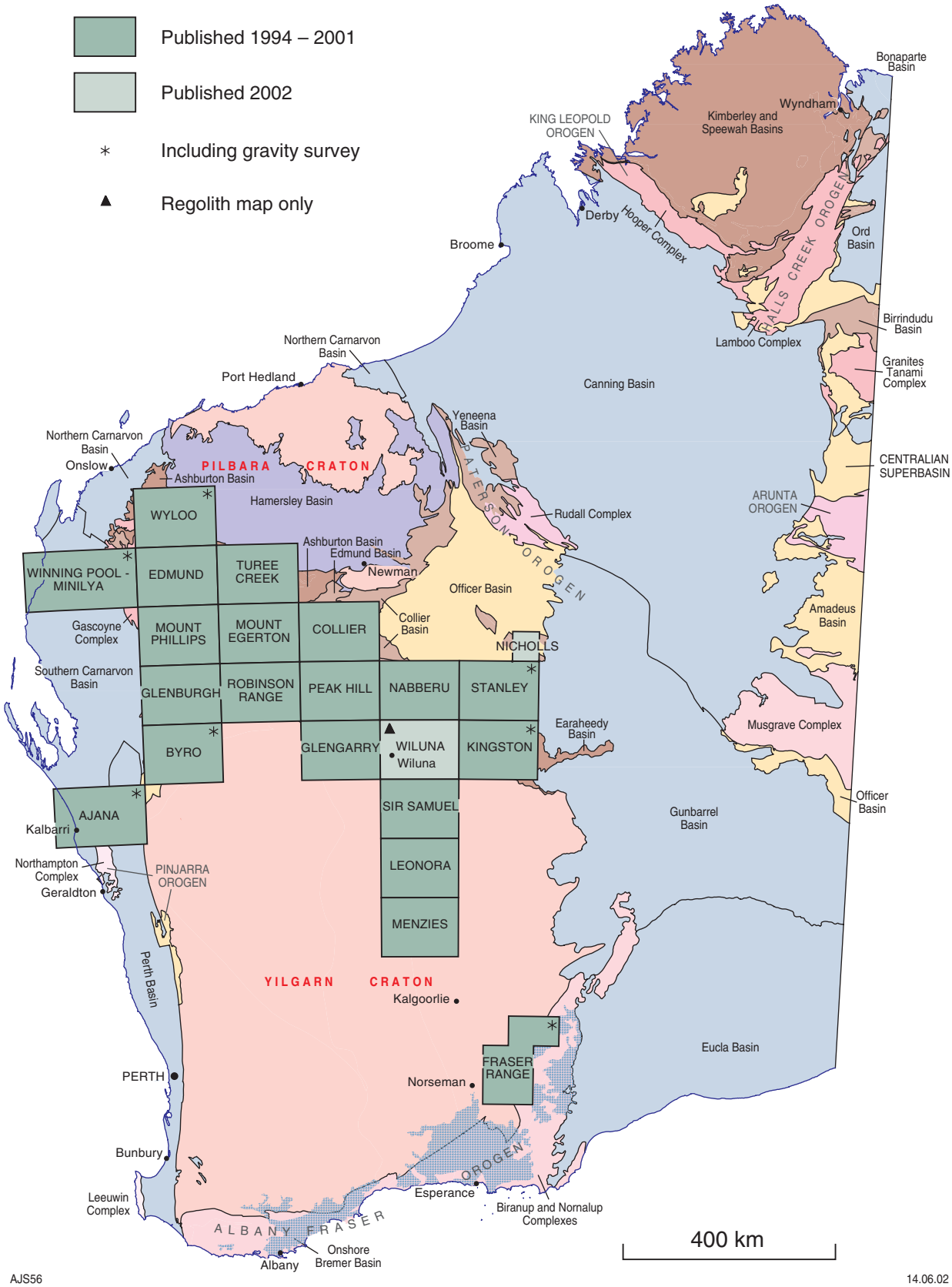

Figure 1. Status of regional regolith and geochemical mapping program maps and Explanatory Notes

INTERPRETED BEDROCK GEOLOGY

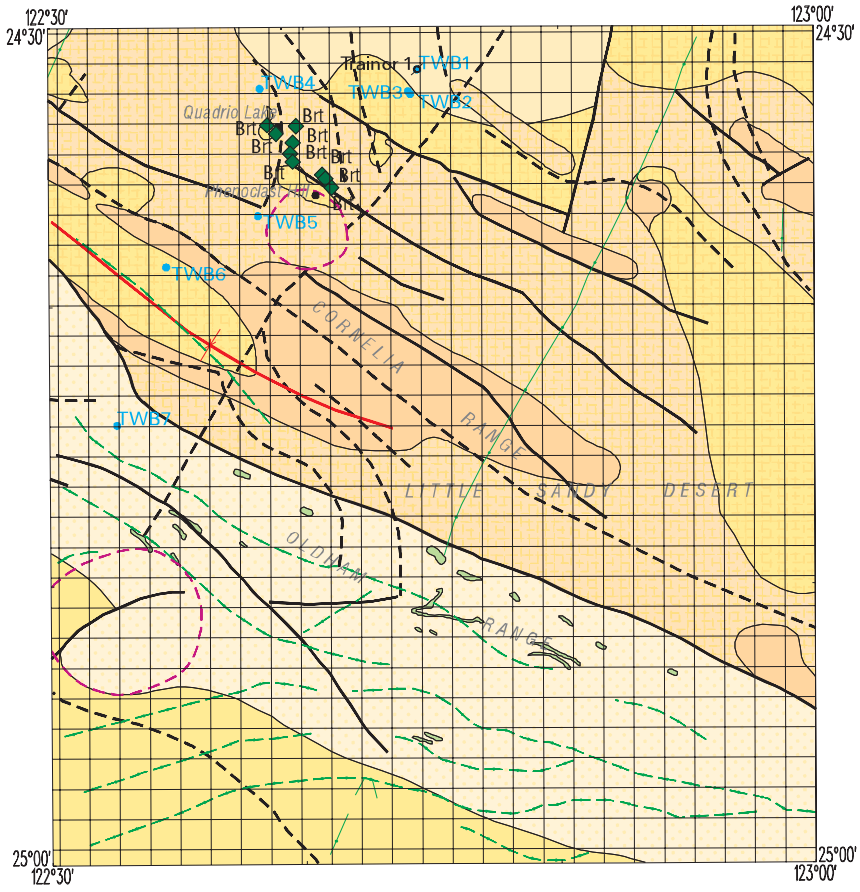

Geological interpretation after Hocking et al. (2000), Myers and Hocking (1998), and Williams (1995)

SCALE 1:500 000

0 5 10 15 20 km

NICHOLLS

SHEET 3448

First Edition 2002

Figure 2

INTERPRETED BEDROCK GEOLOGY

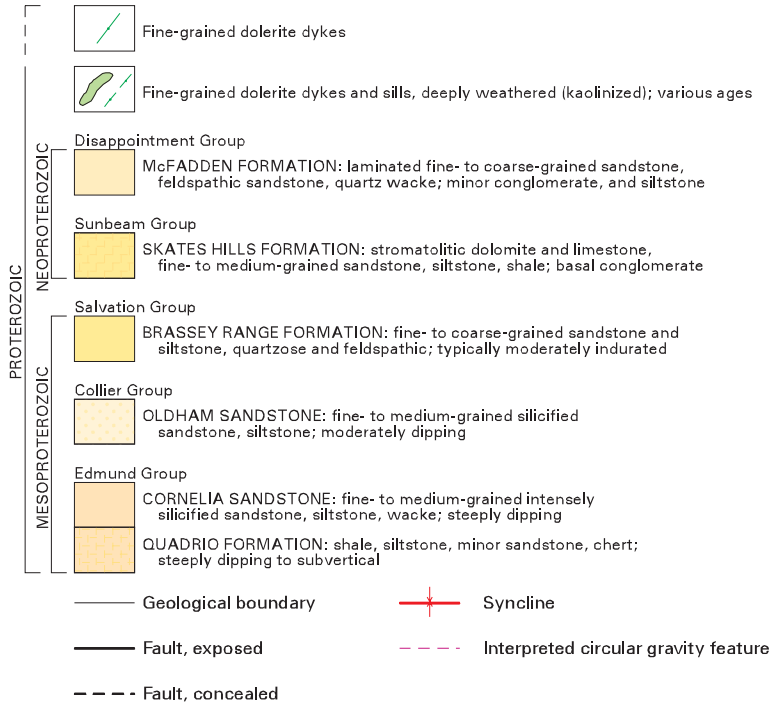

SYMBOLS

	Track
	Watercourse
• *Phenoclast Hill*	Locality
• TWB4	Water bore
Trainor 1	Stratigraphic drillhole
◆	Mineral occurrence
Barite..... Brt	

NICHOLLS

SHEET 3448

First Edition 2002

Figure 2

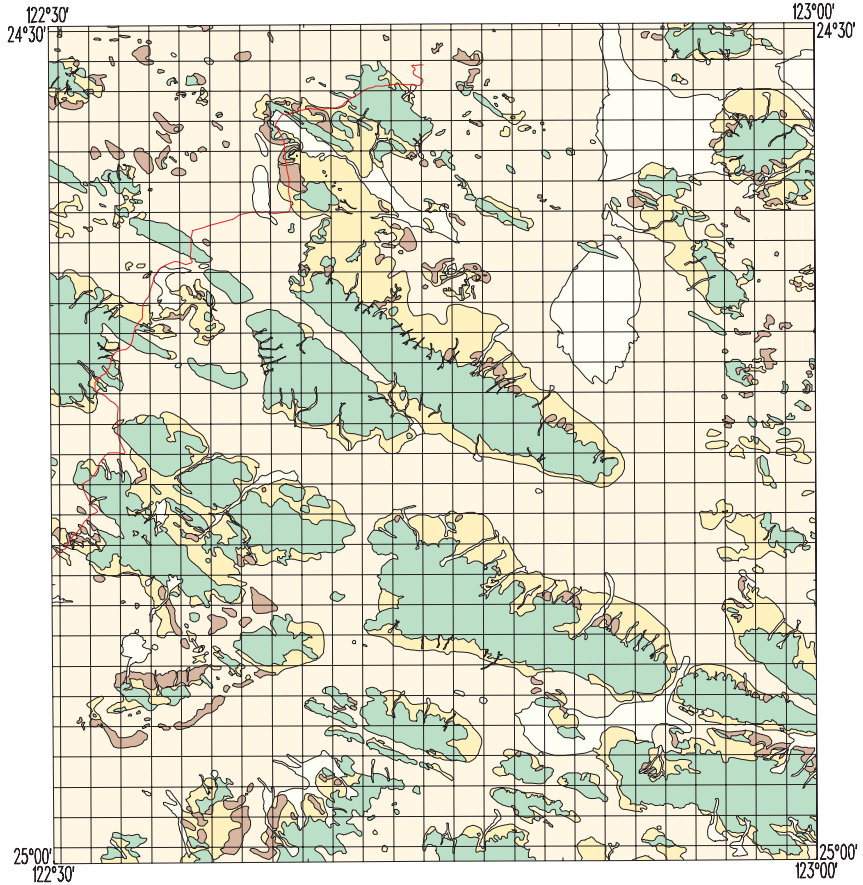

SCALE 1:500 000

0 5 10 15 20 km

GENERALIZED REGOLITH

- Residual
- Exposed
- Colluvial (includes low-gradient slope)
- Alluvial and lacustrine
- Sandplain
- Regolith boundary
- Track

NICHOLLS

SHEET 3448

First Edition 2002

Figure 3

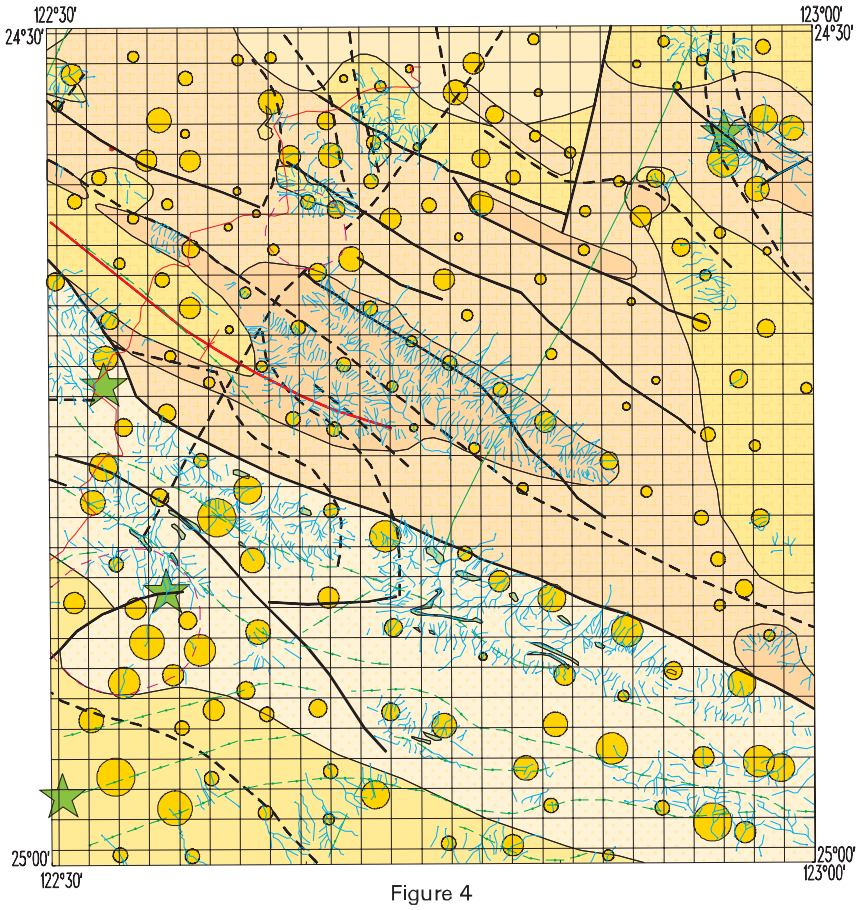

Figure 4

TiO_2

Total digest

Maximum value:
1.4 %

1.0 %

0.6 %

0.1 %

Below 0.1 % theoretical detection limit

> 1.0 %

SCALE 1:500 000

0 5 km

NICHOLLS

3448

First Edition 2002

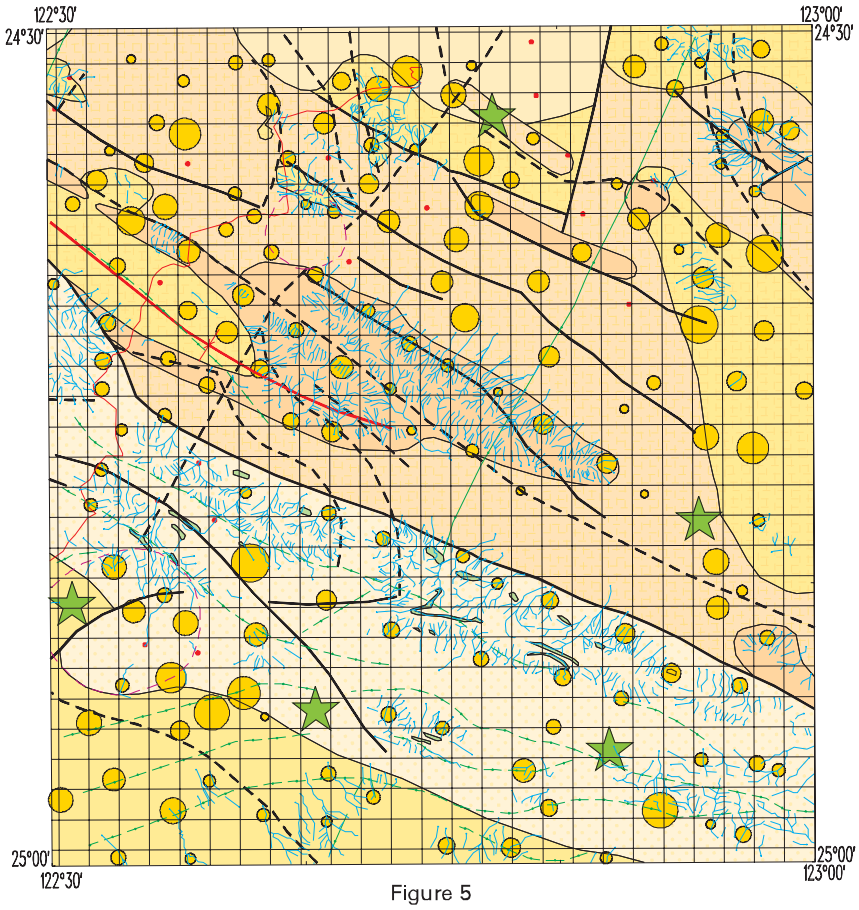

Figure 5

Ti

Partial digest

Maximum value:
17.7 ppm

13.4 ppm

6.8 ppm

0.2 ppm

Below 0.2 ppm theoretical detection limit

> 13.4 ppm

SCALE 1:500 000

0 5 km

NICHOLLS

3448

First Edition 2002

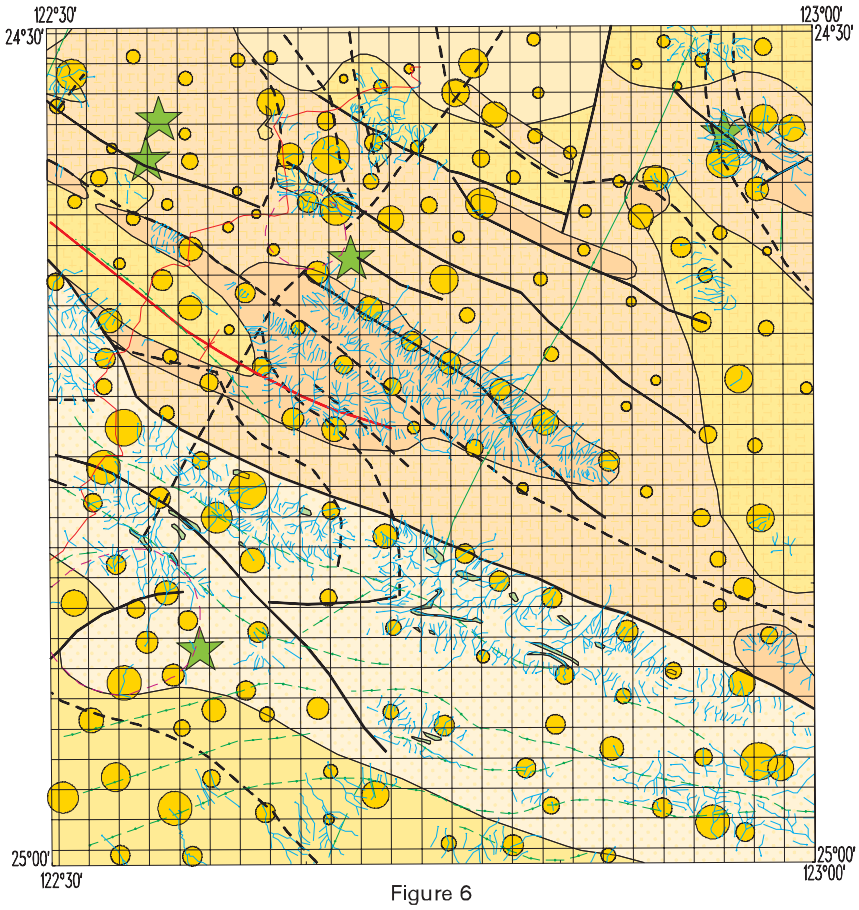

Figure 6

Al_2O_3
Total digest

Maximum value:
17.42 %

12.98 %
7.17 %
1.35 %

Below 0.04 %
theoretical
detection limit

> 12.98 %

SCALE 1:500 000
0 5 km

NICHOLLS

3448
First Edition 2002

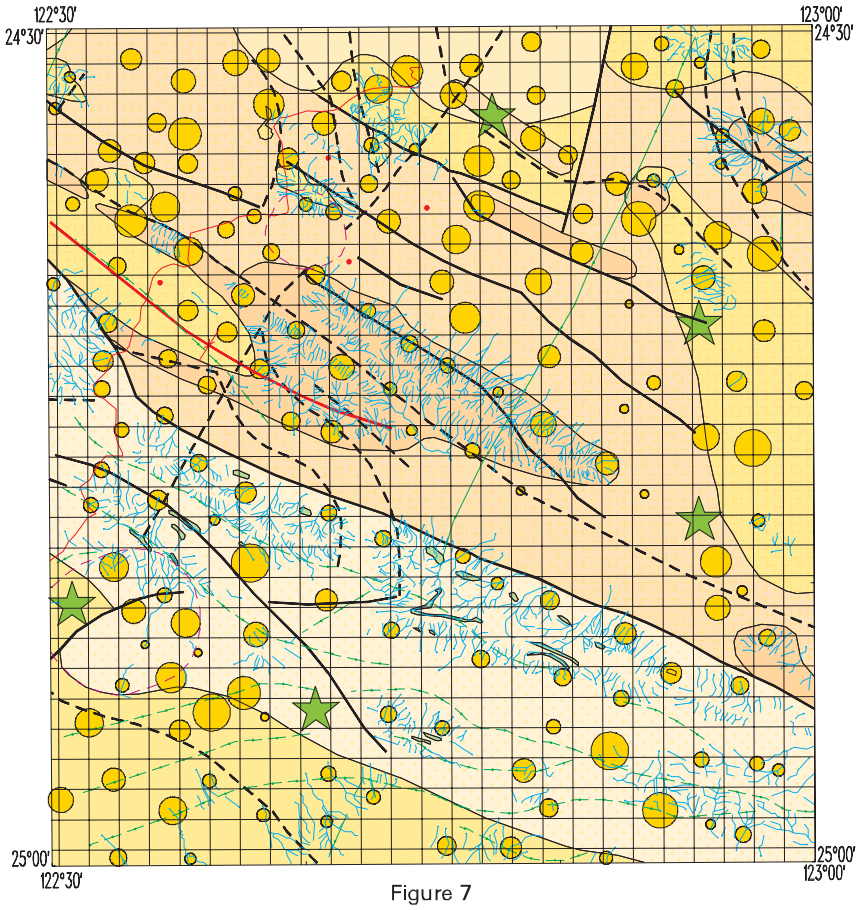

Figure 7

Al
Partial digest

Maximum value:
2714.4 ppm

1914.2 ppm
957.2 ppm
0.2 ppm

Below 0.2 ppm
theoretical
detection limit

> 1914.2 ppm

SCALE 1:500 000
0 5 km

NICHOLLS

3448
First Edition 2002

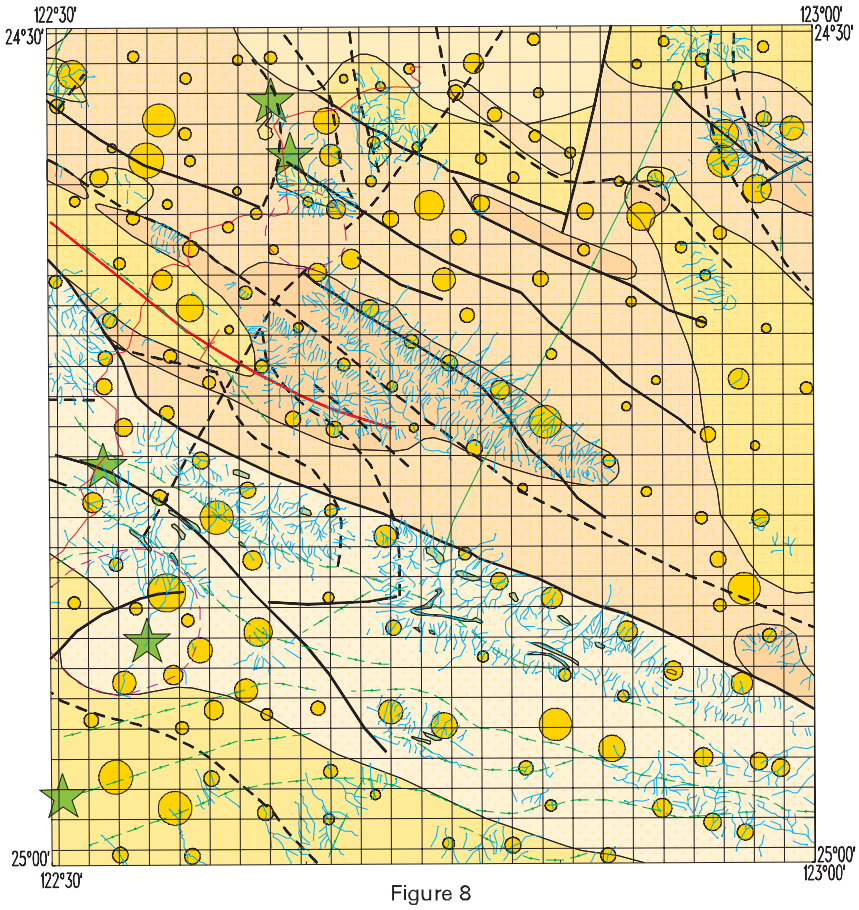

Figure 8

Fe_2O_3
Total digest

Maximum value:
29.94 %

22.71 %
11.82 %
0.92 %

Below 0.02 %
theoretical
detection limit

> 22.71 %

SCALE 1:500 000
0 5 km

NICHOLLS

3448
First Edition 2002

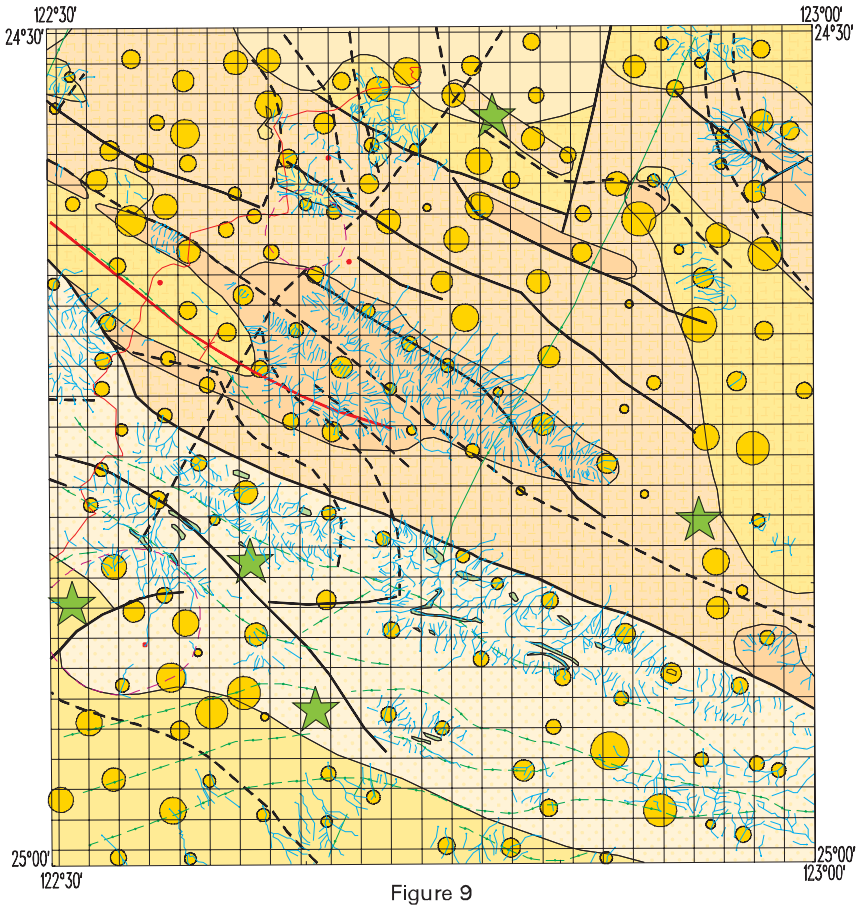

Figure 9

Fe
Partial digest

Maximum value:
1017.1 ppm

758.6 ppm
379.4 ppm
0.2 ppm

Below 0.2 ppm
theoretical
detection limit

> 758.6 ppm

SCALE 1:500 000
0 5 km

NICHOLLS

3448
First Edition 2002

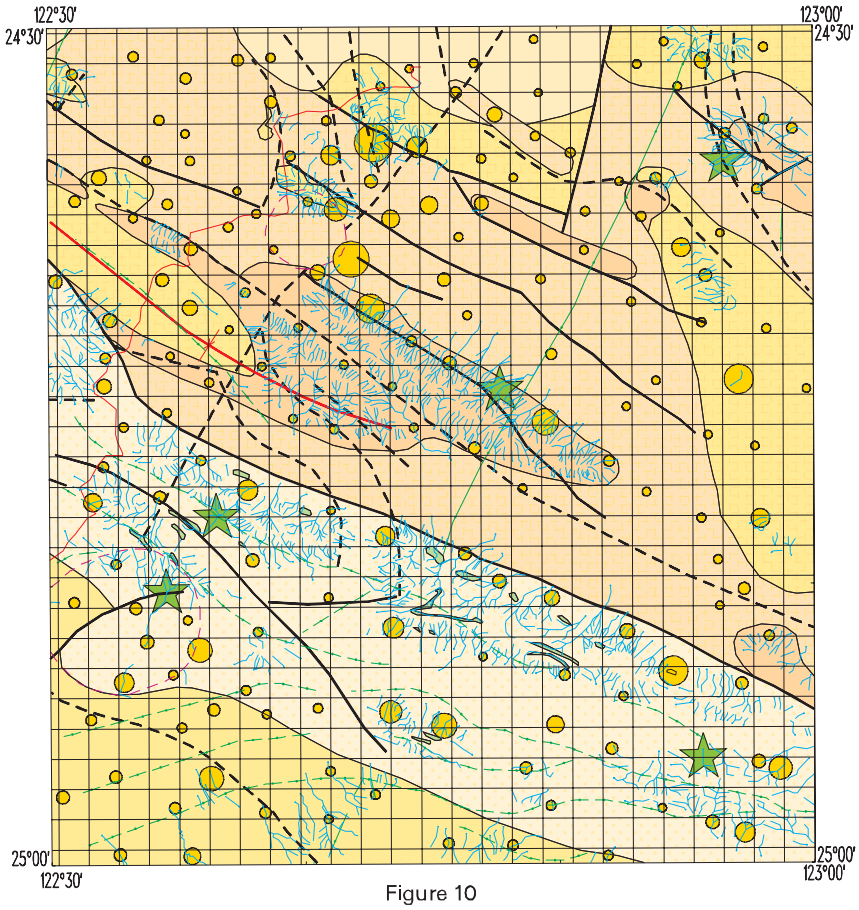

Figure 10

MnO
Total digest

Maximum value:
0.422 %

0.175 %
0.089 %
0.003 %

Below 0.001 %
theoretical
detection limit

> 0.175 %

SCALE 1:500 000
0 5 km

NICHOLLS

3448
First Edition 2002

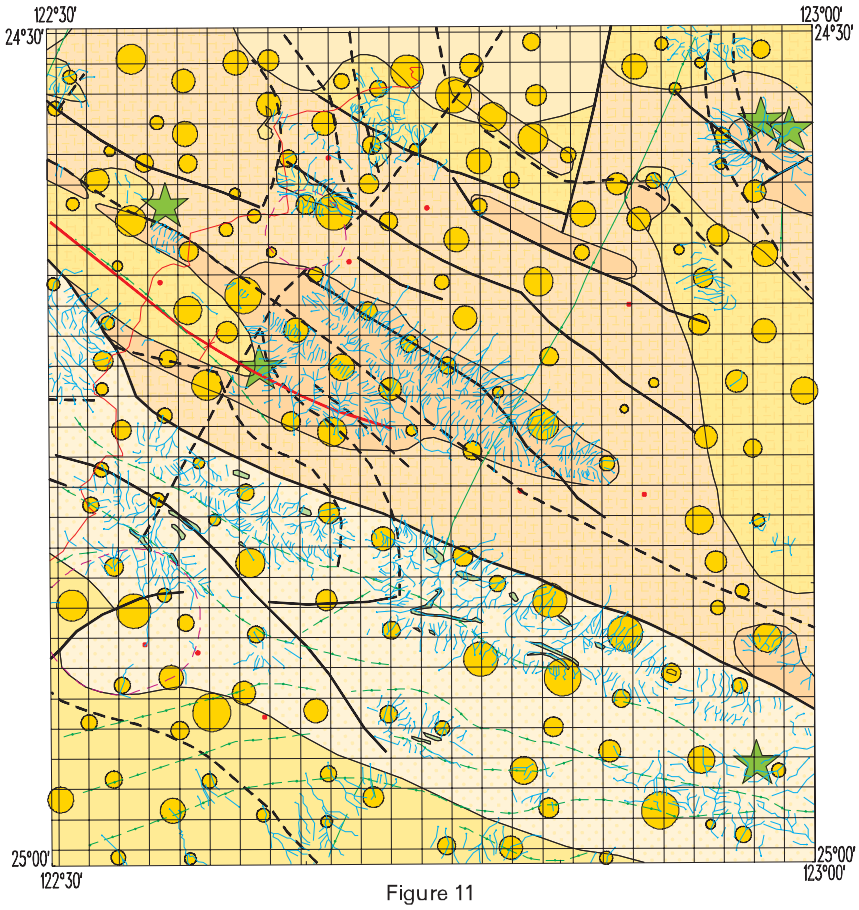

Figure 11

Mn
Partial digest

Maximum value:
14.4 ppm

8.6 ppm
4.4 ppm
0.2 ppm

Below 0.2 ppm
theoretical
detection limit

> 8.6 ppm

SCALE 1:500 000
0 5 km

NICHOLLS

3448
First Edition 2002

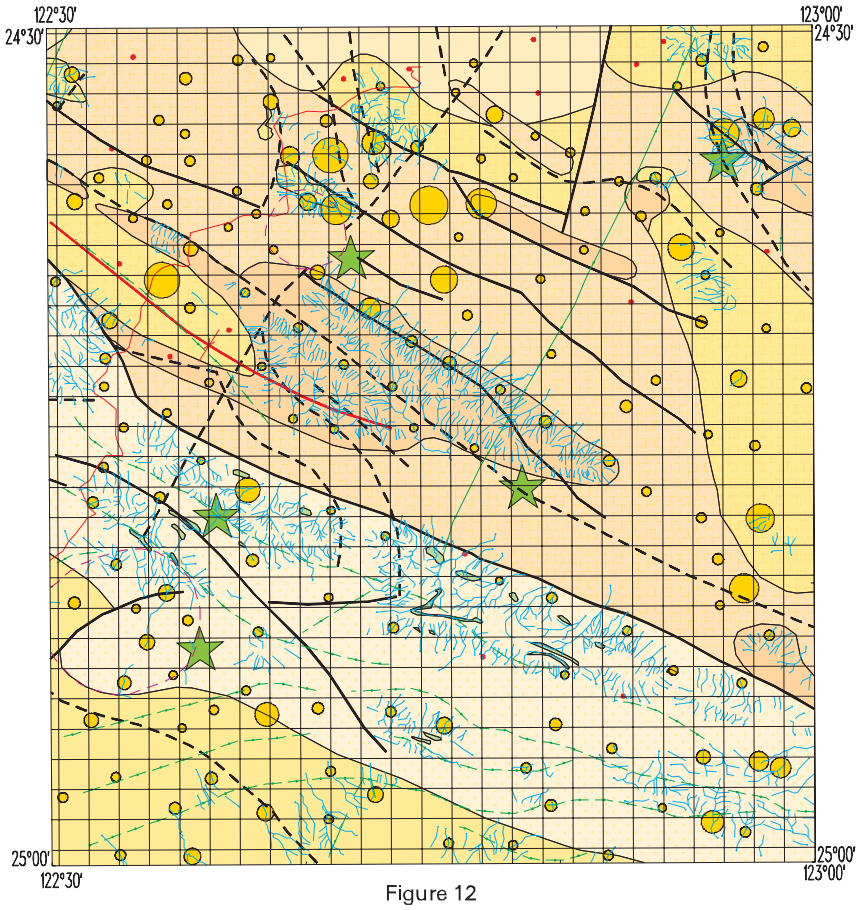

Figure 12

MgO
Total digest

Maximum value:
2.55 %

0.74 %
0.38 %
0.02 %

Below 0.02 %
theoretical
detection limit

> 0.74 %

SCALE 1:500 000
0 5 km

NICHOLLS

3448
First Edition 2002

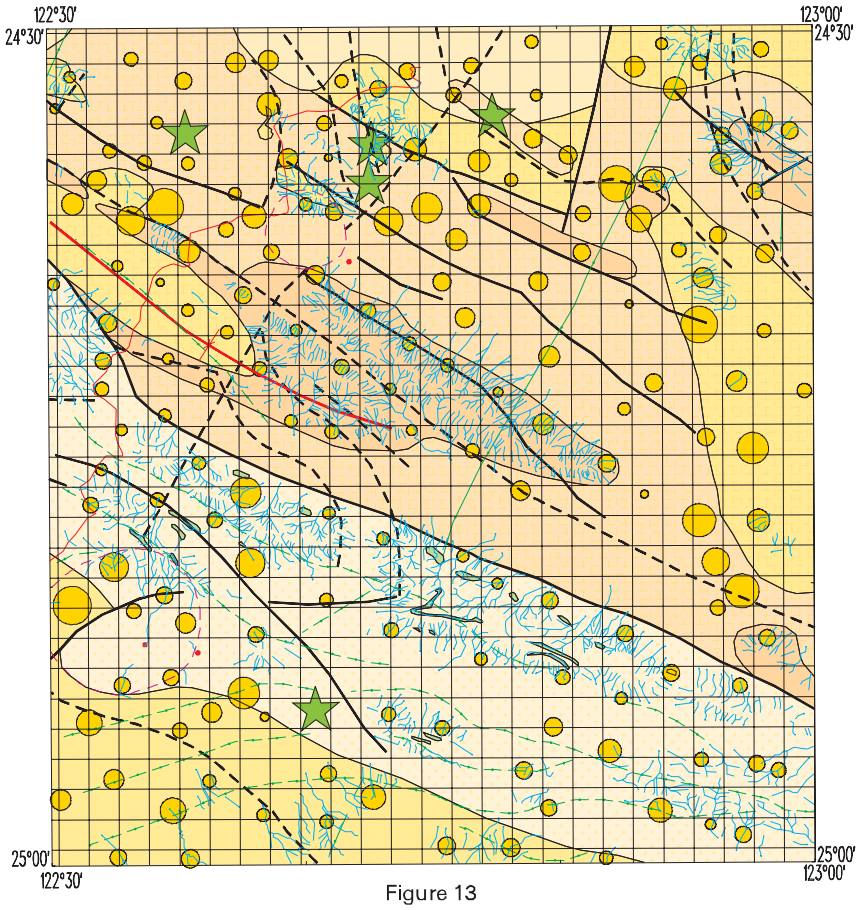

Figure 13

Mg
Partial digest

Maximum value:
101.2 ppm

51.9 ppm
26.1 ppm
0.2 ppm

Below 0.2 ppm
theoretical
detection limit

> 51.9 ppm

SCALE 1:500 000
0 5 km

NICHOLLS

3448
First Edition 2002

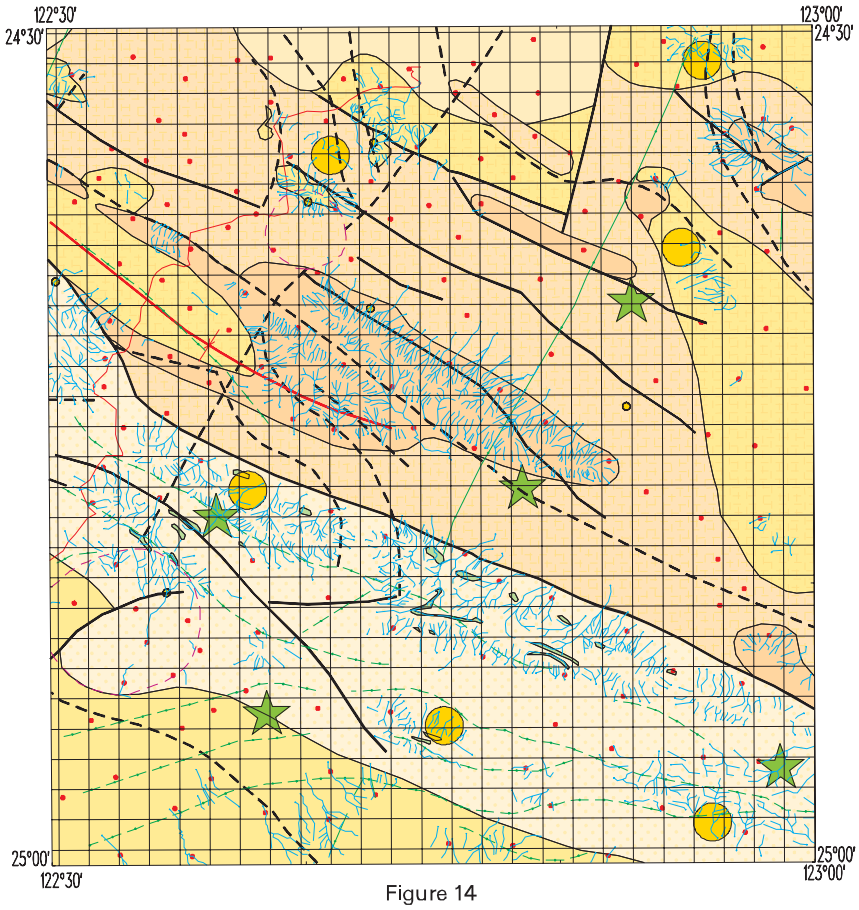

Figure 14

CaO
Total digest

Maximum value:
0.8 %

0.3 %

0.2 %

Below 0.2 %
theoretical
detection limit

> 0.3 %

SCALE 1:500 000
0 5 km

NICHOLLS

3448
First Edition 2002

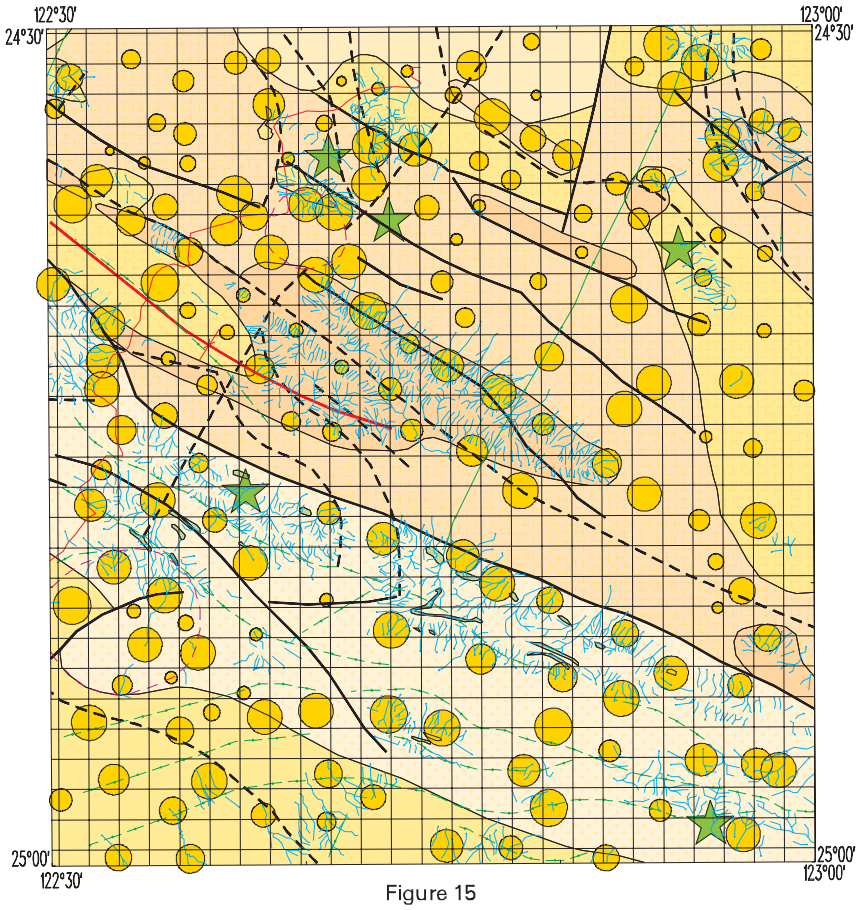

Figure 15

Ca
Partial digest

Maximum value:
246.0 ppm

206.7 ppm

108.6 ppm

10.5 ppm

Below 0.2 ppm
theoretical
detection limit

> 206.7 ppm

SCALE 1:500 000
0 5 km

NICHOLLS

3448
First Edition 2002

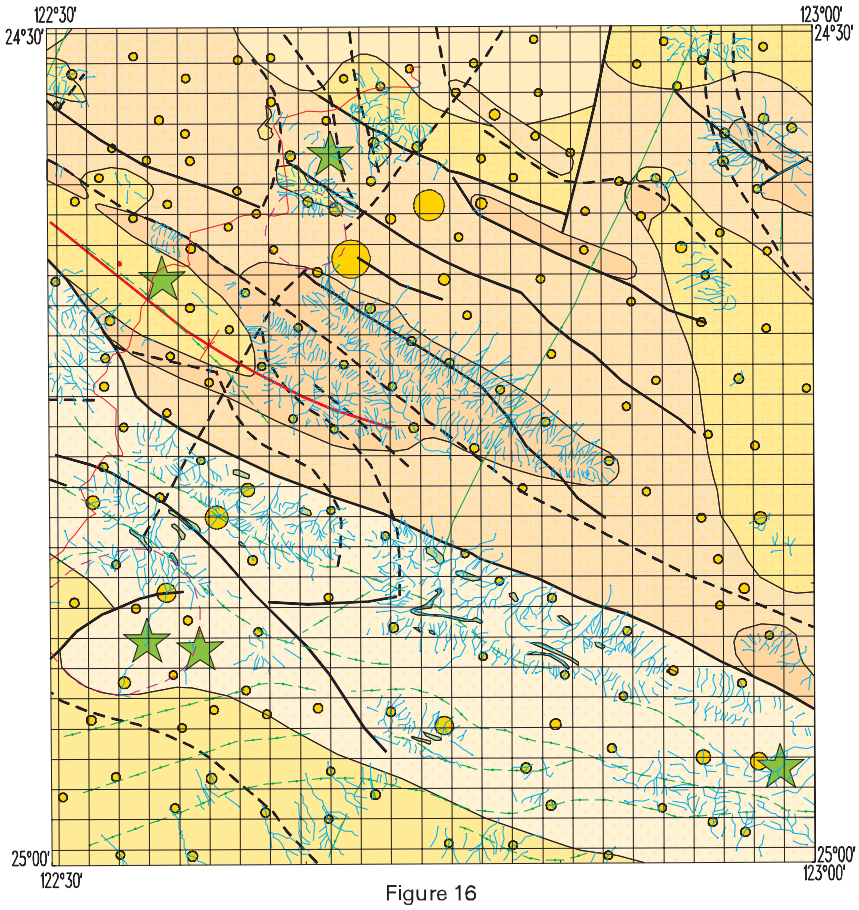

Figure 16

Na_2O

Total digest

Maximum value:
0.623 %

0.311 %

0.158 %

0.004 %

Below 0.004 %
theoretical
detection limit

> 0.311 %

SCALE 1:500 000

0 5 km

NICHOLLS

3448

First Edition 2002

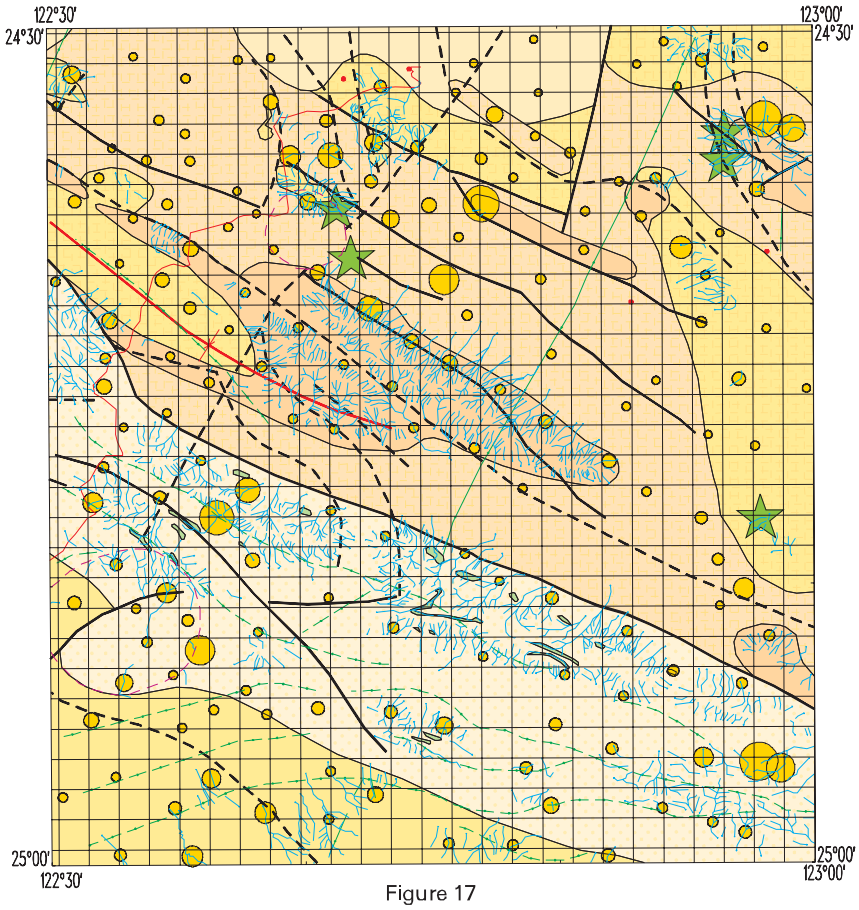

Figure 17

K_2O

Total digest

Maximum value:
4.23 %

2.02 %

1.03 %

0.04 %

Below 0.04 %
theoretical
detection limit

> 2.02 %

SCALE 1:500 000

0 5 km

NICHOLLS

3448

First Edition 2002

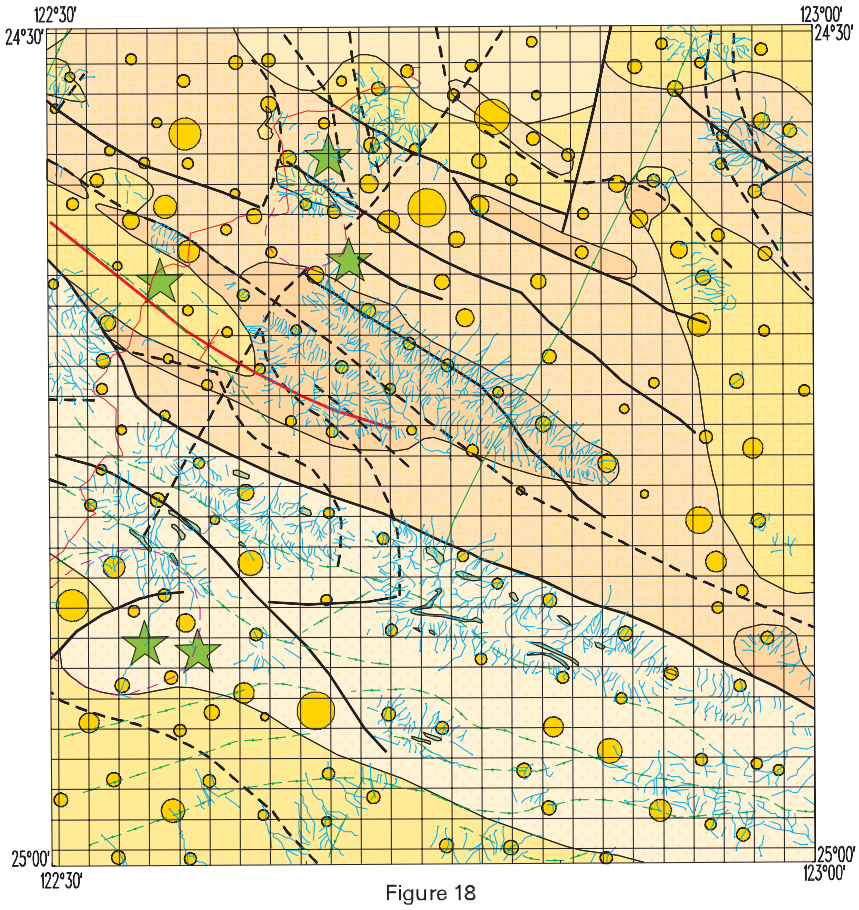

Figure 18

K

Partial digest

Maximum value:
517.6 ppm

210.0 ppm

108.3 ppm

6.5 ppm

Below 0.2 ppm
theoretical
detection limit

> 210.0 ppm

SCALE 1:500 000

0 5 km

NICHOLLS

3448

First Edition 2002

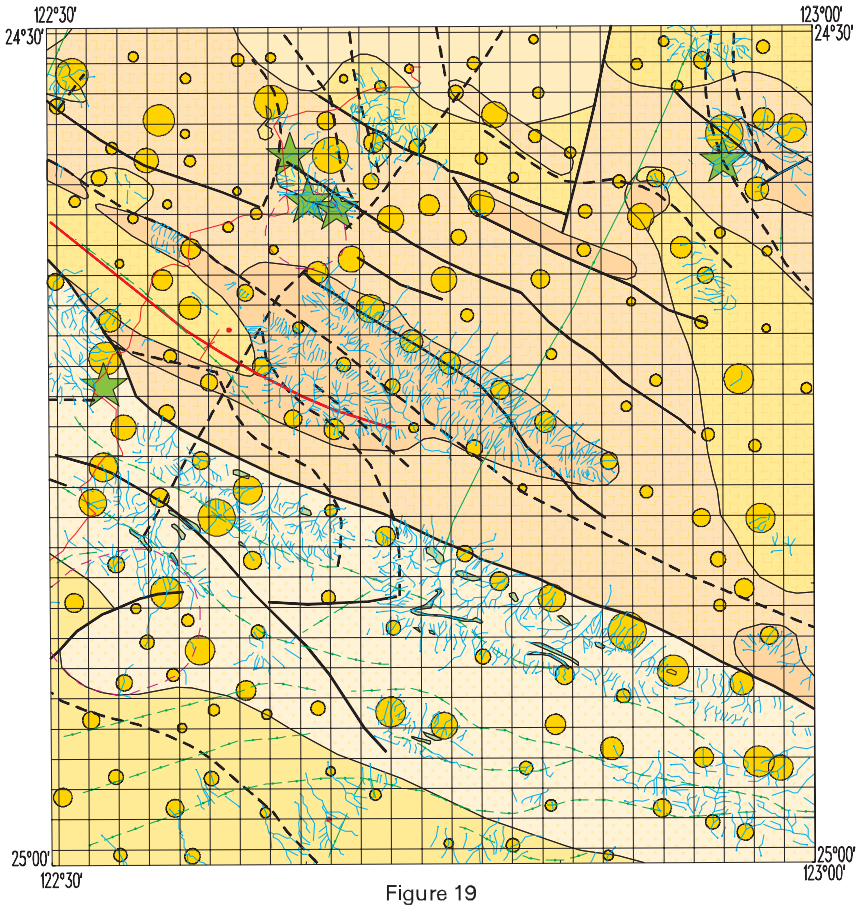

Figure 19

P_2O_5
Total digest

Maximum value:
0.208 %

0.085 %
0.046 %
0.006 %

Below 0.006 %
theoretical
detection limit

> 0.085 %

SCALE 1:500 000
0 5 km

NICHOLLS

3448
First Edition 2002

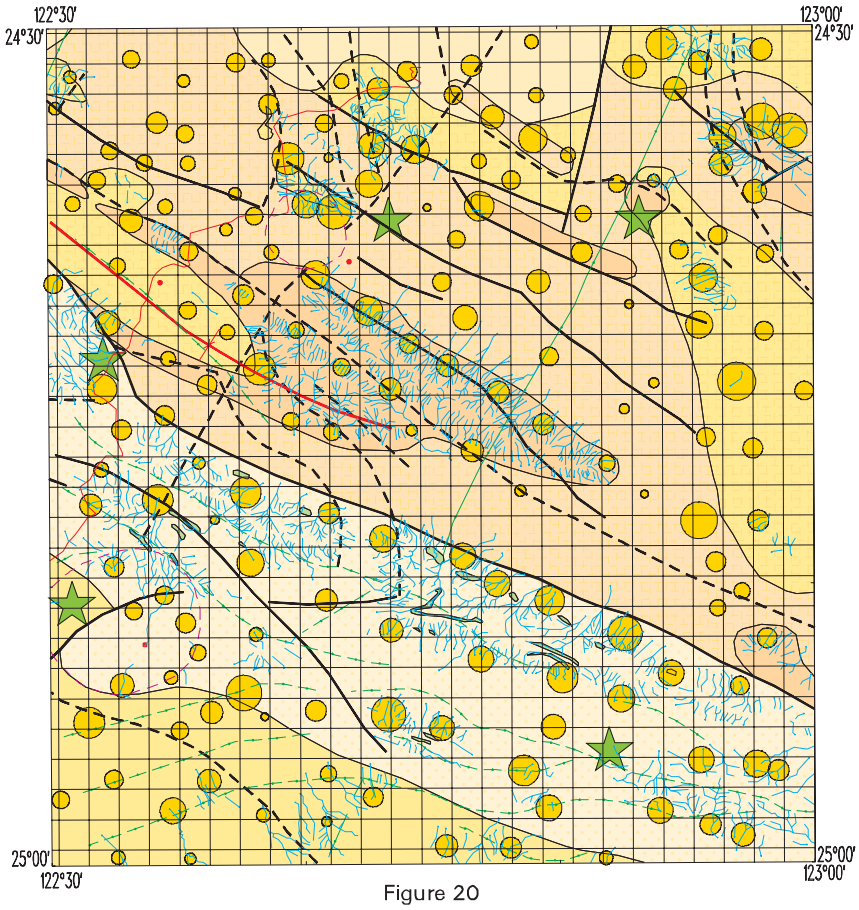

Figure 20

P
Partial digest

Maximum value:
58 ppm

27 ppm
15 ppm
2 ppm

Below 2 ppm
theoretical
detection limit

> 27 ppm

SCALE 1:500 000
0 5 km

NICHOLLS

3448
First Edition 2002

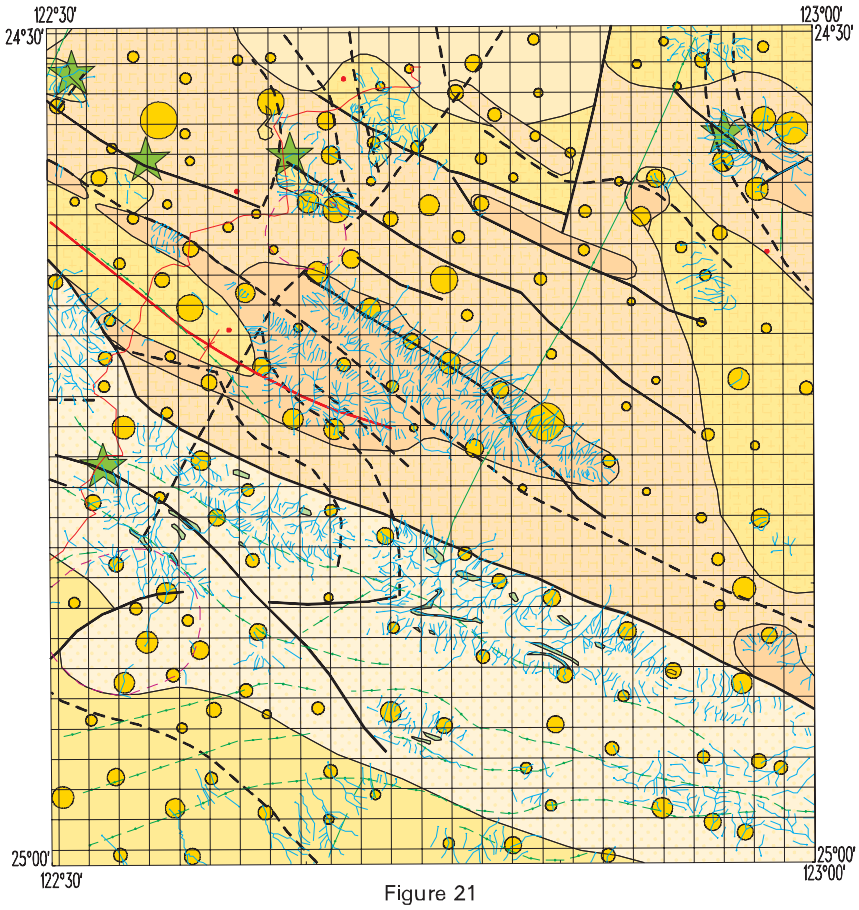

Figure 21

As
Total digest

Maximum value:
49 ppm

27 ppm
14 ppm
1 ppm

Below 1 ppm
theoretical
detection limit

> 27 ppm

SCALE 1:500 000
0 5 km

NICHOLLS

3448
First Edition 2002

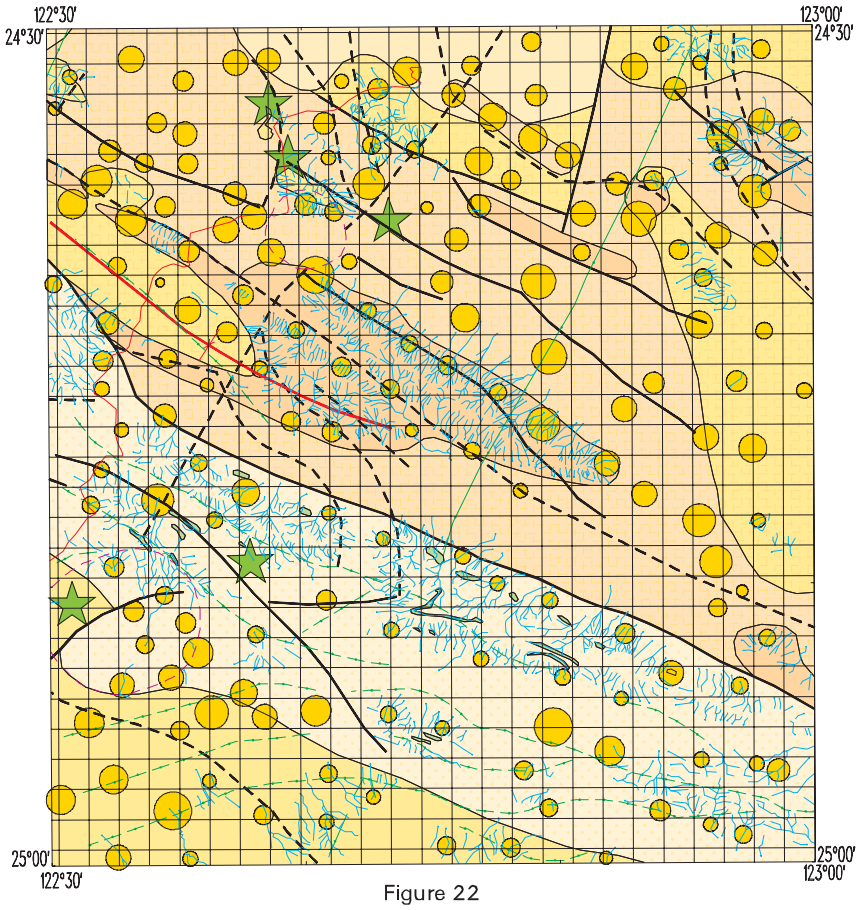

Figure 22

As
Partial digest

Maximum value:
361 ppb

295 ppb
151 ppb
7 ppb

Below 2 ppb
theoretical
detection limit

> 295 ppb

SCALE 1:500 000
0 5 km

NICHOLLS

3448
First Edition 2002

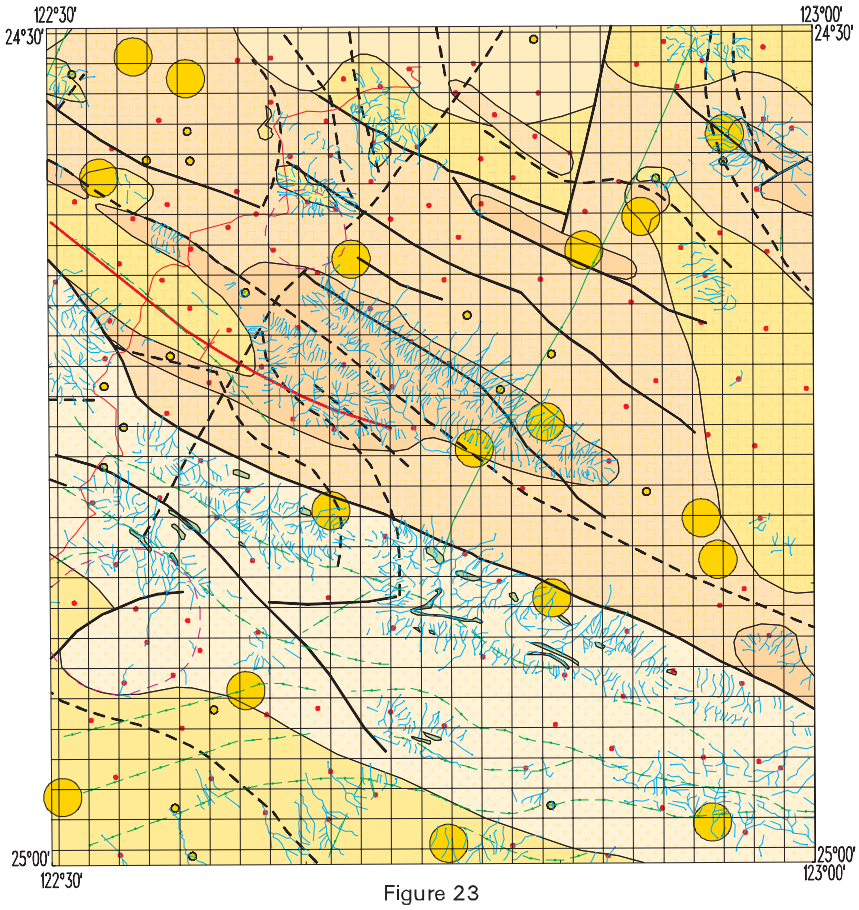

Figure 23

Au
Total digest

Maximum value:
2 ppb

2 ppb

1 ppb

Below 1 ppb
theoretical
detection limit

SCALE 1:500 000
0 5 km

NICHOLLS

3448
First Edition 2002

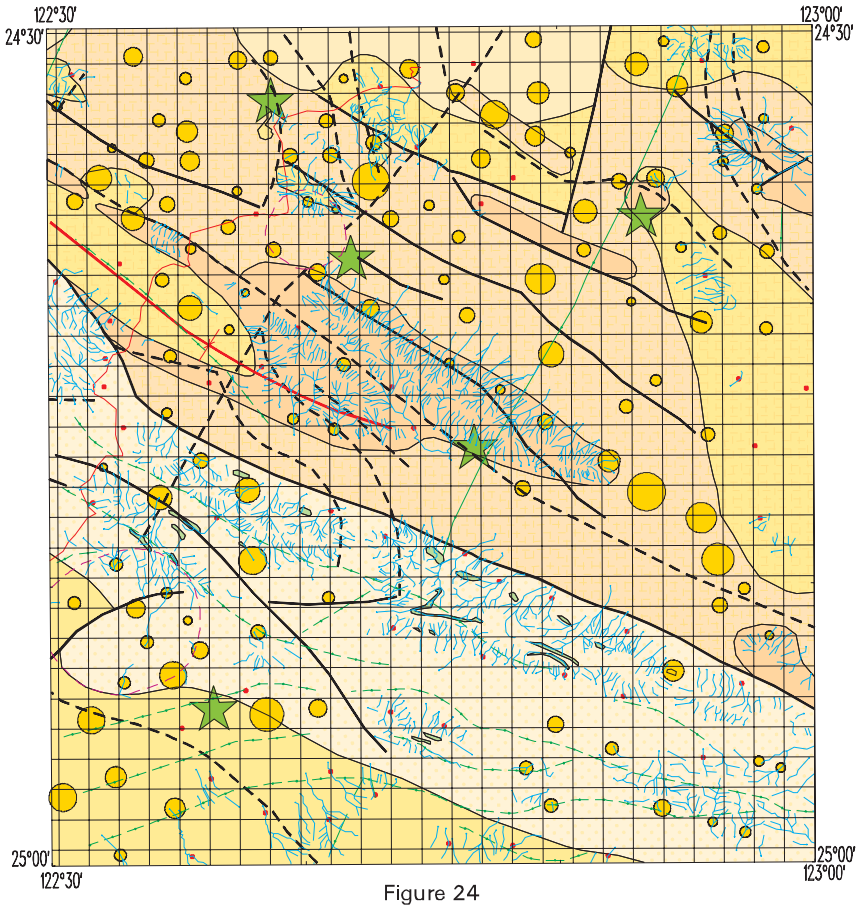

Figure 24

Au
Partial digest

Maximum value:
0.81 ppb

0.41 ppb

0.23 ppb

0.05 ppb

Below 0.05 ppb
theoretical
detection limit

> 0.41 ppb

SCALE 1:500 000
0 5 km

NICHOLLS

3448
First Edition 2002

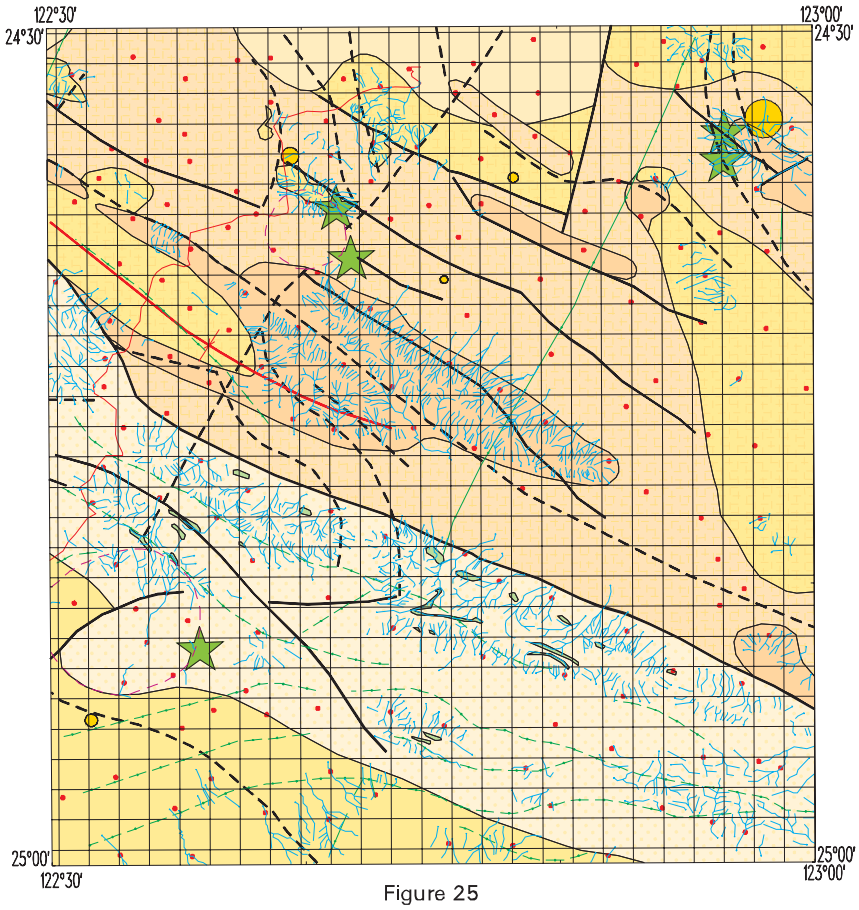

Figure 25

B

Total digest

Maximum value:
109 ppm

75 ppm

63 ppm

50 ppm

Below 50 ppm theoretical detection limit

> 75 ppm

SCALE 1:500 000

0 5 km

NICHOLLS

3448

First Edition 2002

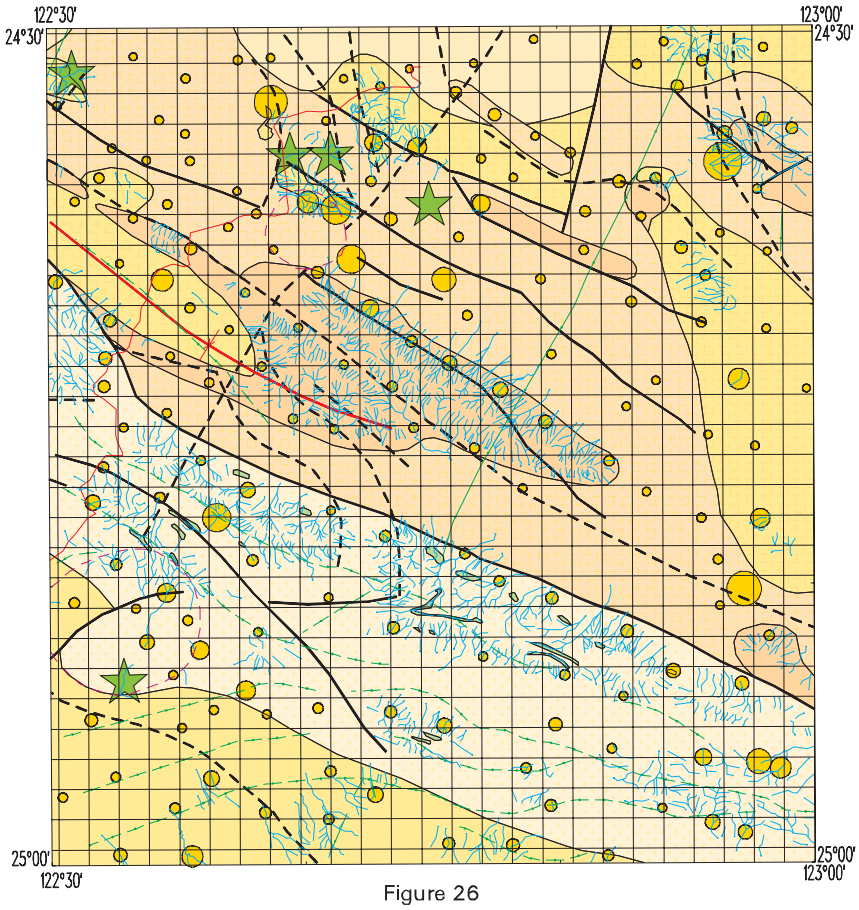

Figure 26

Ba

Total digest

Maximum value:
5003.5 ppm

874.6 ppm

441.8 ppm

9.0 ppm

Below 0.1 ppm theoretical detection limit

> 874.6 ppm

SCALE 1:500 000

0 5 km

NICHOLLS

3448

First Edition 2002

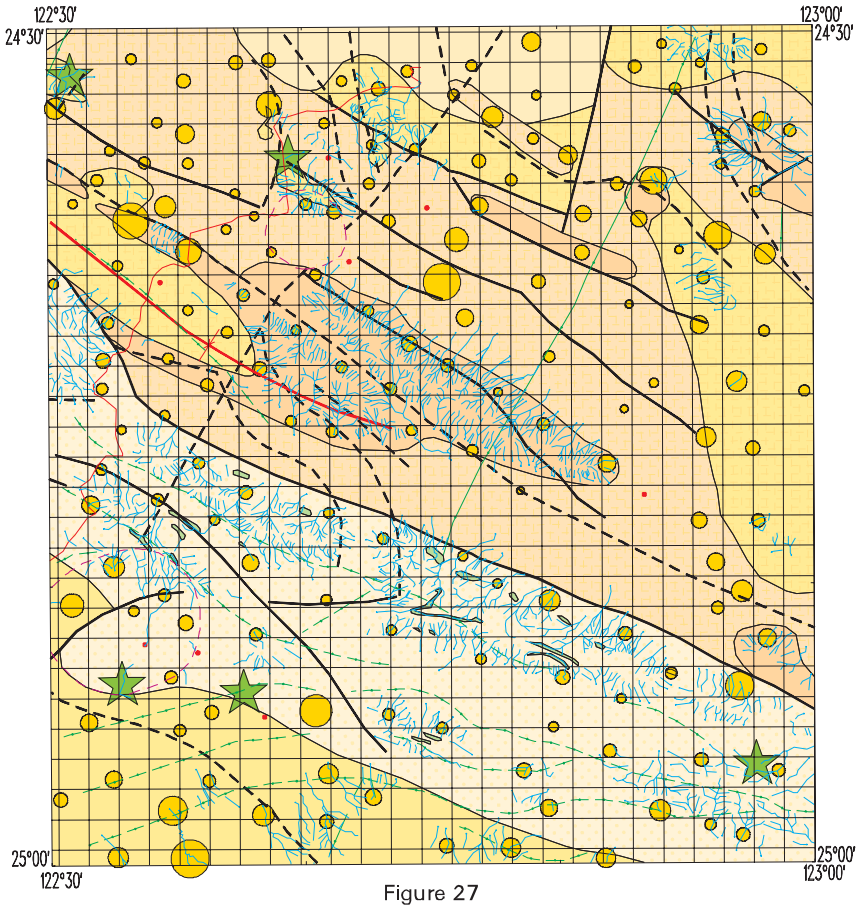

Figure 27

Ba

Partial digest

Maximum value:
10.918 ppm

3.380 ppm

1.693 ppm

0.005 ppm

Below 0.005 ppm theoretical detection limit

> 3.380 ppm

SCALE 1:500 000

0 5 km

NICHOLLS

3448

First Edition 2002

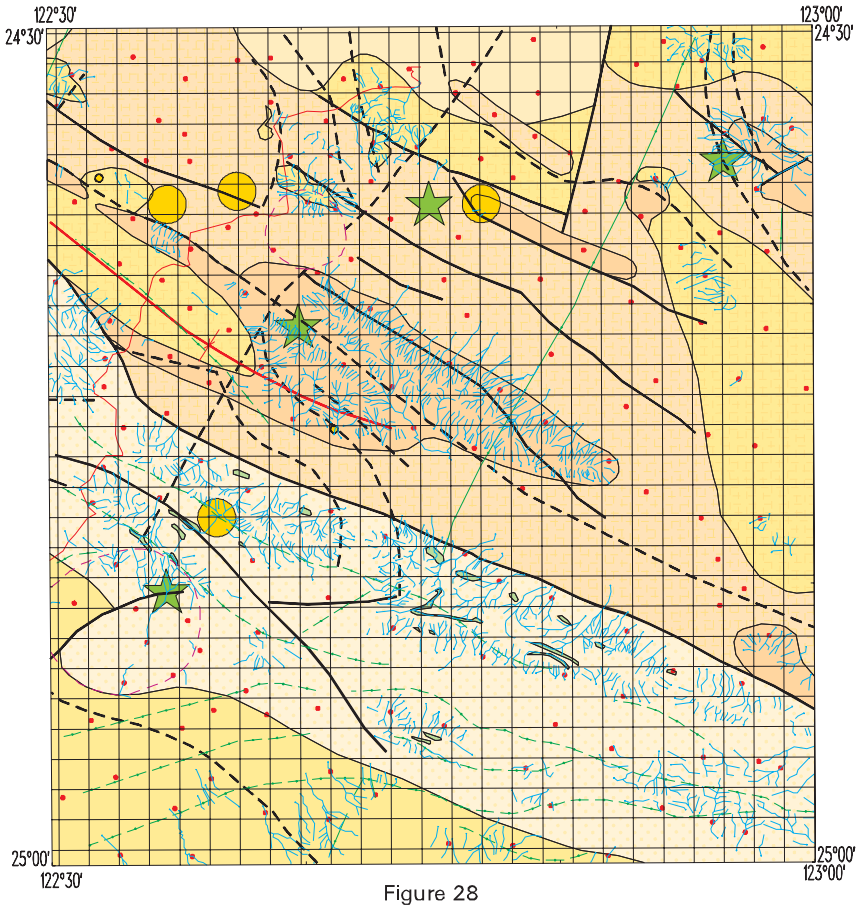

Figure 28

Cd
Total digest

Maximum value:
1.0 ppm

0.2 ppm

0.1 ppm

Below 0.1 ppm
theoretical
detection limit

> 0.2 ppm

SCALE 1:500 000
0 5 km

NICHOLLS

3448
First Edition 2002

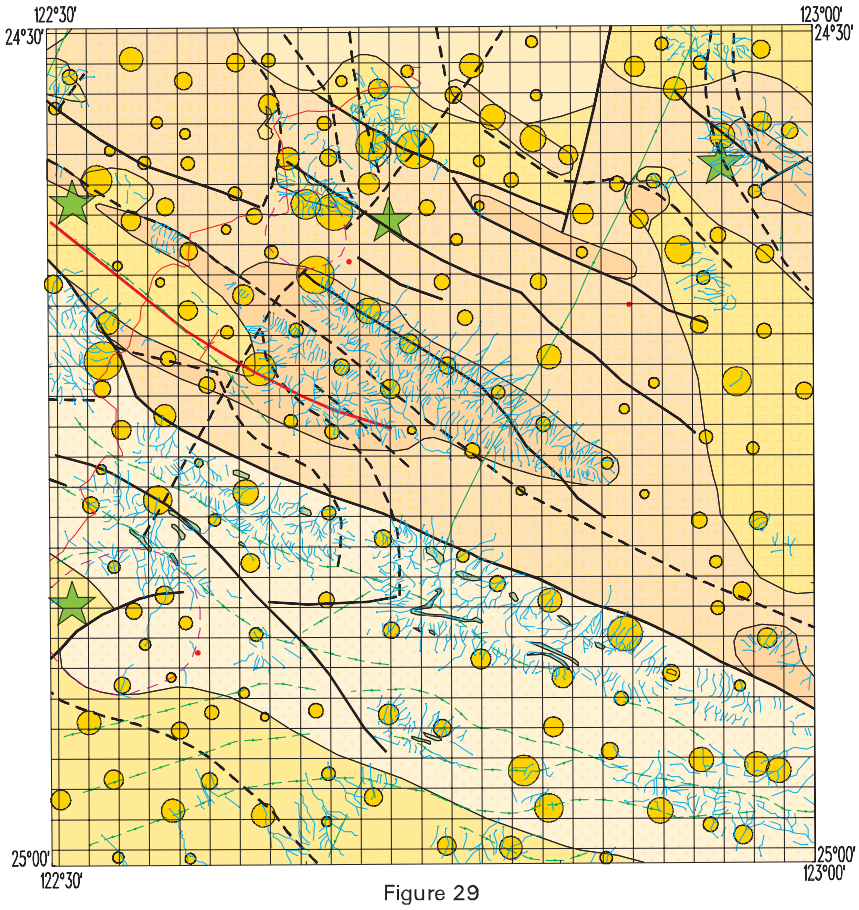

Figure 29

Cd
Partial digest

Maximum value:
27.8 ppb

5.8 ppb

3.2 ppb

0.5 ppb

Below 0.5 ppb
theoretical
detection limit

> 5.8 ppb

SCALE 1:500 000
0 5 km

NICHOLLS

3448
First Edition 2002

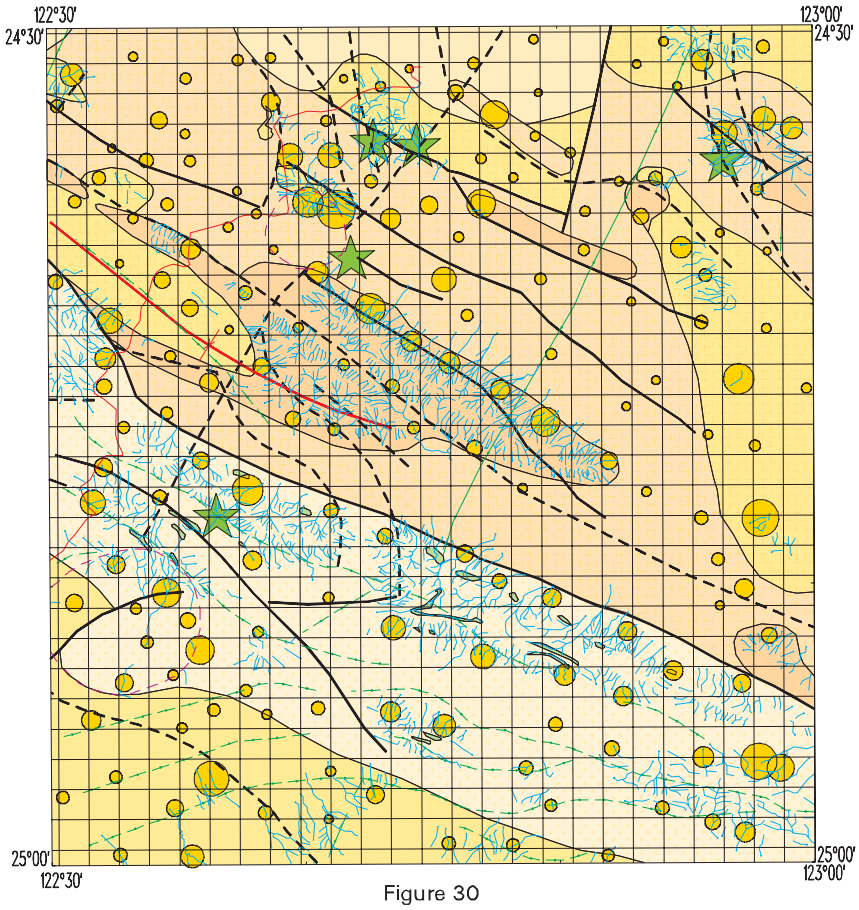

Figure 30

Ce
Total digest

Maximum value:
97.14 ppm

67.42 ppm
35.62 ppm
3.82 ppm

Below 0.01 ppm theoretical detection limit

> 67.42 ppm

SCALE 1:500 000
0 5 km

NICHOLLS

3448
First Edition 2002

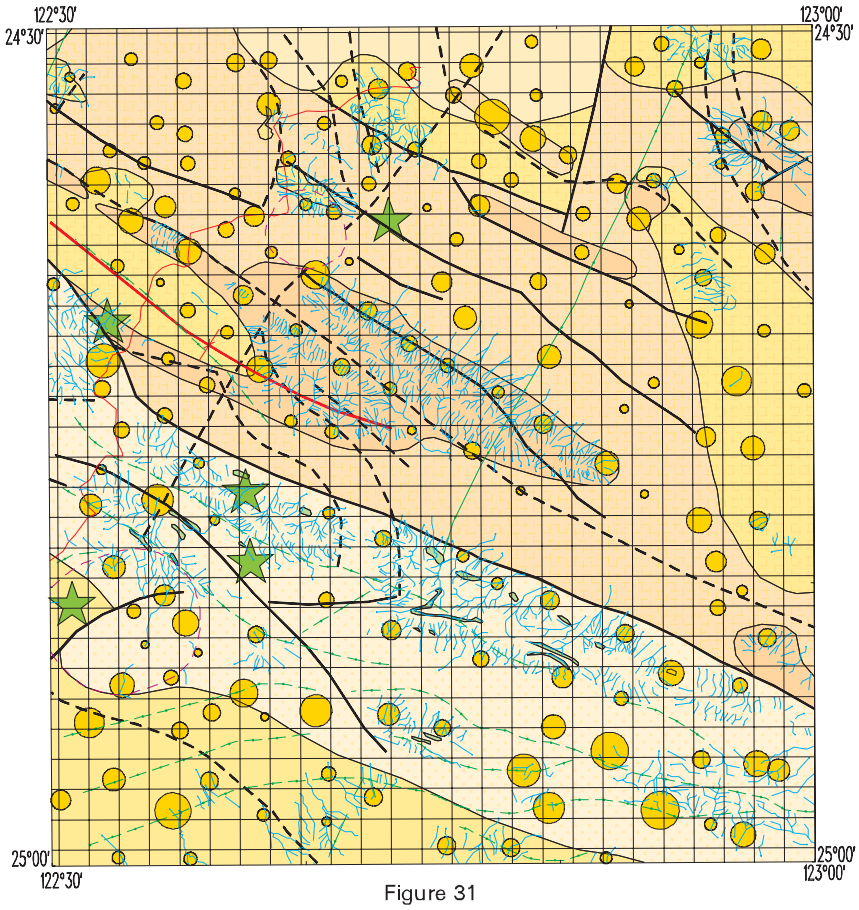

Figure 31

Ce
Partial digest

Maximum value:
5310.67 ppb

2115.81 ppb
1057.96 ppb
0.11 ppb

Below 0.05 ppb theoretical detection limit

> 2115.81 ppb

SCALE 1:500 000
0 5 km

NICHOLLS

3448
First Edition 2002

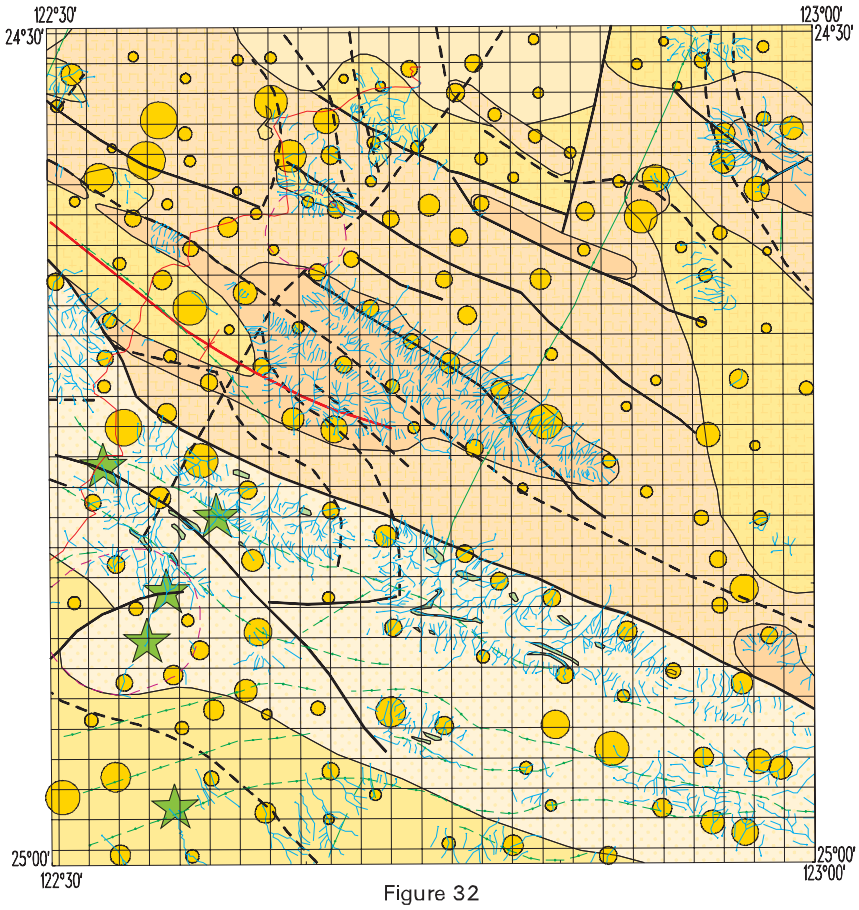

Figure 32

Cr
Total digest

Maximum value:
497 ppm

343 ppm
179 ppm
15 ppm

Below 2 ppm theoretical detection limit

> 343 ppm

SCALE 1:500 000
0 5 km

NICHOLLS

3448
First Edition 2002

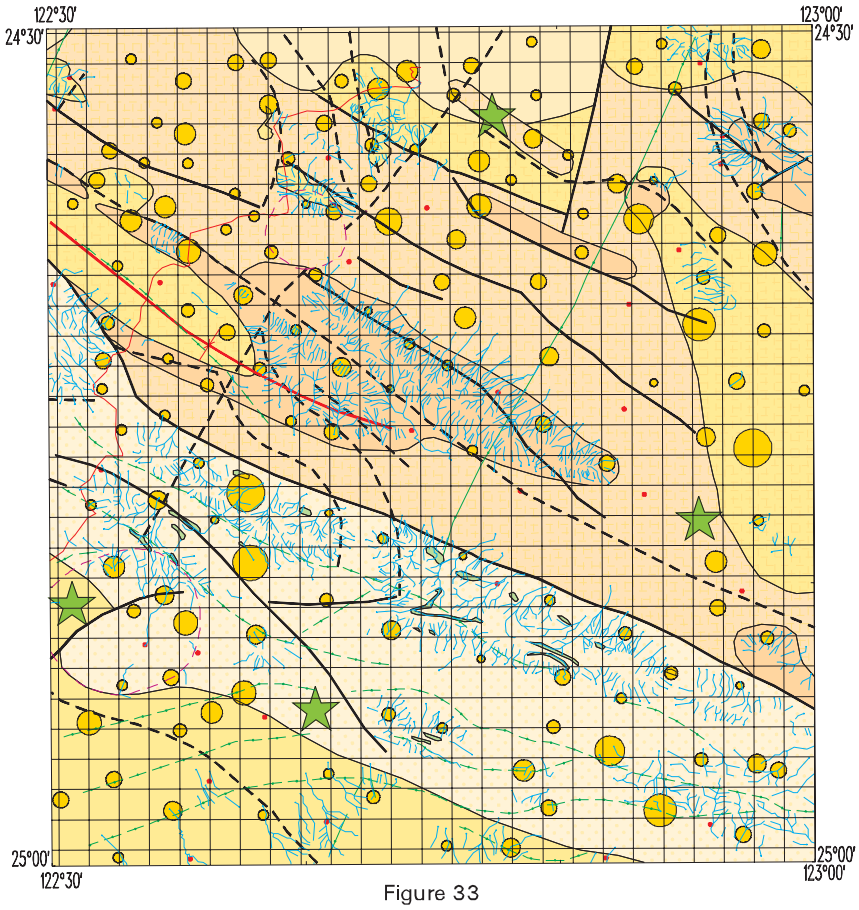

Figure 33

Cr
Partial digest

Maximum value:
1.8 ppm

1.3 ppm
0.8 ppm
0.2 ppm

Below 0.2 ppm theoretical detection limit

> 1.3 ppm

SCALE 1:500 000
0 5 km

NICHOLLS

3448
First Edition 2002

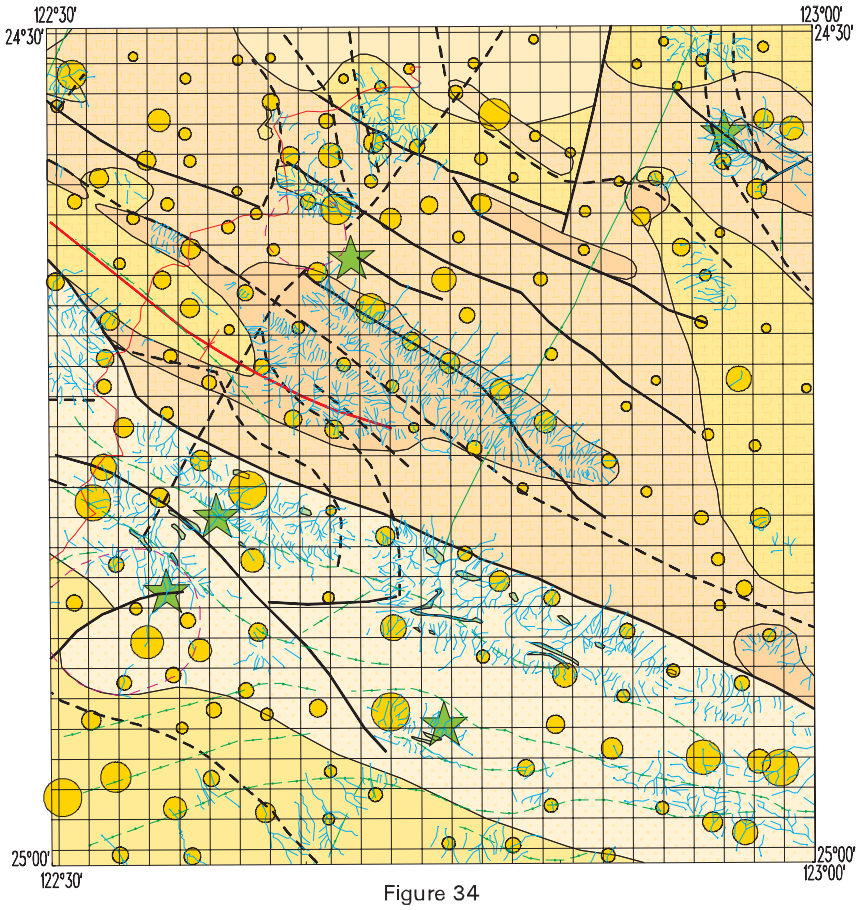

Figure 34

Cu
Total digest

Maximum value:
122 ppm

41 ppm
21 ppm
1 ppm

Below 1 ppm
theoretical
detection limit

> 41 ppm

SCALE 1:500 000
0 5 km

NICHOLLS

3448
First Edition 2002

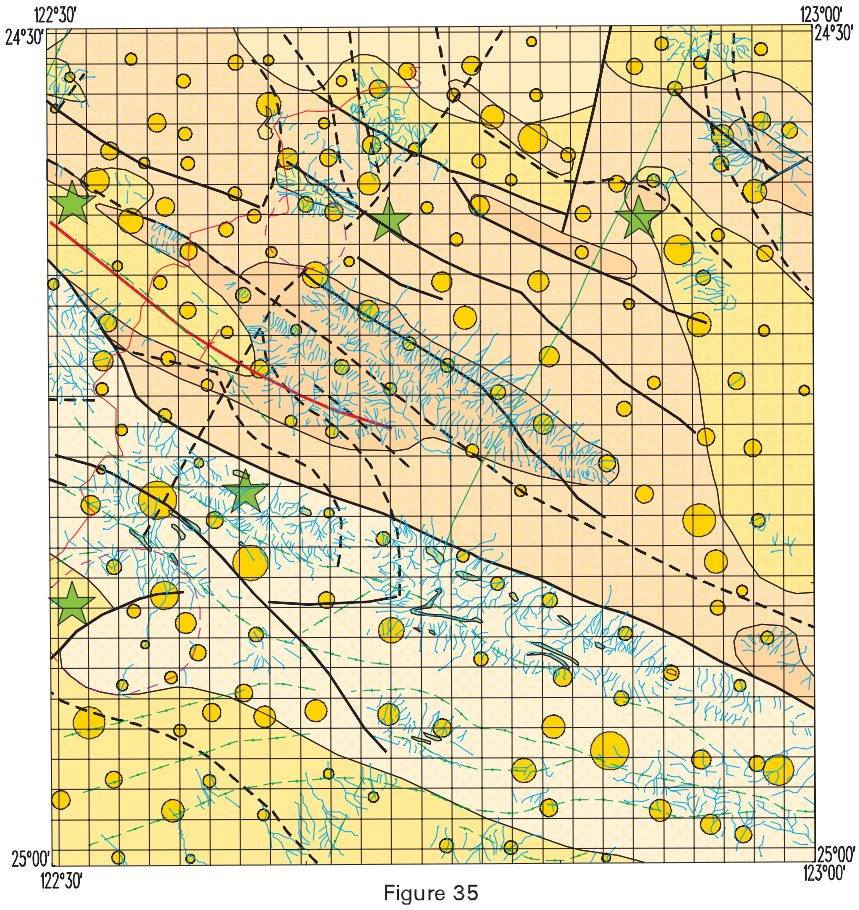

Figure 35

Cu
Partial digest

Maximum value:
4.66 ppm

2.90 ppm
1.61 ppm
0.31 ppm

Below 0.02 ppm
theoretical
detection limit

> 2.90 ppm

SCALE 1:500 000
0 5 km

NICHOLLS

3448
First Edition 2002

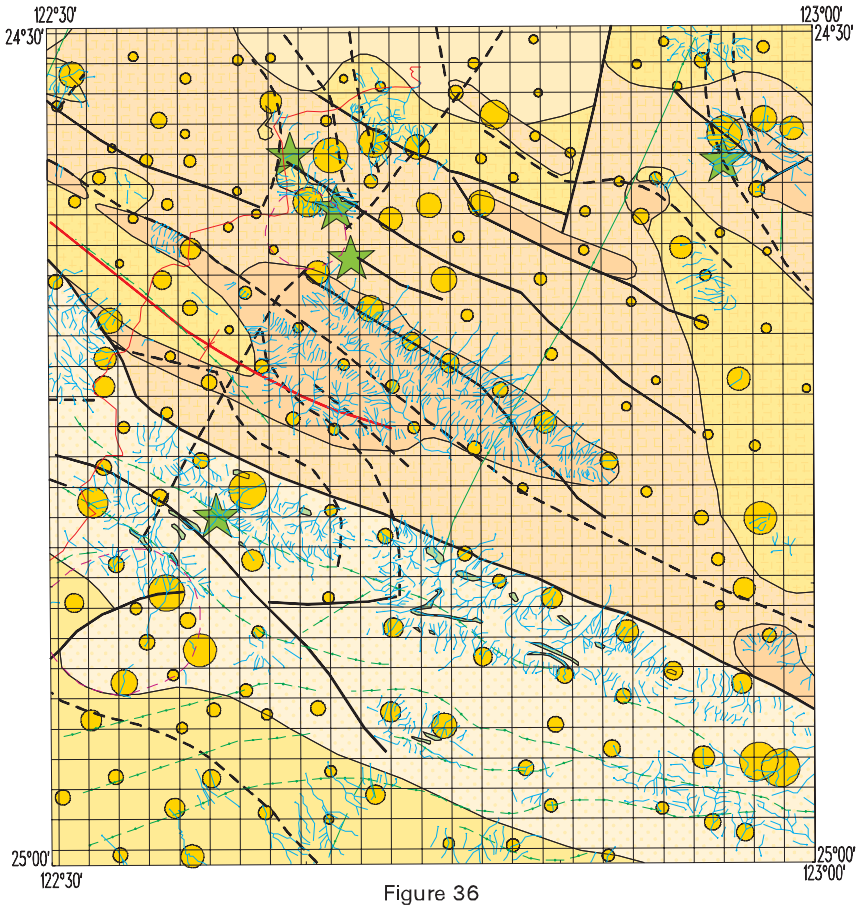

Figure 36

Eu

Total digest

Maximum value:
1.19 ppm

0.94 ppm

0.50 ppm

0.05 ppm

Below 0.01 ppm theoretical detection limit

> 0.94 ppm

SCALE 1:500 000

0 5 km

NICHOLLS

3448

First Edition 2002

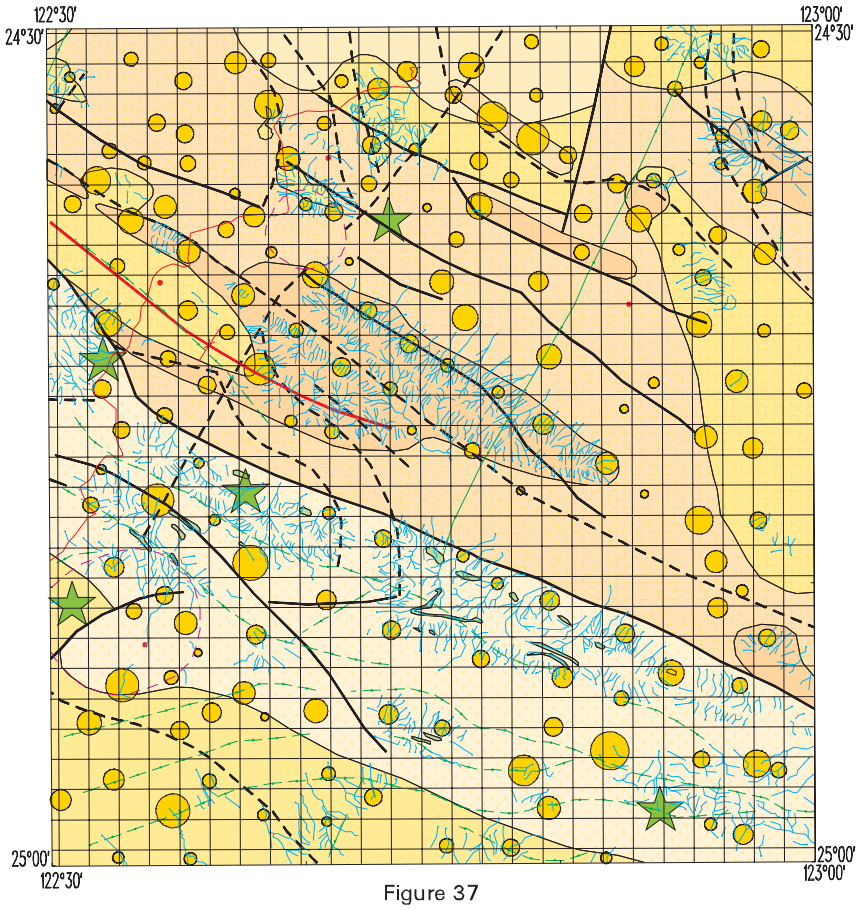

Figure 37

Eu

Partial digest

Maximum value:
73.51 ppb

38.41 ppb

19.22 ppb

0.02 ppb

Below 0.02 ppb theoretical detection limit

> 38.41 ppb

SCALE 1:500 000

0 5 km

NICHOLLS

3448

First Edition 2002

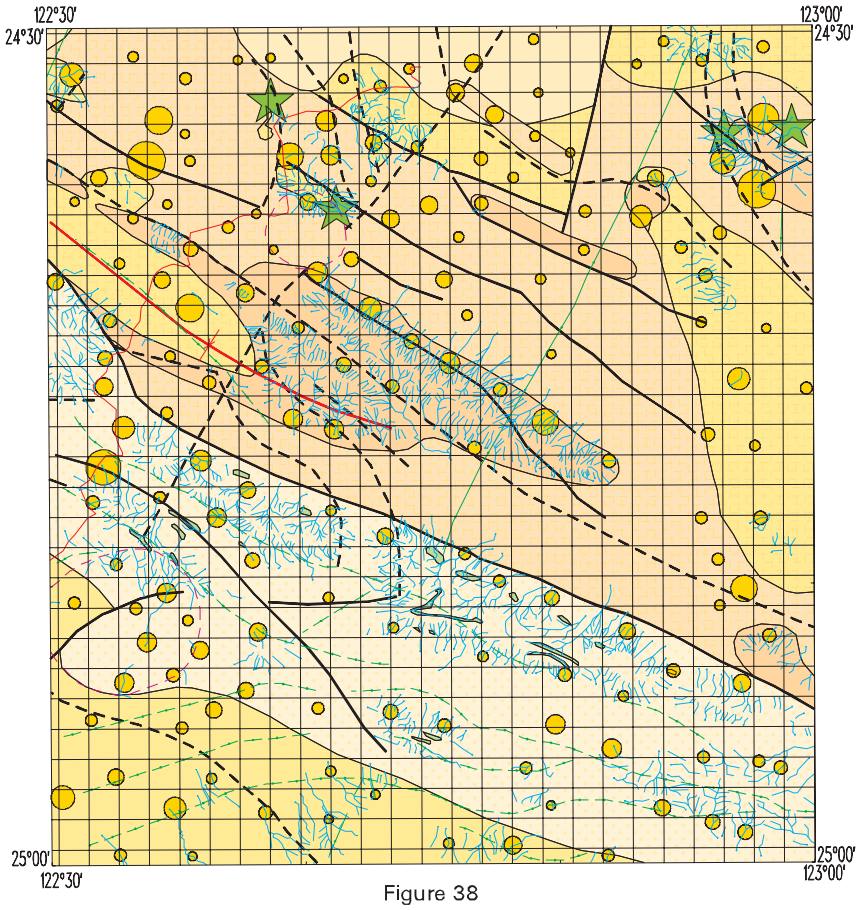

Figure 38

Mo
Total digest

Maximum value:
4.4 ppm

2.3 ppm
1.3 ppm
0.2 ppm

Below 0.1 ppm theoretical detection limit

> 2.3 ppm

SCALE 1:500 000
0 5 km

NICHOLLS

3448
First Edition 2002

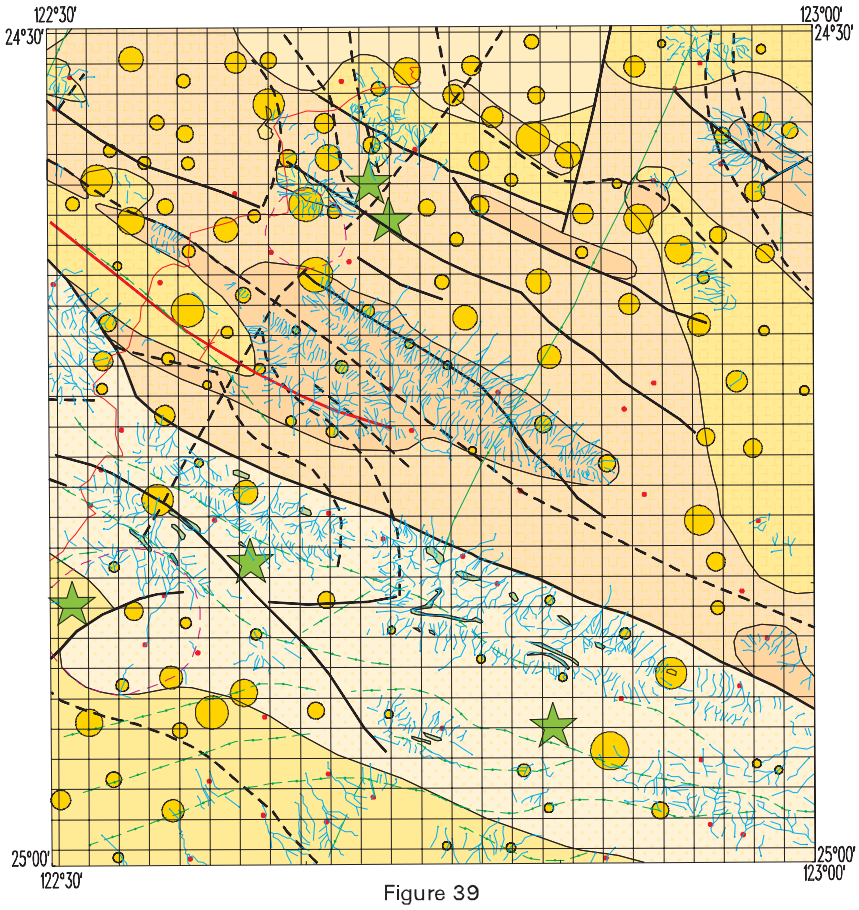

Figure 39

Mo
Partial digest

Maximum value:
83 ppb

46 ppb
28 ppb
10 ppb

Below 10 ppb theoretical detection limit

> 46 ppb

SCALE 1:500 000
0 5 km

NICHOLLS

3448
First Edition 2002

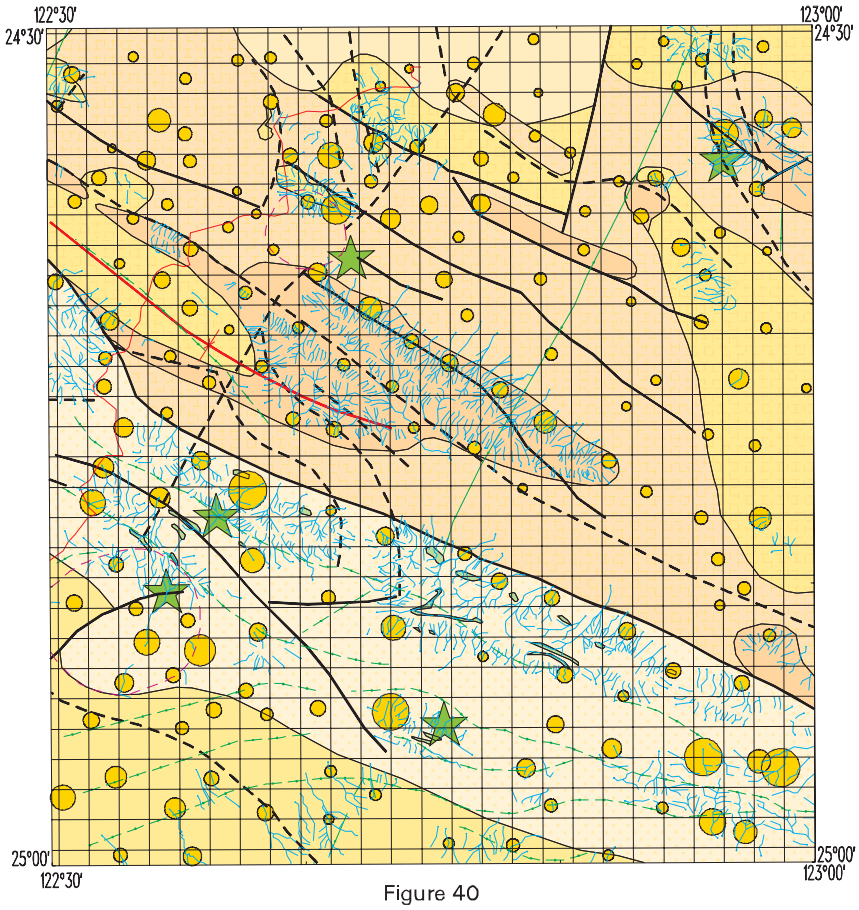

Figure 40

Ni

Total digest

Maximum value:
80 ppm

42 ppm

23 ppm

3 ppm

Below 1 ppm theoretical detection limit

> 42 ppm

SCALE 1:500 000

0 5 km

NICHOLLS

3448

First Edition 2002

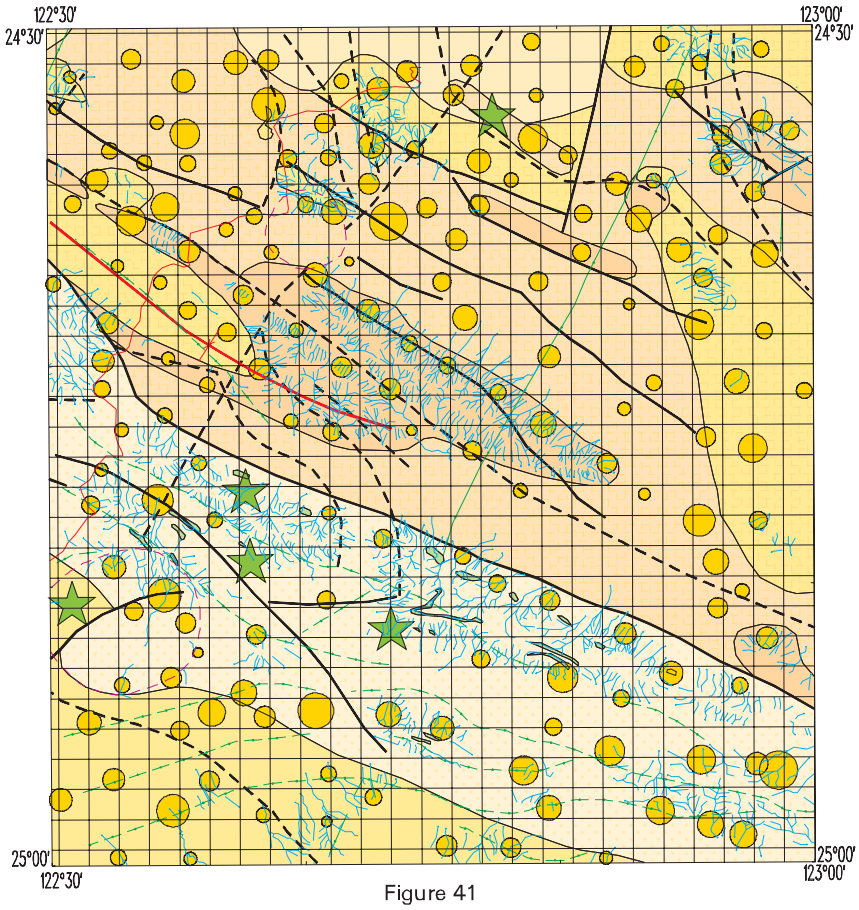

Figure 41

Ni

Partial digest

Maximum value:
1.55 ppm

0.76 ppm

0.39 ppm

0.02 ppm

Below 0.02 ppm theoretical detection limit

> 0.76 ppm

SCALE 1:500 000

0 5 km

NICHOLLS

3448

First Edition 2002

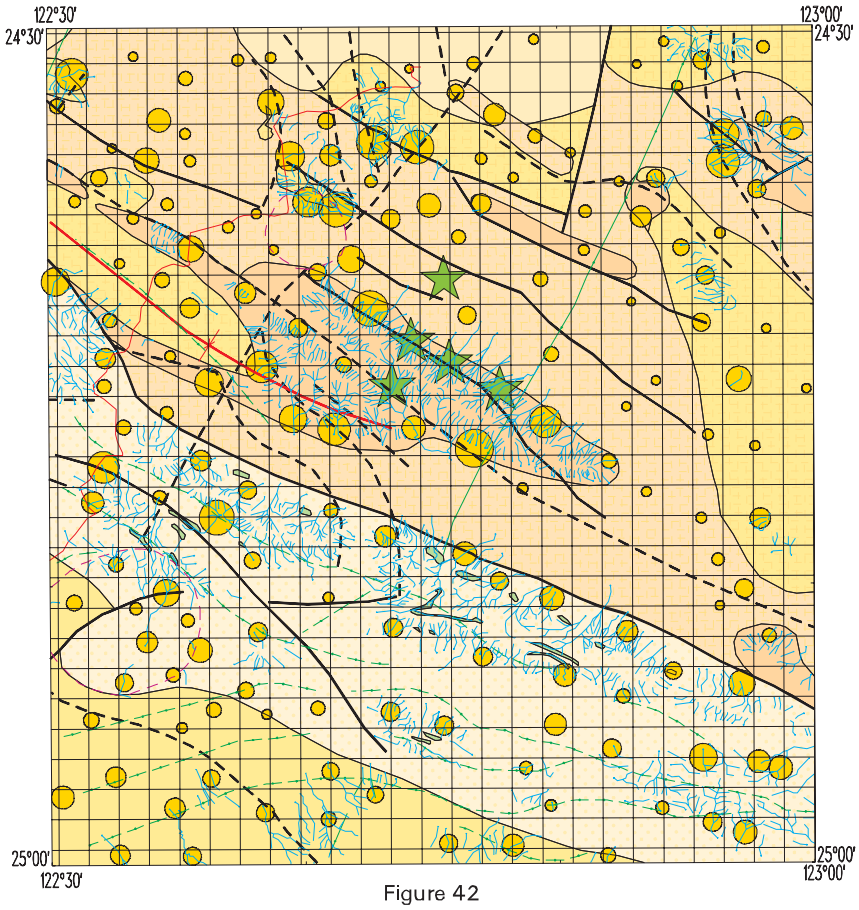

Figure 42

Pb
Total digest

Maximum value:
138 ppm

42 ppm
23 ppm
4 ppm

Below 2 ppm theoretical detection limit

> 42 ppm

SCALE 1:500 000
0 5 km

NICHOLLS

3448
First Edition 2002

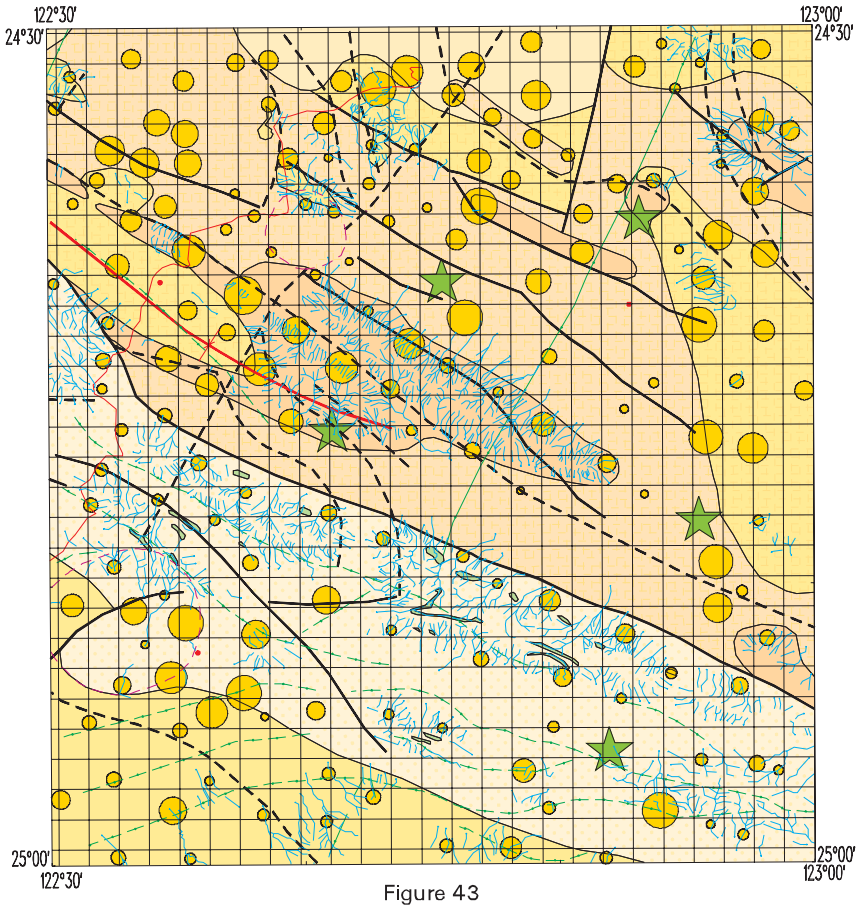

Figure 43

Pb
Partial digest

Maximum value:
1.10 ppm

0.80 ppm
0.41 ppm
0.01 ppm

Below 0.01 ppm theoretical detection limit

> 0.80 ppm

SCALE 1:500 000
0 5 km

NICHOLLS

3448
First Edition 2002

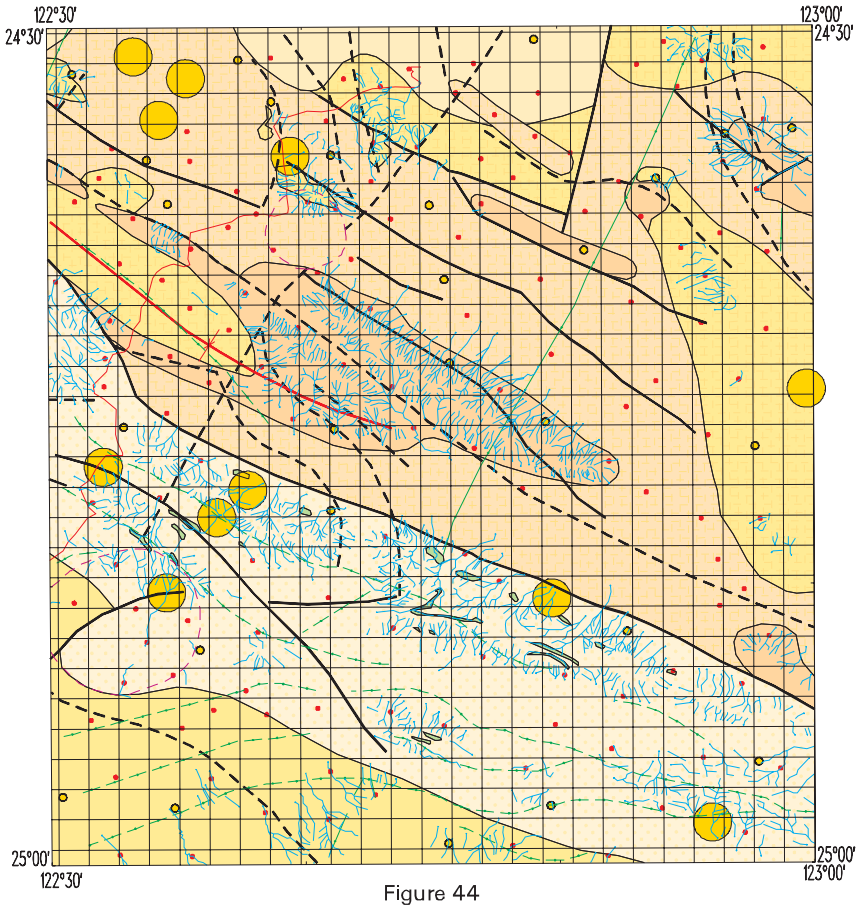

Figure 44

Pd

Total digest

Maximum value:
2 ppb

2 ppb

1 ppb

Below 1 ppb
theoretical
detection limit

SCALE 1:500 000

0 5 km

NICHOLLS

3448

First Edition 2002

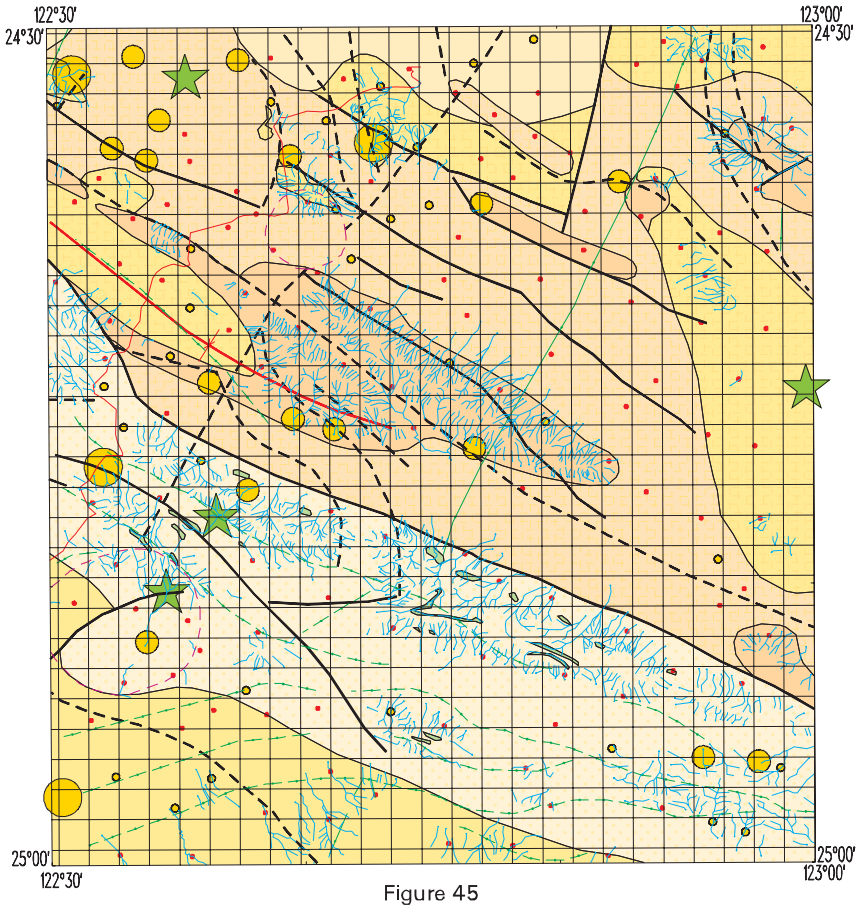

Figure 45

Pt

Total digest

Maximum value:
5 ppb

3 ppb

2 ppb

1 ppb

Below 1 ppb theoretical detection limit

> 3 ppb

SCALE 1:500 000

0 5 km

NICHOLLS

3448

First Edition 2002

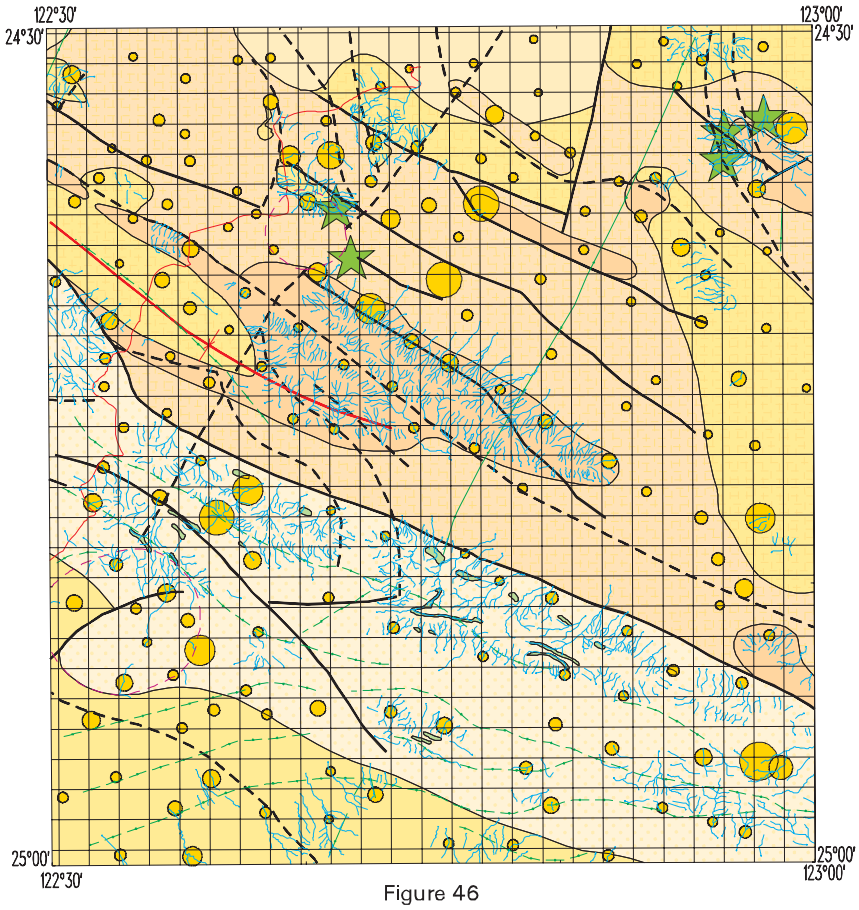

Figure 46

Rb

Total digest

Maximum value:
193.49 ppm

112.75 ppm

57.88 ppm

3.00 ppm

Below 0.05 ppm
theoretical
detection limit

> 112.75 ppm

SCALE 1:500 000

0 5 km

NICHOLLS

3448

First Edition 2002

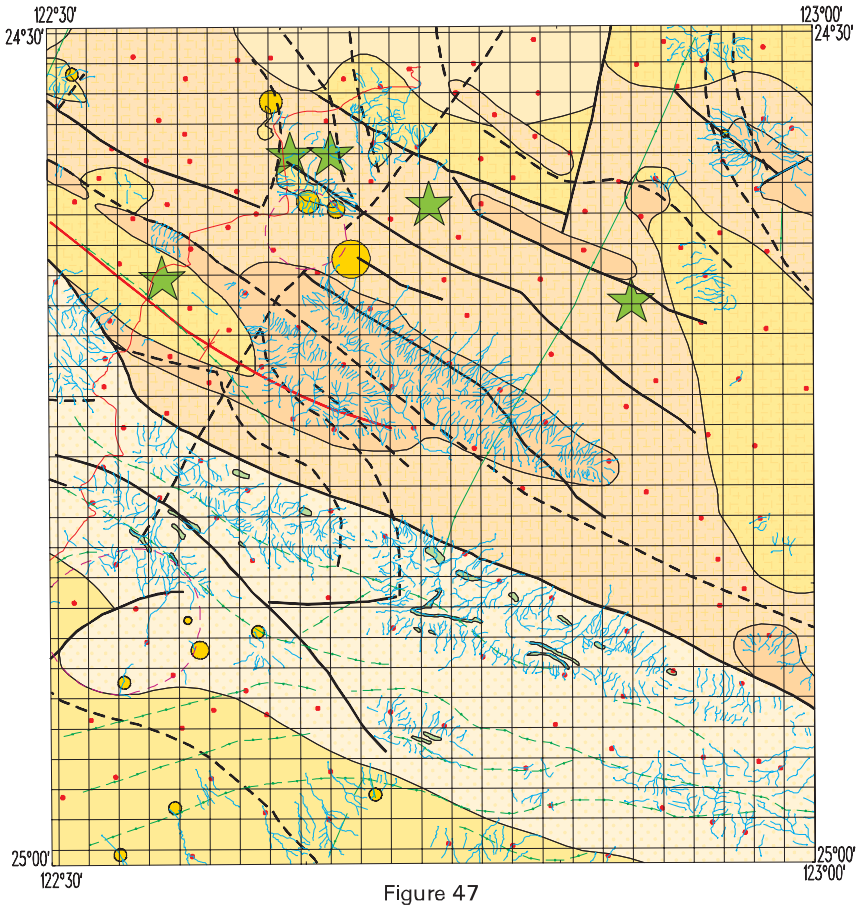

Figure 47

S

Total digest

Maximum value:
0.21 %

0.07 %

0.04 %

0.01 %

Below 0.01 %
theoretical
detection limit

> 0.07 %

SCALE 1:500 000

0 5 km

NICHOLLS

3448

First Edition 2002

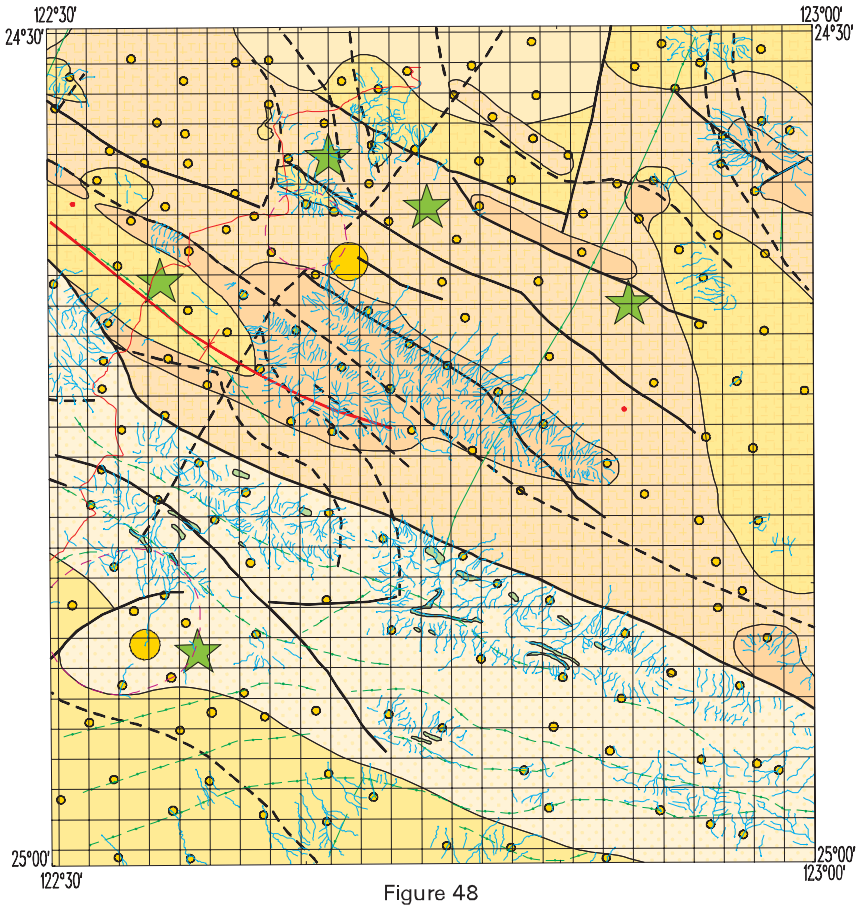

Figure 48

S

Partial digest

Maximum value:
2817 ppm

793 ppm

398 ppm

2 ppm

Below 2 ppm
theoretical
detection limit

> 793 ppm

SCALE 1:500 000

0 5 km

NICHOLLS

3448

First Edition 2002

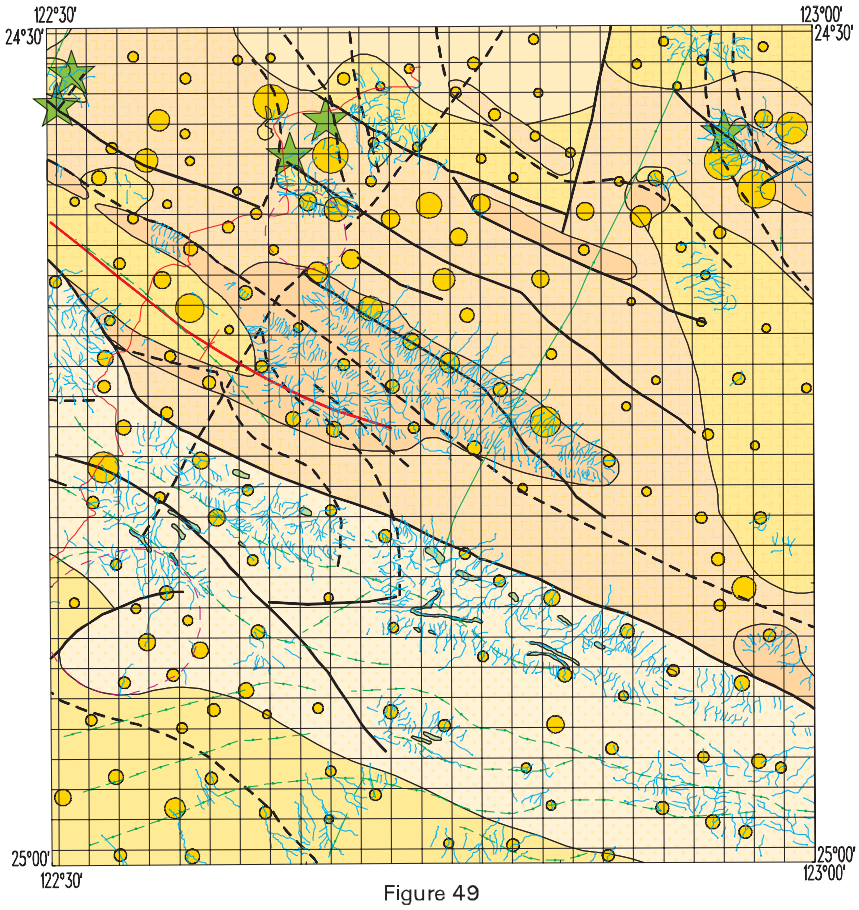

Figure 49

Sb
Total digest

Maximum value:
38.45 ppm

3.42 ppm
1.79 ppm
0.15 ppm

Below 0.05 ppm theoretical detection limit

> 3.42 ppm

SCALE 1:500 000
0 5 km

NICHOLLS

3448
First Edition 2002

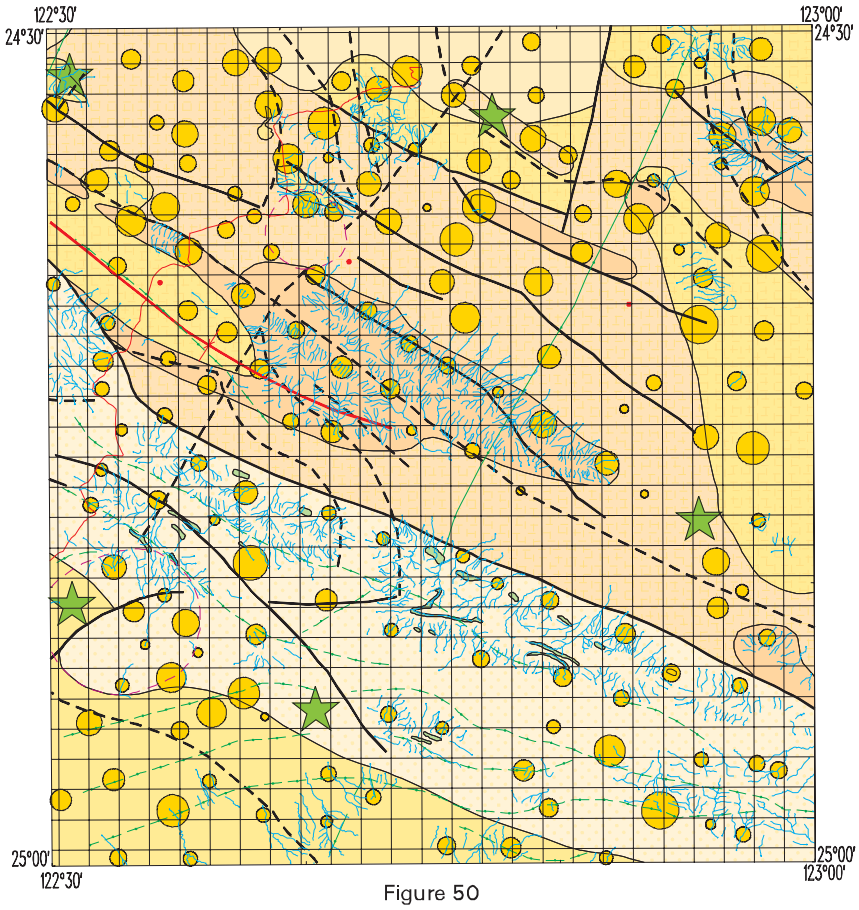

Figure 50

Sb
Partial digest

Maximum value:
5.8 ppb

3.8 ppb
2.0 ppb
0.2 ppb

Below 0.2 ppb theoretical detection limit

> 3.8 ppb

SCALE 1:500 000
0 5 km

NICHOLLS

3448
First Edition 2002

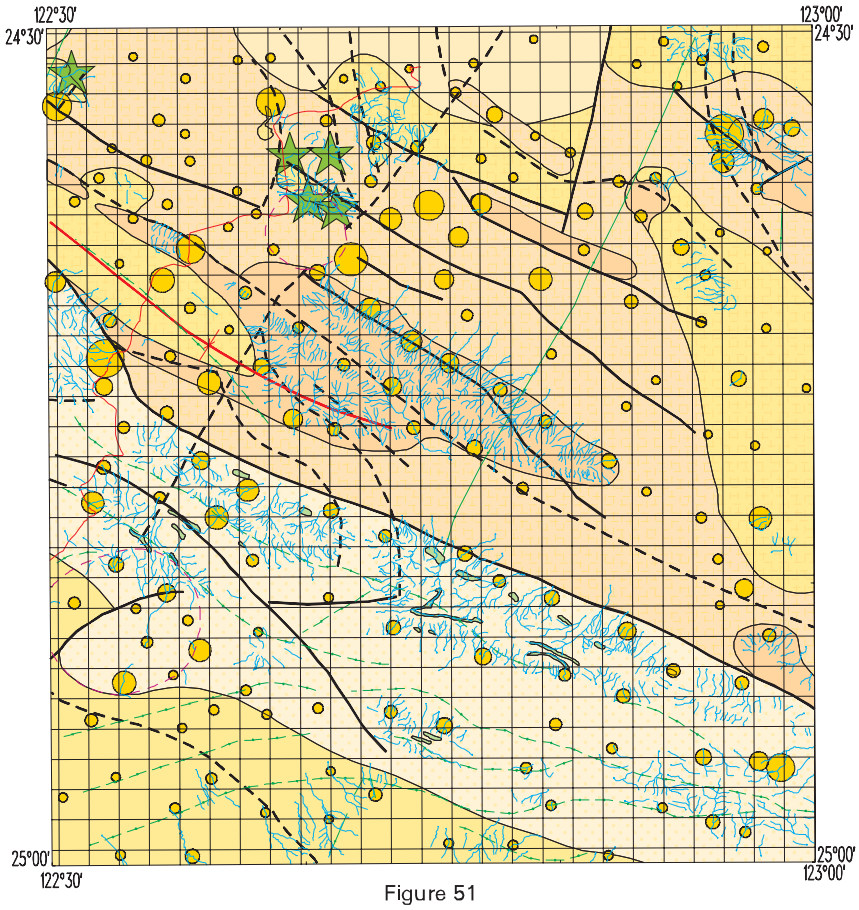

Figure 51

Sr

Total digest

Maximum value:
838.61 ppm

85.98 ppm

44.39 ppm

2.79 ppm

Below 0.05 ppm
theoretical
detection limit

> 85.98 ppm

SCALE 1:500 000

0 5 km

NICHOLLS

3448

First Edition 2002

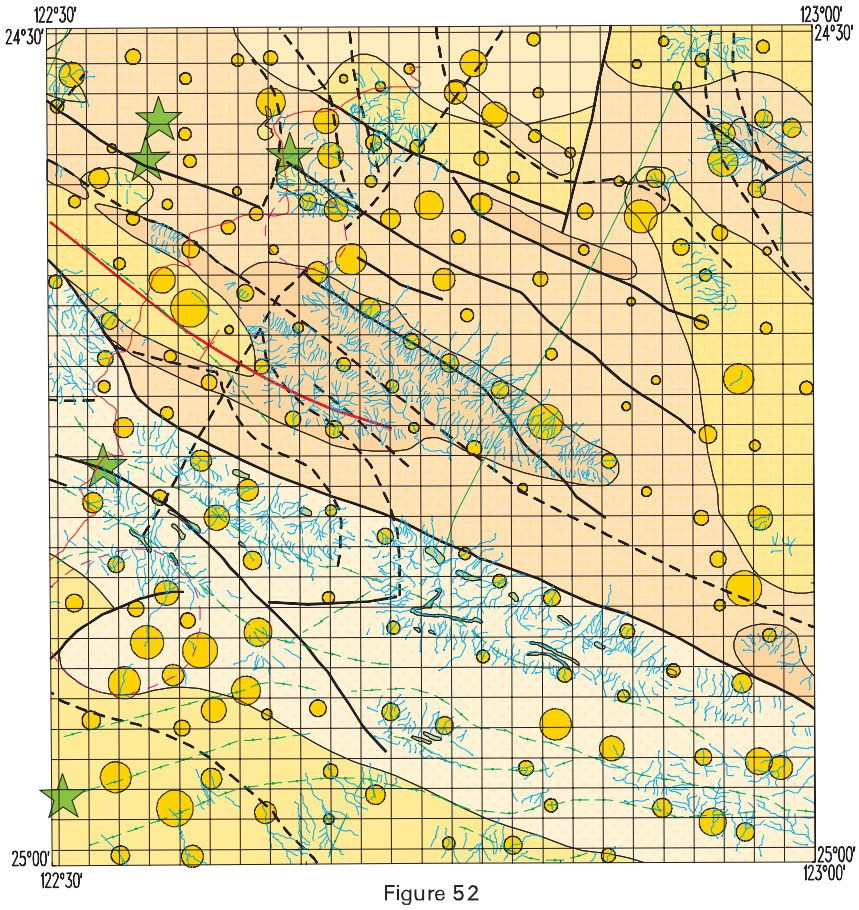

Figure 52

Th

Total digest

Maximum value:
38.75 ppm

20.49 ppm

11.14 ppm

1.78 ppm

Below 0.01 ppm theoretical detection limit

> 20.49 ppm

SCALE 1:500 000

0 5 km

NICHOLLS

3448

First Edition 2002

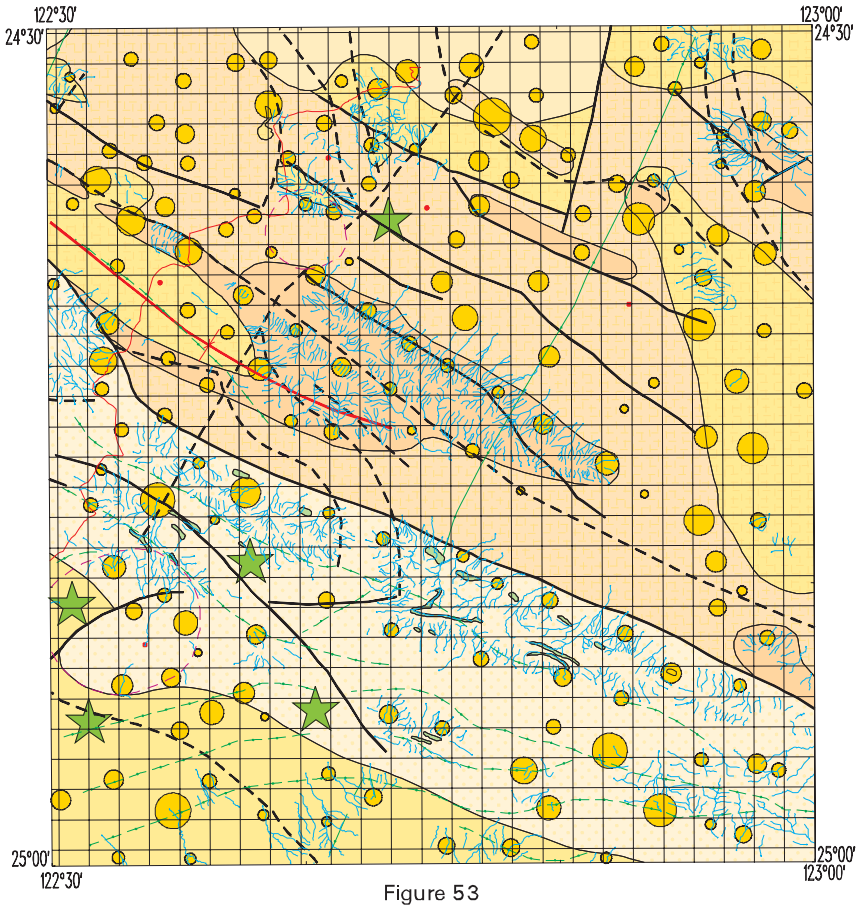

Figure 53

Th

Partial digest

Maximum value:
1635.8 ppb

579.0 ppb

289.6 ppb

0.1 ppb

Below 0.1 ppb theoretical detection limit

> 579.0 ppb

SCALE 1:500 000

0 5 km

NICHOLLS

3448

First Edition 2002

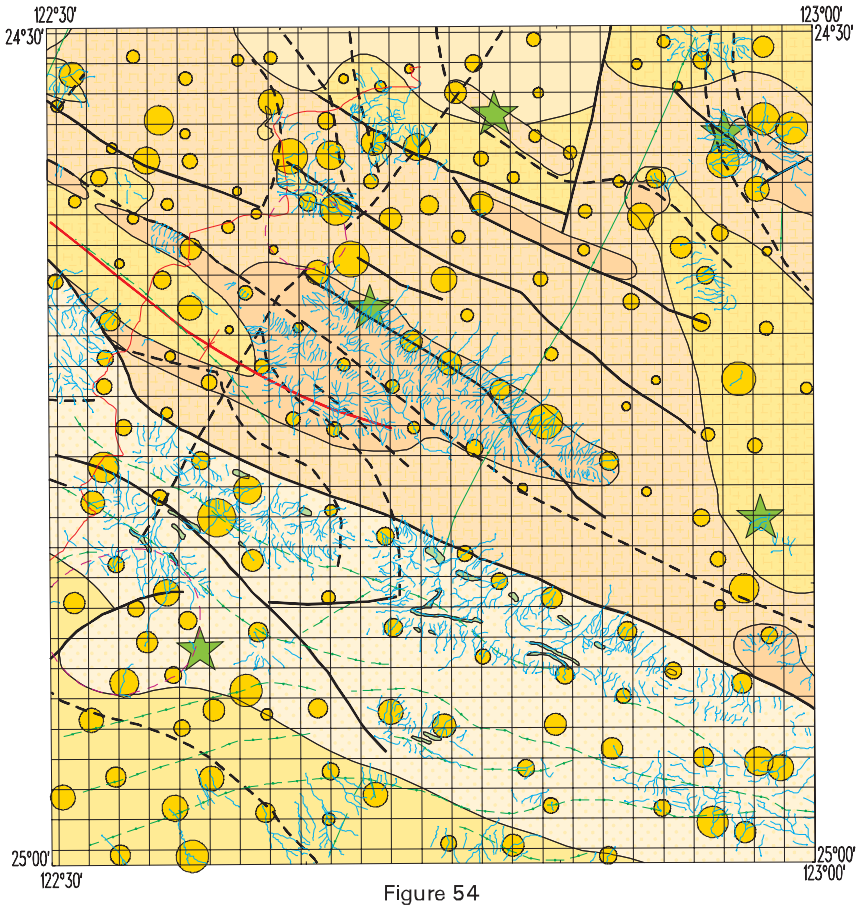

Figure 54

U
Total digest

Maximum value:
3.62 ppm

2.12 ppm
1.16 ppm
0.20 ppm

Below 0.01 ppm
theoretical
detection limit

> 2.12 ppm

SCALE 1:500 000
0 5 km

NICHOLLS

3448
First Edition 2002

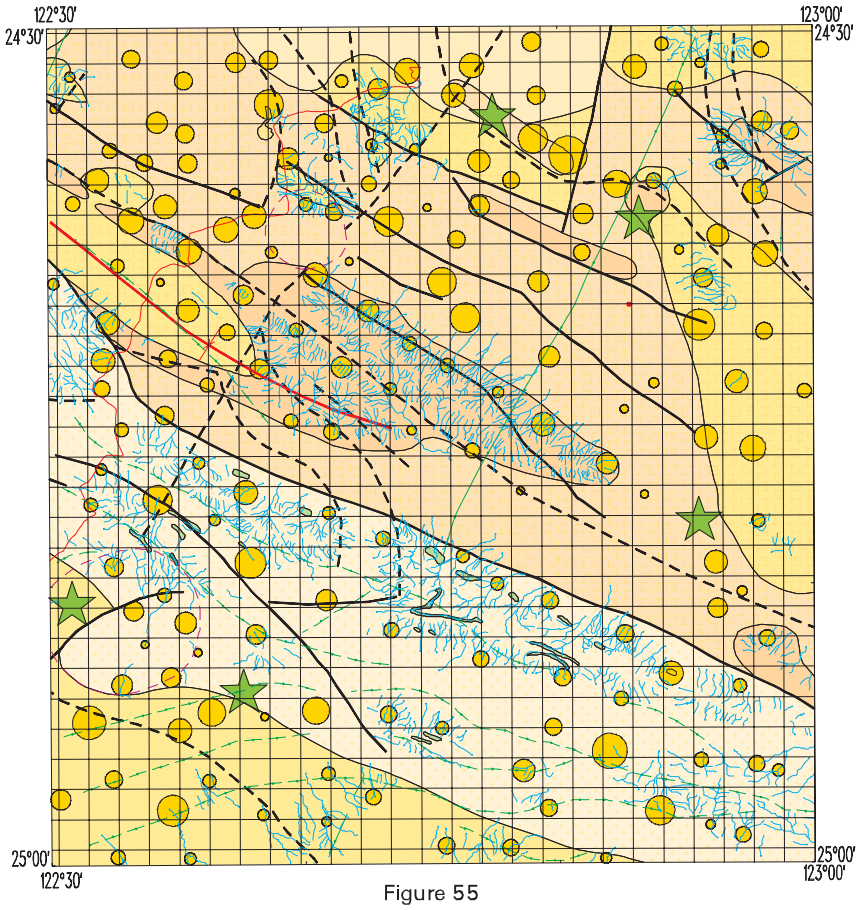

Figure 55

U
Partial digest

Maximum value:
237.5 ppb

100.4 ppb
50.3 ppb
0.1 ppb

Below 0.1 ppb
theoretical
detection limit

> 100.4 ppb

SCALE 1:500 000
0 5 km

NICHOLLS

3448
First Edition 2002

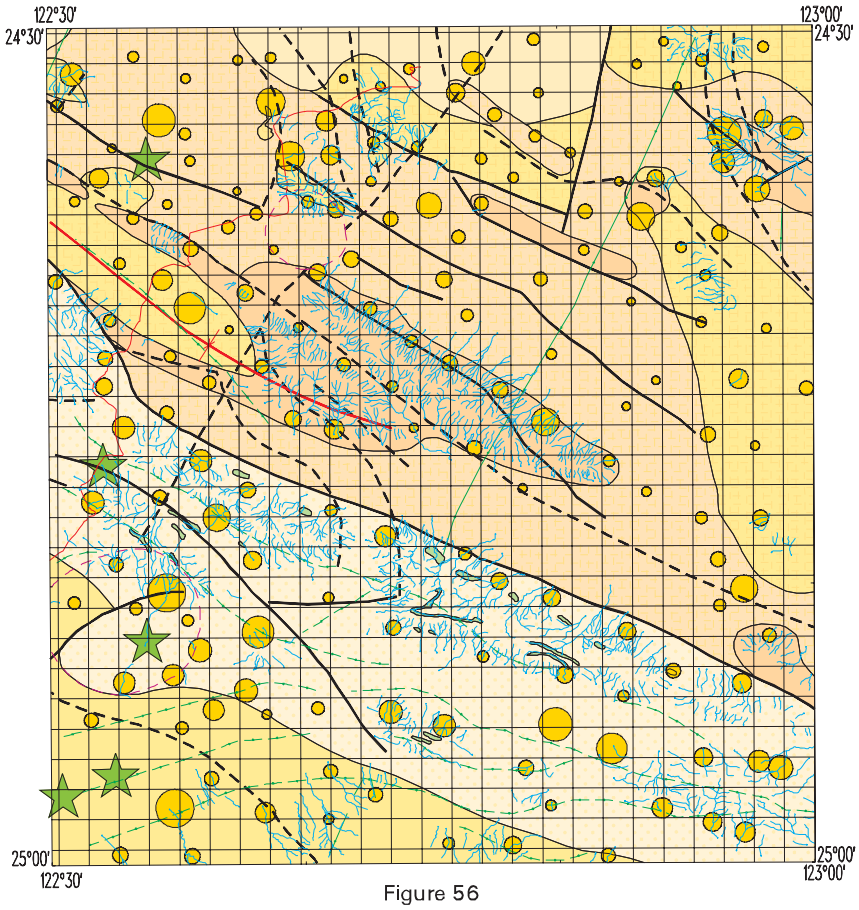

Figure 56

V

Total digest

Maximum value:
575 ppm

381 ppm

198 ppm

14 ppm

Below 2 ppm theoretical detection limit

> 381 ppm

SCALE 1:500 000

0 5 km

NICHOLLS

3448

First Edition 2002

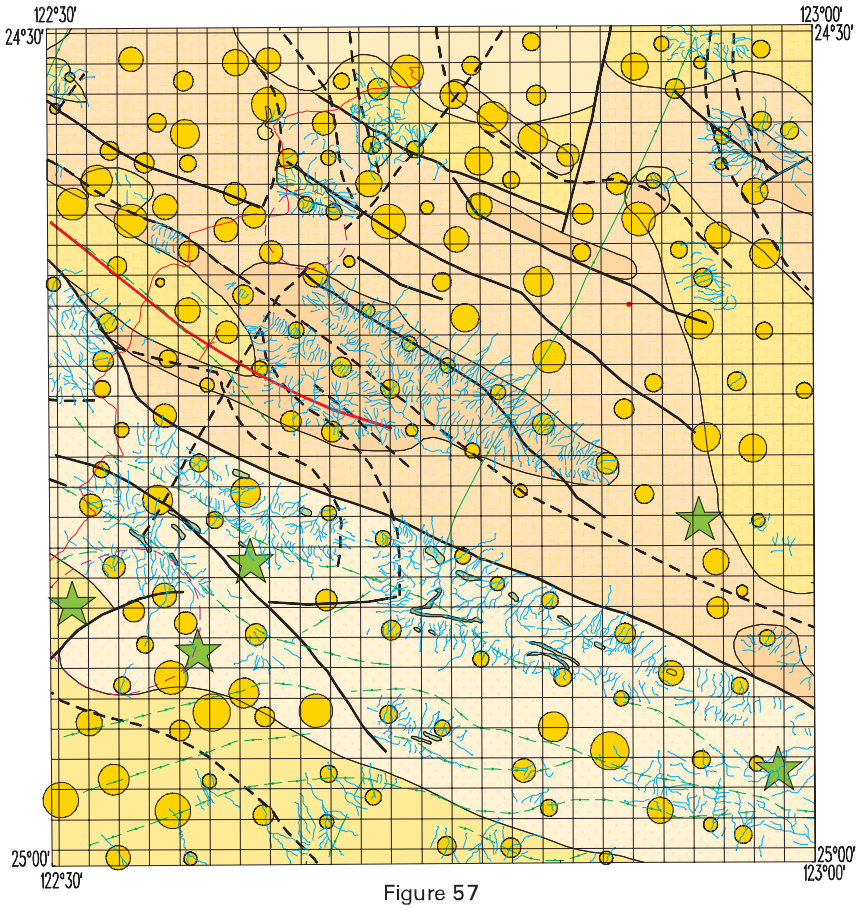

Figure 57

V

Partial digest

Maximum value:
4.7 ppm

3.5 ppm

1.9 ppm

0.2 ppm

Below 0.2 ppm theoretical detection limit

> 3.5 ppm

SCALE 1:500 000

0 5 km

NICHOLLS

3448

First Edition 2002

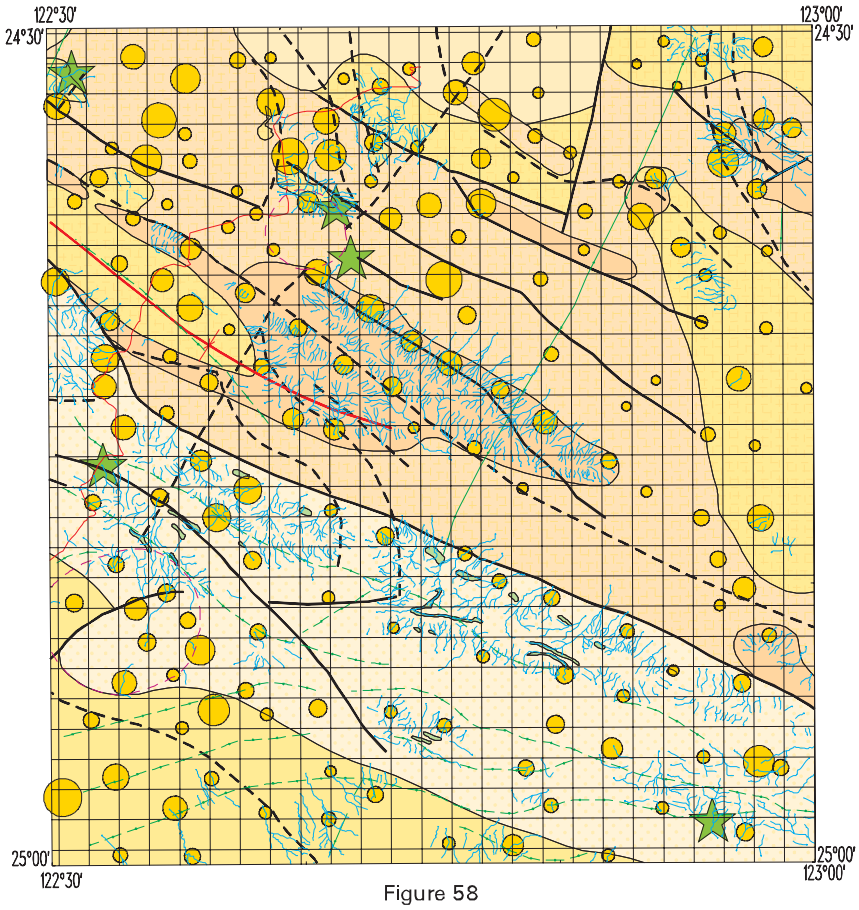

Figure 58

W

Total digest

Maximum value:
7.4 ppm

2.0 ppm

1.1 ppm

0.2 ppm

Below 0.1 ppm theoretical detection limit

> 2.0 ppm

SCALE 1:500 000

0 5 km

NICHOLLS

3448

First Edition 2002

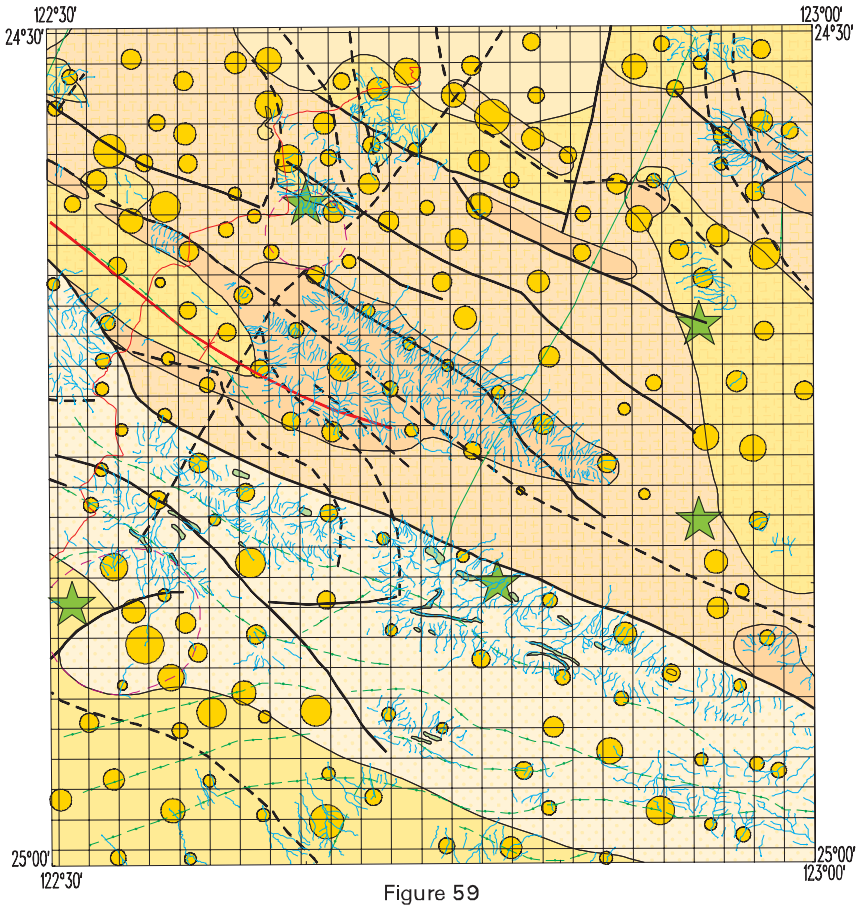

Figure 59

W

Partial digest

Maximum value:
21.4 ppb

10.4 ppb

5.5 ppb

0.5 ppb

Below 0.5 ppb theoretical detection limit

> 10.4 ppb

SCALE 1:500 000

0 5 km

NICHOLLS

3448

First Edition 2002

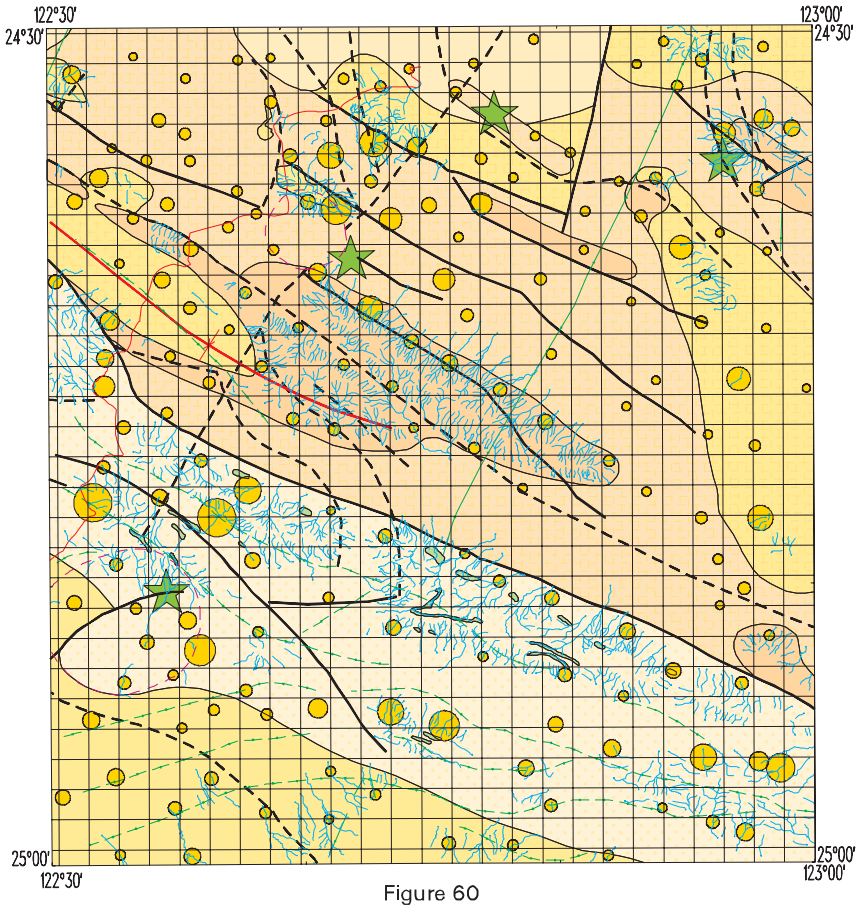

Figure 60

Zn
Total digest

Maximum value:
264 ppm

71 ppm

37 ppm

2 ppm

Below 1 ppm
theoretical
detection limit

> 71 ppm

SCALE 1:500 000

0 5 km

NICHOLLS

3448
First Edition 2002

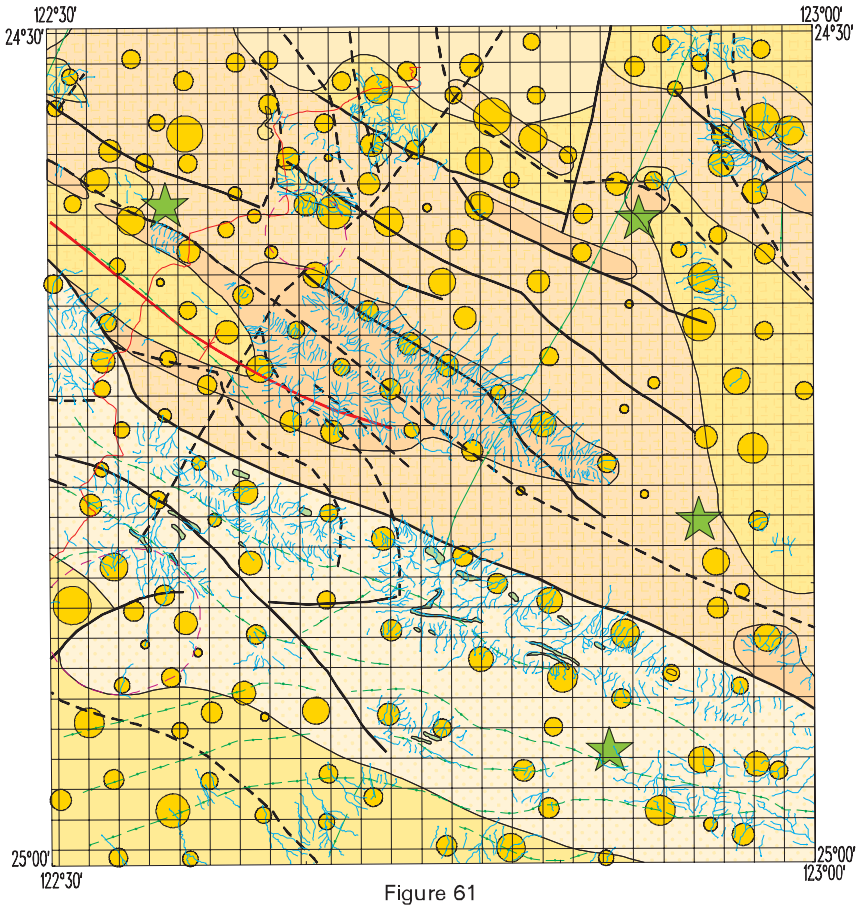

Figure 61

Zn
Partial digest

Maximum value:
1665 ppb

1145 ppb

576 ppb

6 ppb

Below 5 ppb
theoretical
detection limit

> 1145 ppb

SCALE 1:500 000

0 5 km

NICHOLLS

3448
First Edition 2002

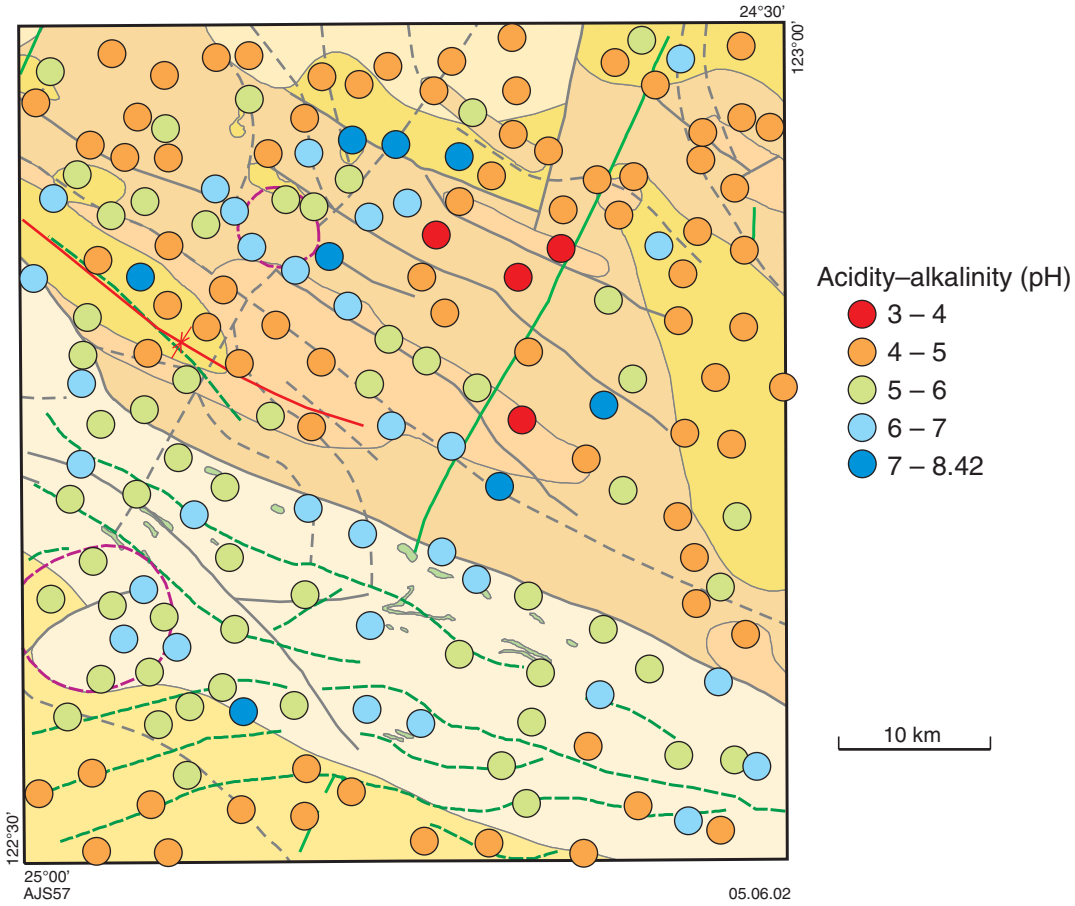

Figure 62. Acidity–alkalinity (pH) on NICHOLLS. Geological symbols as for Figure 63, except for faults and geological boundaries, which are grey

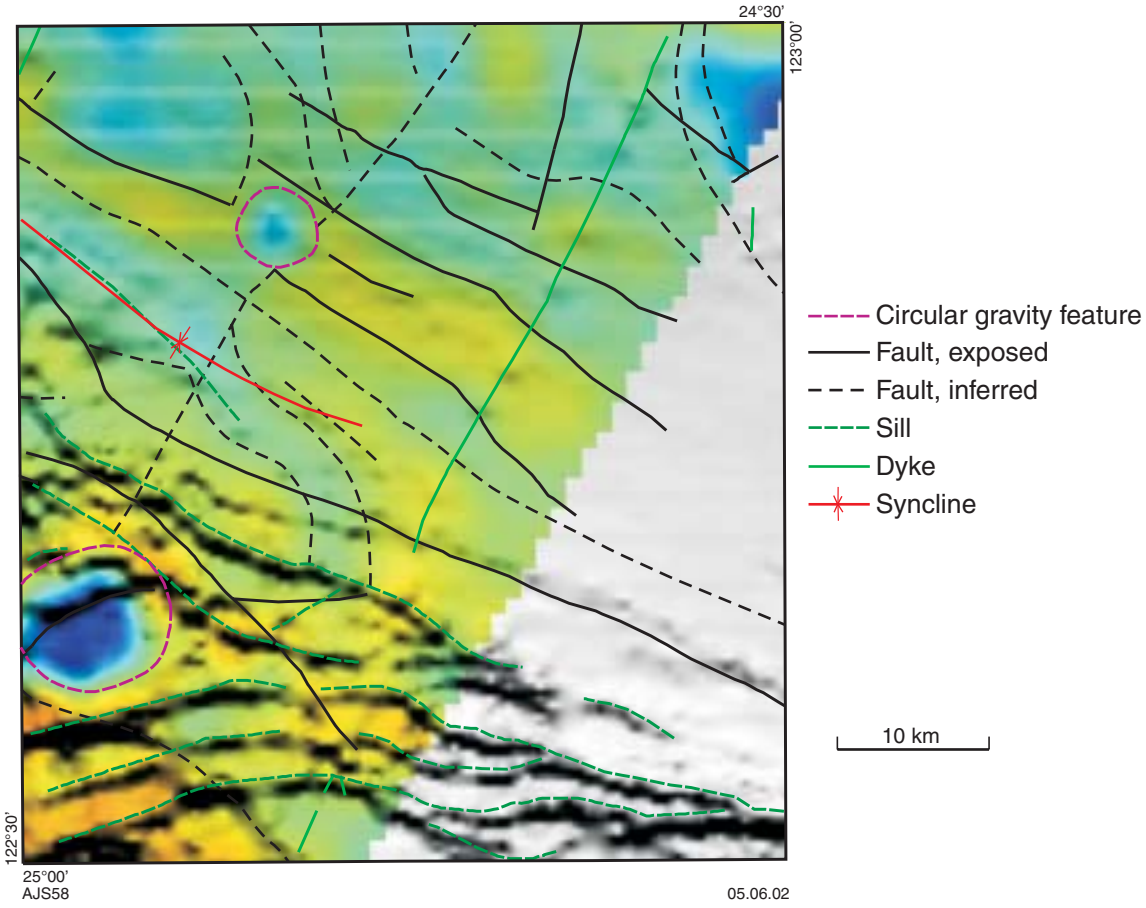

Figure 63. Combined first vertical derivative Bouguer gravity (colour) and TMI image (intensity), and interpreted lineaments on NICHOLLS

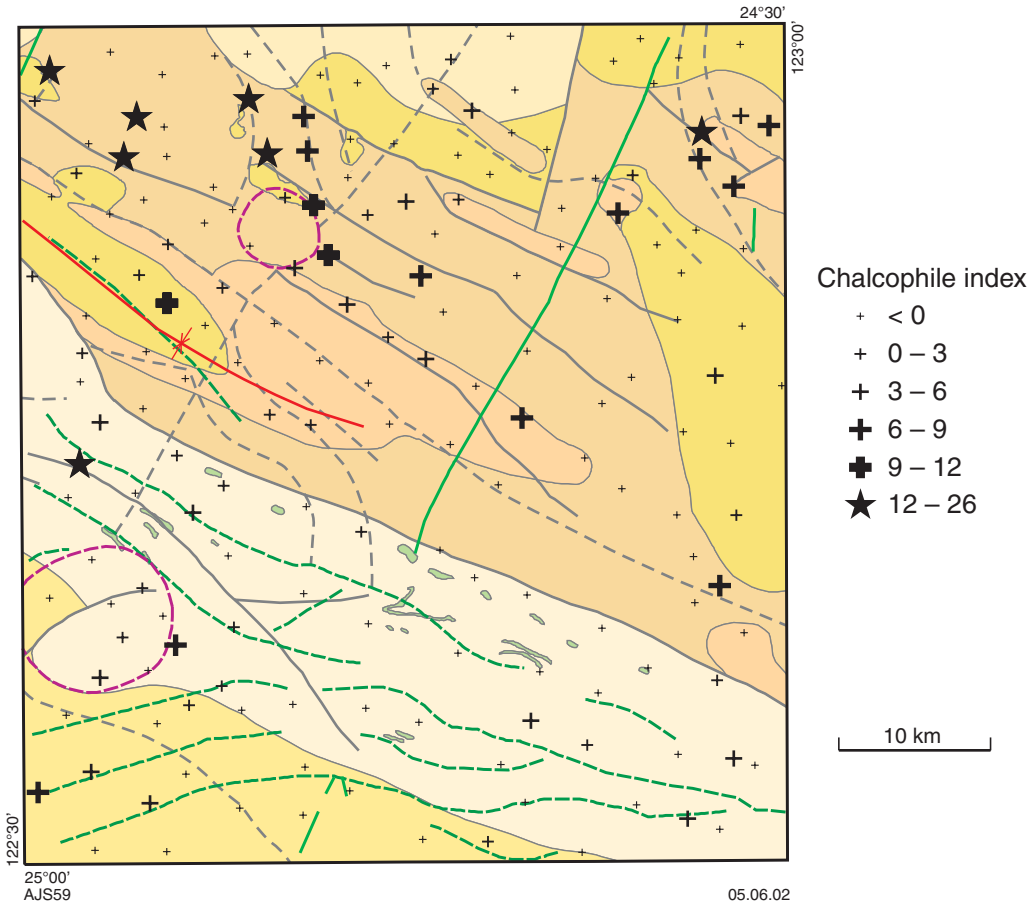

Figure 64. Chalcophile index on Nicholls. Geological symbols as for Figure 63, except for faults and geological boundaries, which are grey

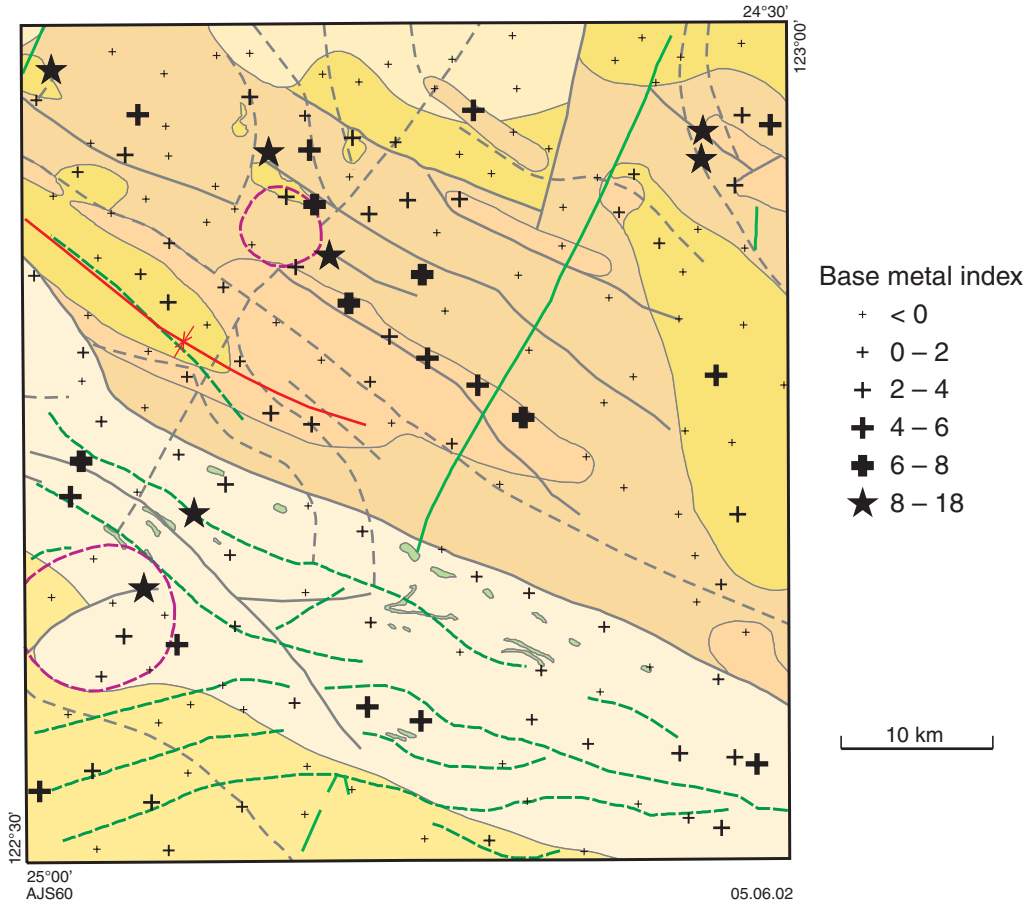

Figure 65. Base metal index on Nicholls. Geological symbols as for Figure 63, except for faults and geological boundaries, which are grey

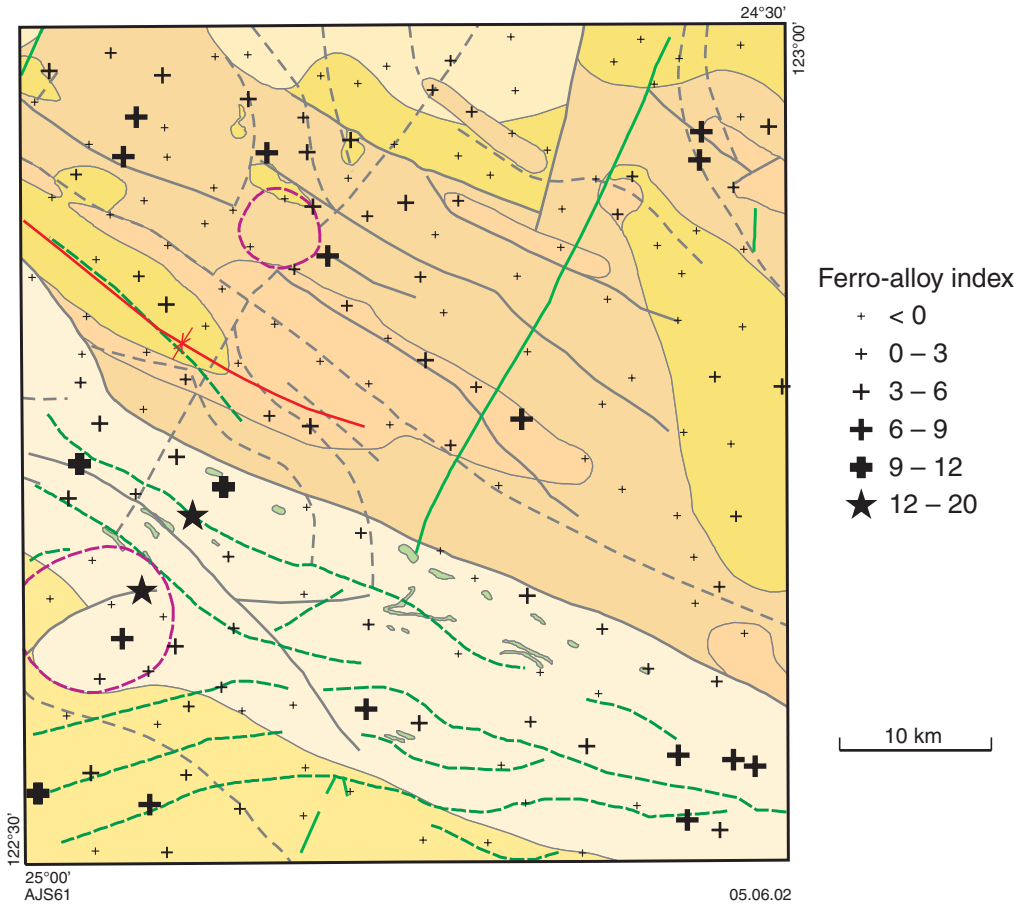

Figure 66. Ferro-alloy index on NICHOLLS. Geological symbols as for Figure 63, except for faults and geological boundaries, which are grey

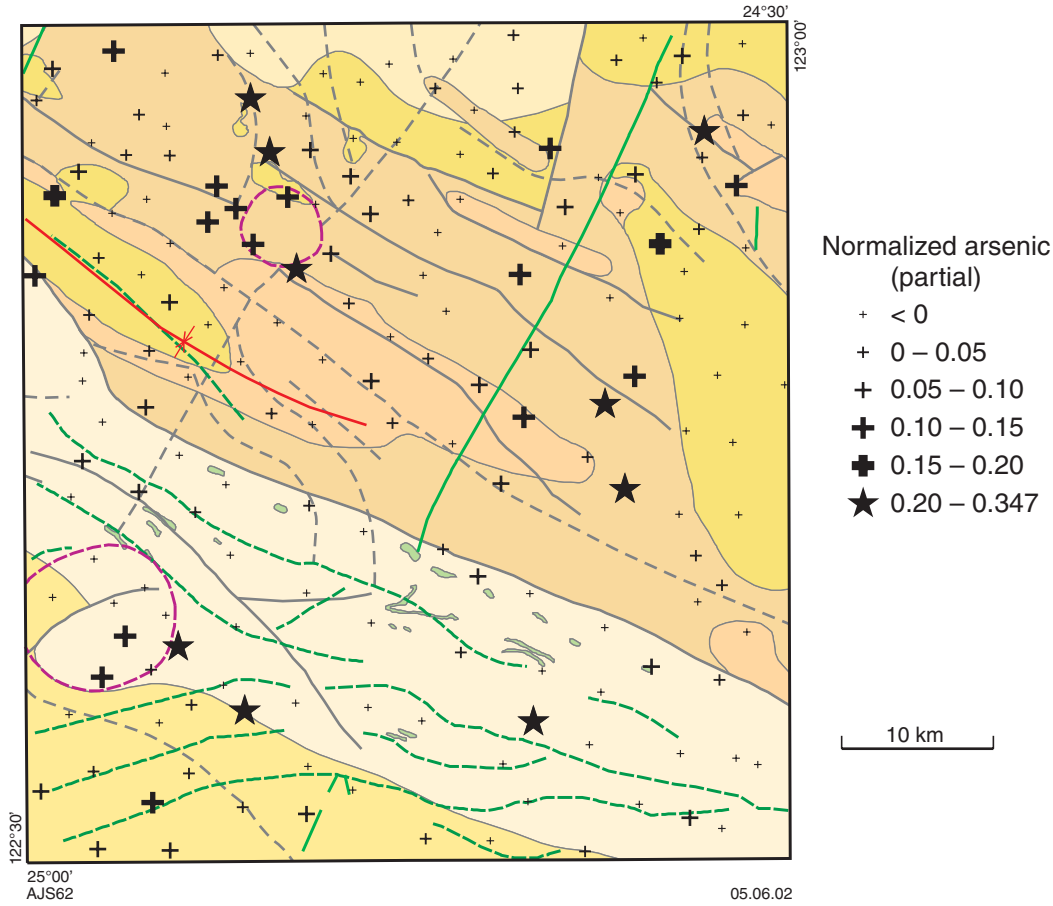

Figure 67. Normalized arsenic (partial) on NICHOLLS. Geological symbols as for Figure 63, except for faults and geological boundaries, which are grey

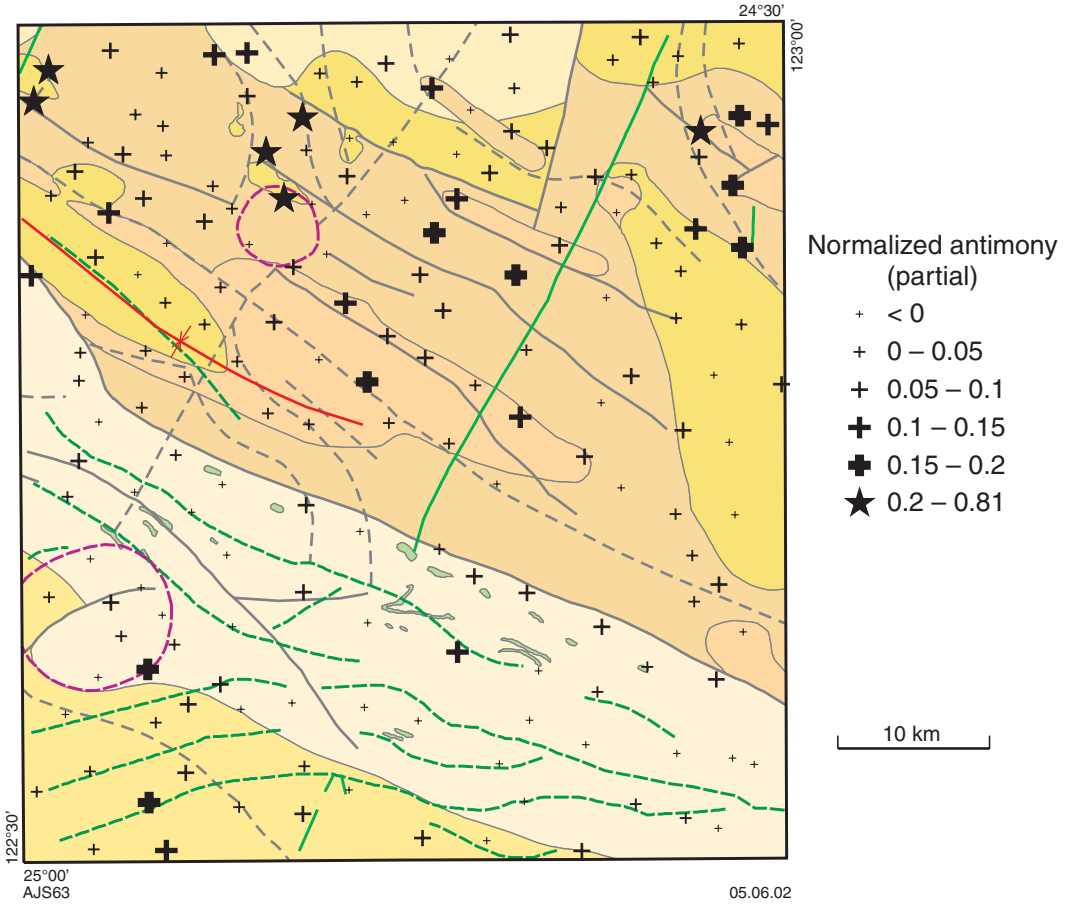

Figure 68. Normalized antimony (partial) on NICHOLLS. Geological symbols as for Figure 63, except for faults and geological boundaries, which are grey

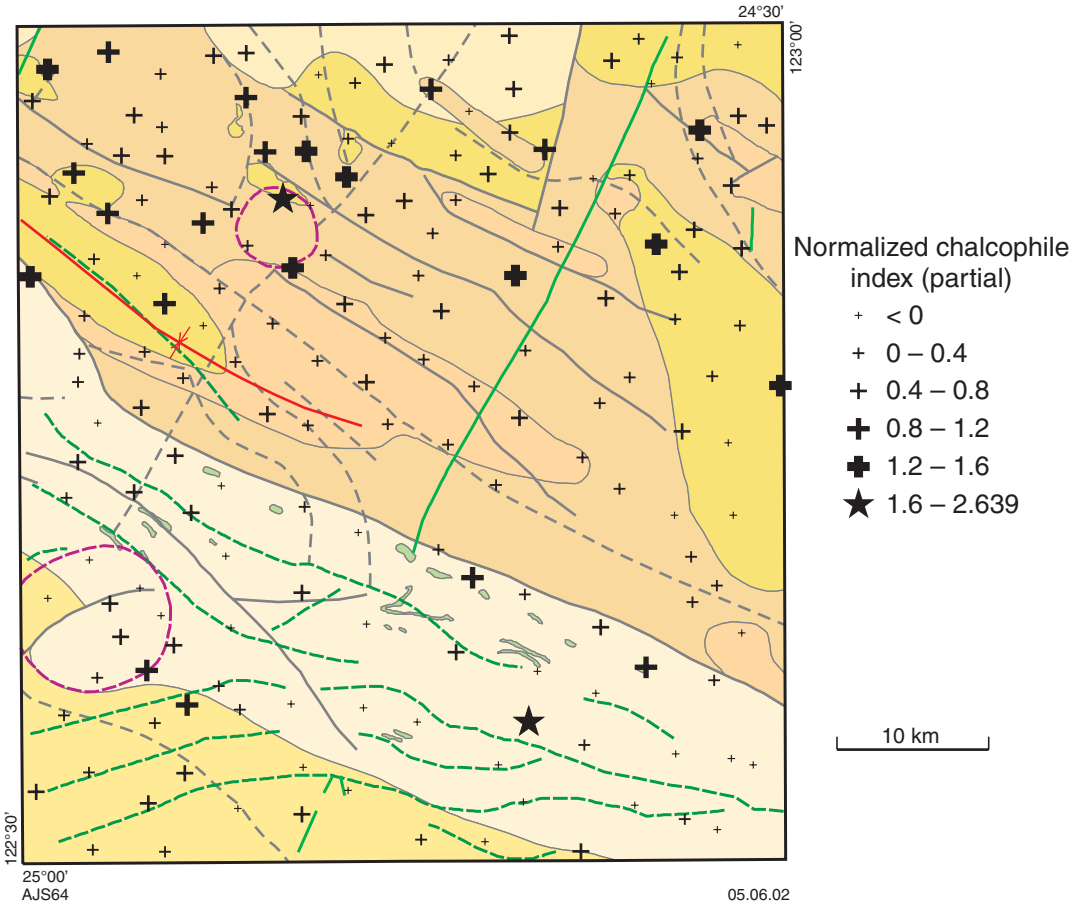

Figure 69. Normalized chalcophile index (partial) on NICHOLLS. Geological symbols as for Figure 63, except for faults and geological boundaries, which are grey

NICHOLLS

AUSTRALIA 1:100 000 REGOLITH GEOCHEMISTRY SERIES | GEOLOGICAL SURVEY OF WESTERN AUSTRALIA | SHEET 3448

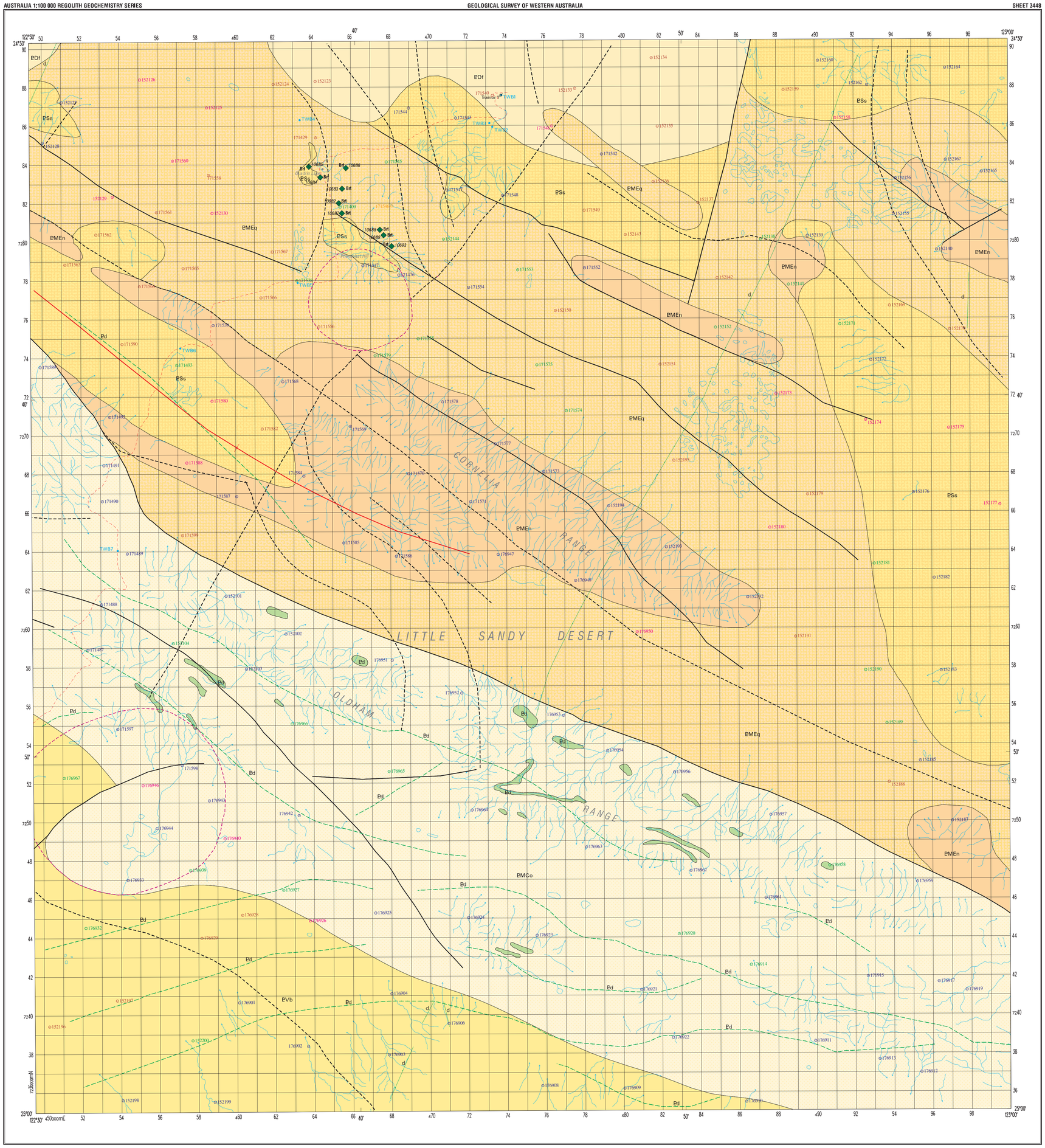

Edited by G. Hall, K. Greenberg, and C. Brien

Cartography by M. Vicentic

Topography from Australian Surveying and Land Information Group, and Department of Land Administration Sheet SG 51-2, 3448

This map was compiled and produced using a Geographic Information System (ArcInfo), and the data are available in digital form

Published by the Geological Survey of Western Australia. Copies of this map, or extracts of the data, are available from the Information Centre, Department of Mineral and Petroleum Resources, 100 Plain Street, East Perth, WA, 6004. Phone (08) 9222 3459, Fax (08) 9222 3444
Web www.mpr.wa.gov.au Email geological_surveys@mpr.wa.gov.au

Gravity and aeromagnetic interpretation by S. I. Shevchenko 2001

Gravity interpretation using: GEOLOGICAL SURVEY OF WESTERN AUSTRALIA, 1996, Savory Basin first vertical derivative of Bouguer gravity image, 1:250 000; Western Australia Geological Survey
Aeromagnetic interpretation using: BMR Trainor regional magnetic survey, project 498, 1984

SHEET INDEX

MAULEIFFE 3248	TRAINOR 3349	SANDRIDGE 3448	CONSTANCE 3549	GRILLETT 3648	TUGALA 3749
	TRAINOR SG 51-2			MADLEY SG 51-3	
WHITE LAKE 3248	BRAGGS 3348	NICHOLLS 3448	SKATES 3548	MADLEY 3648	NANTHONA 3748
MEDAN 3247	GLENAGLE 3347	KAARIMAN 3447	BOUGAUT 3547	NOSSITER 3647	LAMPE 3747
	STANLEY SG 51-6			HERBERT SG 51-7	
DARAMEEDY 3246	LEE STEERE 3346	COONABIBBI 3446	LIBOO 3546	FANE 3646	HERBERT WASH 3746

1:100 000 maps shown in black
1:250 000 maps shown in brown
Gravity survey shown in magenta

Compiled by A. J. Sanders 2001

Sampling by A. J. Sanders

Total sample sites: 175; 91 stream sediment, 28 sheetwash, 18 soil, 1 lake sediment, and 37 sandplain

Analyst: Genalysis Laboratory Services

Method: Total digest
Minimum sample size: 1 kg
Fraction of sample analysed: < 2 mm -> 0.45 mm

Method: Partial digest
Minimum sample size: 0.1 kg
Fraction of sample analysed: < 0.2 mm

Geological interpretation after: HOCKING, R. M., GREY, K., BAGAS, L., and STEVENS, M. K., 2000, Mesoproterozoic stratigraphy in the Oldham Inlier, Little Sandy Desert, Central Western Australia: Western Australia Geological Survey, Annual Review 1999-2000, p 49-56; MYERS, J. S., and HOCKING, R. M., 1998, Geological map of Western Australia, 1:2 500 000 (13th edition): Western Australia Geological Survey; WILLIAMS, I. R., 1995, Trainor, W.A. Sheet SG 51-2 (2nd edition) Western Australia Geological Survey, 1:250 000 Geological Series.

The recommended reference for this map is:
SANDERS, A. J., 2002, Regolith materials, Nicholls, W.A. Sheet SG 51-2, 3448, *in* Geochemical mapping of the Nicholls 1:100 000 sheet *by* A. J. SANDERS: Western Australia Geological Survey, Regolith Geochemistry Explanatory Notes, Plate 1

SAMPLE LOCATIONS

Sample point reference

- 152101 Stream sediment
- 152104 Sheetwash
- 152125 Soil
- 171546 Lake sediment
- 152123 Sandplain

SYMBOLS

- Track
- Watercourse
- Phenoclast Hill — Locality
- TWB4 — Water bore
- Trainor 1 — Stratigraphic drillhole

Water bore locations from STEVENS, M. K., and CARLSEN, G. M., 1998, A compilation and review of data pertaining to the hydrocarbon prospectivity of the Savory Sub-basin, Officer Basin, Western Australia: Western Australia Geological Survey, Record 1998/5, 65p.

MINERAL OCCURRENCES

MINERALIZATION STYLES: ◇ Vein and hydrothermal ú undivided
MINERAL AND ROCK COMMODITY GROUPS: ● Industrial mineral
OCCURRENCE NUMBERS: Numbers refer to GSWA WAMIN mineral occurrence database
KEY TO OPERATING STATUS: *Italic numbers* Mineral occurrence or prospect
MINERAL COMMODITY: Barite..... Brt

INTERPRETED BEDROCK GEOLOGY

PROTEROZOIC

NEOPROTEROZOIC

- d — Fine-grained dolerite dykes
- Bd — Fine-grained dolerite dykes and sills, deeply weathered (kaolinized); where dashed interpreted from aeromagnetic data

Disappointment Group
- EDf — McFADDEN FORMATION: laminated fine- to coarse-grained sandstone, feldspathic sandstone, quartz wacke; minor conglomerate, and siltstone

Sunbeam Group
- EPs — SKATES HILLS FORMATION: stromatolitic dolomite and limestone, fine- to medium-grained sandstone, siltstone, shale; basal conglomerate

Salvation Group
- EPb — BRASSEY RANGE FORMATION: fine- to coarse-grained sandstone and siltstone, quartzose and feldspathic; typically moderately indurated

MESOPROTEROZOIC

Collier Group
- EMCo — OLDHAM SANDSTONE: fine- to medium-grained silicified sandstone, siltstone; moderately dipping

Edmund Group
- EMEn — CORNELIA SANDSTONE: fine- to medium-grained intensely silicified sandstone, siltstone, wacke; steeply dipping
- EMEq — QUADRIO FORMATION: shale, siltstone, minor sandstone, chert; steeply dipping to subvertical

- Geological boundary
- Fault, exposed
- Fault, concealed
- Syncline
- Interpreted circular gravity feature

GENERALIZED REGOLITH

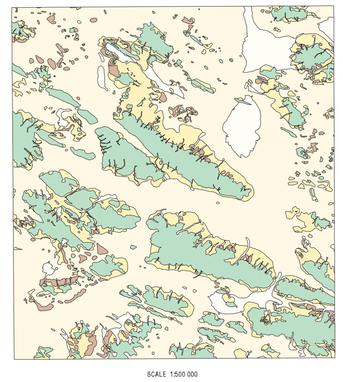

- Residual
- Exposed
- Colluvial (includes low-gradient slope)
- Alluvial and lacustrine
- Sandplain

SCALE 1:500 000

Department of Mineral and Petroleum Resources
CLIVE BROWN, M.L.A., MINISTER FOR STATE DEVELOPMENT
JIM LIMERICK, DIRECTOR GENERAL

Geological Survey of Western Australia
TIM GRIFFIN, DIRECTOR

SCALE 1:100 000

1000 0 1 2 3 4 5 6 7 8 9 10
METRES KILOMETRES

UNIVERSAL TRANSVERSE MERCATOR PROJECTION
VERTICAL DATUM: AUSTRALIAN HEIGHT DATUM
HORIZONTAL DATUM: GEOCENTRIC DATUM OF AUSTRALIA 1994
Grid lines indicate 1 000 metre interval of the Map Grid Australia, Zone 51

GDA The Map Grid Australia (MGA) is based on the Geocentric Datum of Australia 1994 (GDA94) GDA94 positions are compatible within one metre of the datum WGS84 positions

SAMPLE LOCATIONS

REGOLITH GEOCHEMISTRY SERIES

NICHOLLS

SHEET 3448

FIRST EDITION 2002

WARNING: Inks are water soluble and will fade with prolonged exposure to light

NICHOLLS

AUSTRALIA 1:100 000 REGOLITH GEOCHEMISTRY SERIES | GEOLOGICAL SURVEY OF WESTERN AUSTRALIA | SHEET 3448

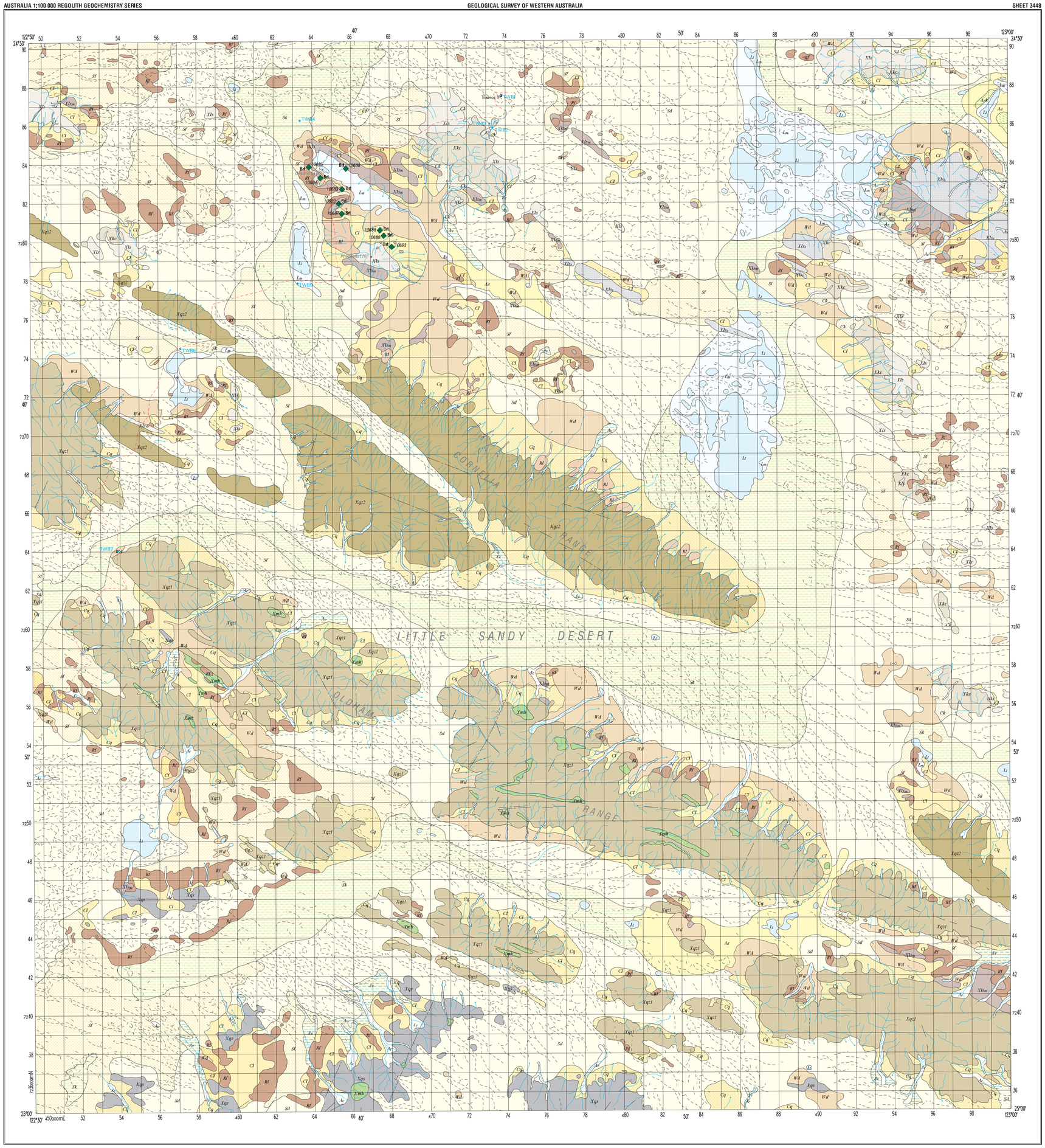

REGOLITH MATERIALS

REFERENCE

RESIDUAL *(R)* Residual sand, duricrust, and gravel derived by weathering in situ; includes proximal reworked material

- *Rf* comprising mainly iron-rich material (ferricrete)
- *Rk* comprising mainly carbonate-rich material (calcrete)
- *Rl* comprising mixed material (ferricrete over either sandstone, shale, or older colluvium)

EXPOSED *(X)* Outcrop of saprock and bedrock, with locally derived sand, silt, clay, and rubble

- *XKc* derived from carbonate-rich bioclastic sedimentary rock (thinly bedded, stromatolitic dolomite and siltstone; largely SKATES HILLS FORMATION)
- *XIs* derived from heterogeneous sedimentary rock (sandstone, siltstone, shale, conglomerate, evaporite, chert, and dolomite; largely SKATES HILLS FORMATION)
- *XIsm* derived from heterogeneous sedimentary rock (shale, siltstone, minor sandstone, and chert; largely QUADRIO FORMATION)
- *XIss* derived from heterogeneous sedimentary rock (sandstone, wacke, and minor shale, and banded chert; largely CORNELIA SANDSTONE)
- *Xmh* derived from ferromagnesian hypabyssal rock (dolerite; typically deeply weathered)
- *Xqs* derived from quartz-rich sillicilastic sedimentary rock (sandstone and siltstone; largely BRASSEY RANGE FORMATION)
- *Xqz1* derived from quartz-rich silicified sedimentary rock (sandstone and siltstone; OLDHAM SANDSTONE)
- *Xqz2* derived from quartz-rich silicified sedimentary rock (sandstone, siltstone, wacke; CORNELIA SANDSTONE)

COLLUVIAL *(C)* Unconsolidated and semi-consolidated silt, sand, gravel, and rubble

- *Cf* comprising mainly iron-rich material
- *Ck* derived mainly from carbonate-rich rock
- *Cl* derived from mixed rock types and heterogeneous sedimentary rocks
- *Cq* derived mainly from quartz-rich rock (sandstone, and minor wacke)

LOW-GRADIENT SLOPE *(W)* Sand- and clay-dominated colluvium and sheetwash

- *Wd* undivided

ALLUVIAL *(A)* Cobbles, gravel, sand, silt, and clay

- *Ac* in alluvial channels
- *Ad* in drainage depressions
- *Adk* in drainage depressions; carbonate-rich (calcrete)
- *Av* in alluvial fan or floodout

LACUSTRINE *(L)* Clay, silt, sand, gravel, and evaporitic material, largely related to palaeodrainages

- *Ld* in playas and lakes
- *Lm* in mixed dune and playa terrain

SANDPLAIN *(S)* Eolian, colluvial and residual sand

- *Sd* undivided
- *Sf* in sandplain environment with ironstone pebble veneer; locally eolian
- *Sk* in sandplain environment with low dunes; sand and calcrete filling older drainage depressions (palaeodrainages)

SYMBOLS

- Regolith boundary
- Breakaway
- Dune crest
- Landsat lineament
- Track
- Watercourse
- • *Phenacolast Hill* Locality
- • TWB4 Water bore
- ⌀ Trainor 1 Stratigraphic drillhole

Water bore locations from STEVENS, M. K., and CARLSEN, G. M., 1998, A compilation and review of data pertaining to the hydrocarbon prospectivity of the Savory Sub-basin, Officer Basin, Western Australia: Western Australia Geological Survey, Record 1998/5, 65p.

MINERAL OCCURRENCES

MINERALIZATION STYLES
◇ Vein and hydrothermal ú undivided

MINERAL AND ROCK COMMODITY GROUPS
● Industrial mineral

OCCURRENCE NUMBERS
Numbers refer to GSWA WAMIN mineral occurrence database

KEY TO OPERATING STATUS
Italic numbers Mineral occurrence or prospect

MINERAL COMMODITY
Barite..... Brt

INTERPRETED BEDROCK GEOLOGY

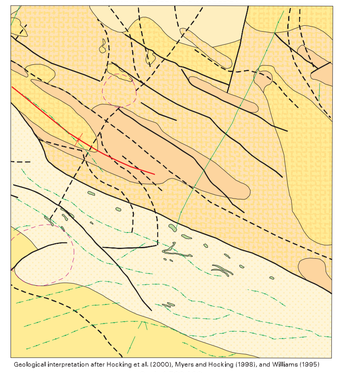

Geological interpretation after Hocking et al. (2000), Myers and Hocking (1998), and Williams (1995)

Scale 1:500 000

- Fine-grained dolerite dykes
- Fine-grained dolerite dykes and sills, deeply weathered (kaolinized); where dashed interpreted from aeromagnetic data

PROTEROZOIC — MESOPROTEROZOIC

- Disappointment Group: McFADDEN FORMATION: laminated fine- to coarse-grained sandstone, feldspathic sandstone, quartz wacke; minor conglomerate, and siltstone
- Sunbeam Group: SKATES HILLS FORMATION: stromatolitic dolomite and limestone, fine- to medium-grained sandstone, siltstone, shale; basal conglomerate
- Salvation Group: BRASSEY RANGE FORMATION: fine- to coarse-grained sandstone and siltstone, quartzose and feldspathic; typically moderately indurated
- Collier Group: OLDHAM SANDSTONE: fine- to medium-grained silicified sandstone, siltstone; moderately dipping
- Edmund Group: CORNELIA SANDSTONE: fine- to medium-grained intensely silicified sandstone, siltstone, wacke; steeply dipping
- QUADRIO FORMATION: shale, siltstone, minor sandstone, chert; steeply dipping to subvertical

- Geological boundary
- Syncline
- Fault, exposed
- Interpreted circular gravity feature
- Fault, concealed

Department of Mineral and Petroleum Resources
CLIVE BROWN, M.L.A., MINISTER FOR STATE DEVELOPMENT
JIM LIMERICK, DIRECTOR GENERAL

Geological Survey of Western Australia
TIM GRIFFIN, DIRECTOR

SCALE 1:100 000

1000 0 1 2 3 4 5 6 7 8 9 10
METRES KILOMETRES

UNIVERSAL TRANSVERSE MERCATOR PROJECTION
VERTICAL DATUM: AUSTRALIAN HEIGHT DATUM
HORIZONTAL DATUM: GEOCENTRIC DATUM OF AUSTRALIA 1994
Grid lines indicate 1 000 metre interval of the Map Grid Australia, Zone 51

GDA The Map Grid Australia (MGA) is based on the Geocentric Datum of Australia 1994 (GDA94)
GDA94 positions are compatible within one metre of the datum WGS84 positions

Edited by G. Hall, K. Greenberg, and C. Brien

Cartography by M. Vicentic

Topography from Australian Surveying and Land Information Group, and Department of Land Administration Sheet SG 51-2, 3448

This map was compiled and produced using a Geographic Information System (ArcInfo), and the data are available in digital form

Published by the Geological Survey of Western Australia. Copies of this map, or extracts of the data, are available from the Information Centre, Department of Mineral and Petroleum Resources, 100 Plain Street, East Perth, WA, 6004. Phone (08) 9222 3459, Fax (08) 9222 3444
Web www.mpr.wa.gov.au Email geological_survey@mpr.wa.gov.au

SHEET INDEX

MAUDIETTE 3249	TRAINOR 3349	SANDRIDGE 3449	CONSTANCE 3549	GIBLETT 3649	TUGALA 3749
	TRAINOR SG 51-2			MADLEY SG 51-3	
WHITE LAKE 3248	BRASSEY 3348	NICHOLLS 3448	SKATES 3548	MADLEY 3648	NANTHONIA 3748
MUDAN 3247	GLENAYLE 3347	KARRABIN 3447	BOUGAUT 3547	NOSSITER 3647	LAMPS 3747
	STANLEY SG 51-6			HERBERT SG 51-7	
EARAHEEDY 3246	LEE STEERE 3346	COONARIBBE 3446	LINKS 3546	FANE 3646	HERBERT WASH 3746

1 : 100 000 maps shown in black
1 : 250 000 maps shown in brown
Gravity survey shown in magenta

Compiled by A. J. Sanders 2001

Field observations 2000-2001 by A. J. Sanders

Compiled using: Landsat TM images (1994 data); ASTER images (2000 data); 1995 images 1:50 000 scale black and white aerial photography; WILLIAMS, I. R., 1995, Trainor, W. A. Sheet SG51-2 (2nd edition); Western Australia Geological Survey, 1:250 000 Geological Series; and field observations 2000-2001.

The recommended reference for this map is:
SANDERS, A. J., 2002, Regolith materials, Nicholls, W.A. Sheet SG 51-2, 3448, *in* Geochemical mapping of the Nicholls 1:100 000 sheet *by* A. J. SANDERS; Western Australia Geological Survey, Regolith Geochemistry Explanatory Notes, Plate 2

REGOLITH MATERIALS

REGOLITH GEOCHEMISTRY SERIES

NICHOLLS

SHEET 3448

FIRST EDITION 2002

WARNING: Inks are water soluble and will fade with prolonged exposure to light